EVALUATION OF THE BATCH PRESS AS A LABORATORY TOOL TO SIMULATE HIGH AND MEDIUM-PRESSURE ROLLER CRUSHERS

by

JAN CORNELIUS RUDOLPH VAN SCHOOR

Submitted in partial fulfilment of the requirements for the degree

MAGISTER

in

METALLURGICAL ENGINEERING

in the

FACULTY OF ENGINEERING, BUILT ENVIRONMENT AND INFORMATION TECHNOLOGY

University of Pretoria

30 November 2012

ACKNOWLEDGEMENTS

SOLI DEO GLORIA

TABLE OF CONTENTS

Nomenclature:

d = Particle size defined in the Rosin-Rammler formula (µm)

E = Energy per unit mass consumed (kWh/ton)

F = Feed size to a crusher or mill (in general) (µm)

F_{80} = 80% mass passing size of the feed (µm)

F_{50} = 50% mass passing size of the feed (µm)

F_{25} = 25% mass passing size of the feed (µm)

Kic = Fracture toughness of material, and in this formula

σ = The stress needed for crack propagation and

a = The crack length (µm)

m = Constant, the so-called Rosin-Rammler slope.

n = Factor characteristic of the comminution device, product size range and material. This factor describes the relationship between product size and energy consumption $E \propto 1/P^n$

OWi = Operating work index, determined by measuring the energy consumption, feed size and product size for the specific device (kWh/ton)

P = Product size of the crusher or mill (in general) (µm)

P_{80} = 80% mass passing size of the product (µm)

P_{50} = 50% mass passing size of the product (µm)

P_{25} = 25% mass passing size of the product (µm)

Wi = Work index, a factor that depends on the comminution device, Bond work index in the case of ball mills (kWh/ton)

x = Screen aperture (µm)

Y = Cumulative size distribution (% passing)

ABSTRACT

High and medium-pressure roller crushers operate on the principle of inter-particle crushing by crushing material in a packed bed. Although reference in the study is made to high-pressure roller crushers, the work was done with medium–pressure roller crushers i.e. the Loesche mill and the Horomill. The difference in pressures between these equipment and high-pressure grinding rolls (HPGR) from measurements done by FCB, the supplier of the Horomill, was that the medium-pressure equipment operates at pressures of 30 MPa whilst the HPGR operates at pressures as high as 100 MPa. In this study, the differences between single particle and inter-particle crushing and the applicability of the batch press to predict the energy consumption and particle size distributions for medium-pressure roller crushers were investigated. Two phases of crushing were identified and investigated. The first phase occurs when the material is still being drawn into the gap between the rollers. The second phase, called packed bed crushing, occurs when the material is in the gap between the rollers. Crushing and milling energy requirements are discussed with specific reference to the energy models proposed by Bond and Rittinger along with the shortcomings of both these models. These models postulate that the comminution energy is an inverse function of product size. This is proven to be true in this study, but where certain constants are suggested in the aforementioned correlations, this study revealed that these constants are not fixed for all applications but varies for different types of ore. The results were determined for 80% as well as 50% mass passing size. Kick proposed that the energy requirements are a function of the reduction ratio. A model used for roller crushers that is similar to what Kick proposed was also investigated. This was also found to be valid but again, the coefficients in the model vary for the different materials. A new method for predicting the work index of an ore for inter-particle crushing was investigated, which involves using a piston press in which a bed of material is pressed to a predetermined pressure. The proposed method was evaluated using pilot test data obtained with a Horomill, as well as with a pilot Loesche mill. The results indicate that the correlation between the batch press and the pilot mills are poor. The Rosin-Rammler description for particle size distribution was applied and compared with other descriptions. The particle size descriptions of products from the batch press and pilot mills were compared and although there are differences, the batch press can be used to prepare material for initial research in a project. From this study it is clear that, especially

when tests are done on an unknown ore body, a work index such as Bond's, cannot be used for plant design and economic studies unless some pilot plant tests are done to confirm the relationship between energy consumed and product size.

CHAPTER 1

PROBLEM STATEMENT

1.1   INTRODUCTION

Inter-particle crushing is achieved when a bed of particles, rather than single particles, is subjected to forces high enough to cause fracture of the particles. This is at present achieved with medium- and high-pressure roller crushers and to some extent in cone crushers operating under choke feed conditions. Although the crushing and milling of material with medium- and high-pressure roller crushers is not new in the world of comminution, its application in the mining industry is still in the early stages. Medium-pressure roller crushers have been in use for over 30 years to mill coking coal for pulverised coal injection in blast furnaces, manganese dioxide and various minerals in the cement industry. Limiting over-grinding is a major potential advantage of inter-particle crushing. To pursue this benefit, a large-scale roller crusher (Loesche) was installed at Foskor in order to limit the over-grinding of apatite. Over-grinding of apatite causes significant losses during flotation. In the late 1980's, Schönert (1988), focused on one of the advantages of inter-particle crushers, namely a potential saving in energy. He found that by milling material with high-pressure roller crushers, energy savings of as high as 50% could be achieved compared to ball mills. Work done by Eicke (1979), Kanda et al (1996), Fandrich et al (1997), Lim and Weller (1998), Mayerhauser (1990), Norgate and Weller (1994), Schönert (1991), Schwechten and Milburn (1990), and Van der. Meer (1997), confirmed that this significant increase in efficiency could indeed be achieved.

Another advantage, and this is where focus in this field should be, is the narrower particle size distributions that can be achieved compared to ball and rod milling. In most beneficiation processes too much fine material, normally expressed as minus 38 μm material, leads to a loss of valuable minerals. Flotation recovery of the fine fractions is lower, magnetic separation of minus 38 μm material is more difficult and under normal circumstances high slimes contents has a negative impact on beneficiation. Viljoen, et al (2001), and Van der Linde and Bester (1998), confirmed this for the flotation of nickel and phosphate ores respectively. The lack of focus on the advantage of changing the particle size distribution to improve downstream

1

beneficiation processes is surprising in view of the major benefits that can be achieved. The reasons are that the mining industry is very conservative to changes in technology, due in part to the high cost involved in introducing new technology in existing plants and the added risk in introducing new technology in green field projects. From a research perspective, the lack of internationally accepted test equipment and procedures contribute to the lack of focus in this field.

1.2   PROBLEM STATEMENT

The first challenge facing researchers in this field is to know whether the commonly used comminution laws and particle size descriptions apply to inter-particle crushing. The second is to design bench-scale methods and procedures, i.e. small-scale tests, to predict the performance of production equipment. With regard to the latter, Daniel (2001), proposed that the simulation of the HPGR should be done in three stages. The first is the portion of the feed that is by-passed in the crushers. This happens at the edges of the rollers where material is not pressed to the same extent as in the middle. This is a number that the suppliers of the HPGR must provide. In the case of the Loesche mill there is no bypass. The second stage is when material is crushed from the feed size to the gap size between the rollers. Particles larger than the gap size are crushed as single particles. Daniel (2001), suggested the Whiten crusher model for simulation of this stage. Of note is that there is not a fixed gap size. Particles larger than the gap size as well as particles with compression strength higher than the applied pressure will open the bed resulting in a certain amount of single particle crushing. The third stage is when the particles are compressed in the bed in an inter-particle mode. For the Loesche or Horomill, i.e. medium pressure mills, the percentage single particle crushing is expected to be higher than in a HPGR, where higher pressures are applied. The gap size varies more with lower pressures. This might lead to less favourable comparisons between the batch press and the medium pressure pilot mills.

2

1.2.1 ENERGY RELATIONSHIPS

When considering the comminution behaviour of particles, either as single particles or in a packed bed, one needs a mathematical model to describe two aspects of the characteristic behaviour of material:

- The relationship between the degree of comminution and the energy input and
- The description of the size distribution of the product.

The energy needed to mill material to a specific particle size was proposed by Austin (1964), to be inversely related to some function of the product size for relative large size reductions:

$$E \propto 1/(P_{80})^n \hspace{4cm} 1$$

Where: E = Energy consumed per unit mass

P_{80} = 80% mass passing screen size of the material (µm)

n = Factor characteristic of the comminution device, product size range and material.

The P_{80} parameter is extensively used in the design of ball and rod mill circuits and was well researched by Bond for the design of mills by Allis Minerals (Bond, 1952). The factor n changes with degree of comminution. This was researched by Hukki (1975). Hukki used calcite and crushed the material to products over a large size range. He found that the energy consumption per ton is as expected, an inverse function of particle size (P_{80}), but also that it increases strongly at smaller particle sizes, as indicated in figure 1.
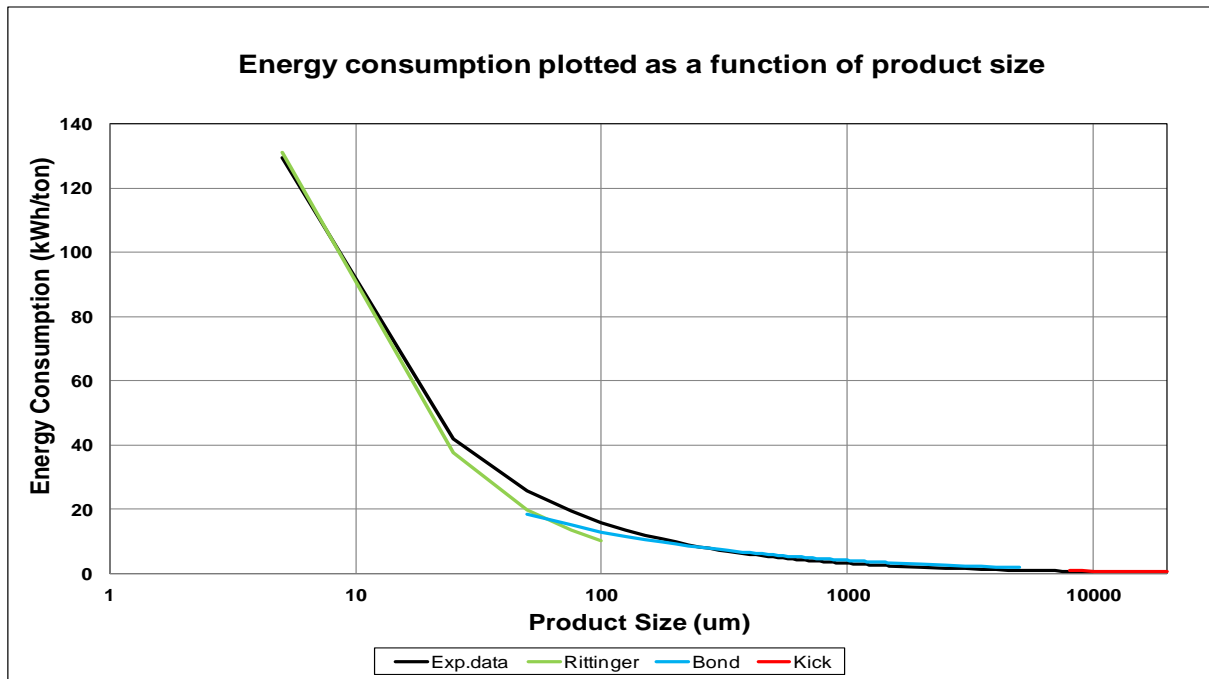
Figure 1: Energy requirements for comminution of limestone as determined by Hukki (1975), illustrating the range of applicability of Kick's, Bond's and Rittinger's laws as indicated by the different applicable values for the exponent in the equation $E \propto (P80)^n$.

The energy consumption per unit mass vs. particle size relationship may be divided into three regions, larger than 10000 μm, between 10000 μm and 100 μm and smaller than 100 μm. Above 10000 μm the energy consumption per unit mass is independent of size, between 100 μm and 10000 μm the exponent approximates –0.5 and below 100 μm it approximates –1. These regions define the so called "comminution laws" of Kick, Bond and Rittinger, respectively.

The region above 10 mm approximates Kick's law which states that the energy needed to crush a piece of rock is a function of the reduction ratio (Jankovic et all, 2008):

$$E \propto \ln(F_{80}/P_{80}) \hspace{4cm} 2$$

Bond found that for the size ranges typical of ball mills, the energy consumed per unit mass is inversely related to the square root of the product size for a constant feed size, i.e.

4

$$E \propto 1/(P_{80})^{0.5} \qquad\qquad 3$$

Or more specifically (Bond, 1952):

$$E = 10W_{iB} (1/(P_{80})^{0.5} - 1/(F_{80})^{0.5}) \qquad\qquad 4$$

Where: E = Energy consumed per unit mass (kWh/ton)

F_{80} = 80% mass passing size of the feed (μm).

W_{iB} = Bond work index (kWh/ton), i.e. the energy required to mill material from relative large feed sizes to a P_{80} of 100 μm.

P_{80} = 80% mass passing size of the product (μm).

Note that the value of the constant 10 in the equation relates to the fact that if the P_{80} is 100 μm and the feed size is large, the square root of P_{80} becomes 10. Thus the energy consumed equals the work index.

For fine product sizes, i.e. below 100 μm, the energy needed to mill a single particle increases exponentially. In this range the energy consumed is inversely related to product size Austin (1964):

$$E = 100W_{iR} (1/P_{80} - 1/F_{80}) \qquad\qquad 5$$

Where: WiR = Work index as described by Rittinger, as with Bond, the energy needed per unit mass to mill material to a P_{80} of 100 μm.

However, there is reason to believe that the size ranges where the different laws apply might differ for different applications. A better description would be as follows:

$$E = Wi(100^{n})(1/P_{80}^{n} - 1/F_{80}^{n}) \qquad\qquad 6$$

Where: Wi = Work index

n = is the coefficient applicable to the specific system, i.e. material, apparatus and product sizes.

The work index of a material is the energy per ton needed to mill material from a very large size ($1/F_{80} \approx 0$) to a product size of 100 µm. For the energy to equal the work index the inverse of the product size must be 1 when P_{80} is 100 µm. Thus a term 100^n is added.

$$Wi = E/(100^n)/(1/P_{80}^n - 1/F_{80}^n) \qquad\qquad 7$$

In the tests done in this study, the term operating work index is used (OWi). It has the same meaning in the equations. The difference is that in a large part of the industry, when this value is determined from plant or test data, it is referred to as an operating work index whereas a work index refers to a number determined in a recognised batch test such as the Bond work index.

Kapur et al (1990), as well as Daniel (2001), found that there is a power relationship between reduction ratio and consumption per unit mass for roller mills.

$$F_{50}/P_{50} = aE^n + 1 \qquad\qquad 8$$

or

$$E = k((F_{50} - P_{50})/P_{50}))^{1/n} \qquad\qquad 9$$

Where: a, n, k = constants.

E = Energy consumed per unit mass (kWh/ton)

From their work it is suggested that the value of n for roller crushers is 1. However their work was done with conventional roller mills. It is believed that this would differ for medium- and high pressure roller crushers.

Where Bond and Rittinger define energy as a function of the inverse of the product size, Kick, as shown in equation 2, expresses energy per unit mass consumed as a function of reduction ratio. Hukki suggested that Kick's law is valid at large product sizes. Although, in this study, material is milled to product sizes that correlates with what is described by Bond and Rittinger, it is advisable to also follow a different approach. Since the relationship as indicted in equation 8 and 9 and that of Kick are

6

similar and already found to describe roller crushers, it will be investigated in this study.

There are three reasons why it is expected that the comminution laws as stated by Bond and Rittinger might not be valid in medium- and high pressure roller crushers. The first can be seen from figure 1. There is an area where neither Rittinger nor Bond describes the experimental data. It is unlikely that the value of n will change from 0.5 to 1.0 at an exact unique product size. There must be a transition from 0.5 to 1.0. The conclusions that Hukki made was with limestone, and it is likely that the size ranges will be different for different ore types. The second reason has to do with the fact that ball mills and crushers were used for the tests by Bond. In ball mills individual particles are nipped between balls and in crushers the particles are nipped between the crushing elements and very little packed bed comminution occurs. It therefore can not be assumed that what this concept will apply to medium- and high pressure roller crushers. The last and perhaps the most important reason has to do with the fact that the different laws apply to different particle size ranges.

Whenever a particle is subjected to a compressive force, tensile forces excited within the particle may cause a crack to develop inside the material. The energy needed to grow this crack is a function of the length of the crack, the inherent toughness of the material and the surface energy required to create the new surface area resulting from crack growth. Ore consists of various mineral particles bonded together. When crushed, ore will start to crack firstly along major flaws or cracks. These flaws are caused by acts of nature such as movements in the ore crust and mostly by the blasting process used in the mining of the ore. Crushing of the large lumps of ore will also excite smaller flaws in the ore that may act as loci where secondary cracks can develop. Eventually, as the lumps of ore decrease in size, the number as well as the size of the flaws will also decrease. The stress required for crack propagation is an inverse function of the flaw size (Guy, 1960):

$$K_{ic} = f \: \sigma \: (\pi a)^{0.5} \qquad\qquad\qquad 10$$
$$\sigma \: \alpha \: 1/(a)^{0.5} \qquad\qquad\qquad 11$$

Where: K_{ic} = Fracture toughness of the material, $(Pa,m^{0.5})$

σ = Stress needed for crack propagation (Pa) and

7

a = Crack length. (m)

This explains why the energy consumption is small with large particles, which typically contains large flaws and increases almost exponentially at smaller sizes.

With inter-particle crushing the power consumption per ton is generally lower than with ball mill and cone crushing. Kapur et al (1992), as well as Kellerwessel (1990), did work with copper and gold ores. They indicated that when material is crushed in a packed bed, numerous flaws are excited on the grain boundaries between mineral particles whilst the particles are still fairly large, i.e. above 3 mm. It can therefore be expected that when the material is crushed to smaller sizes the energy requirements will be lower than expected, due to the numerous micro cracks already present in the material. From figure 1 it follows that Bond's law applies at intermediate sizes and Rittinger's law at the smaller ranges. The result of the induced flaws might well change the size at which the value of n changes to -0.5 and –1. Whenever a comminution circuit is researched, the assumption should not be made that any of the laws apply. A better approach would be to determine the relation between product size and energy consumption, and from these data determine the value for the factor n in the formula $E \propto 1/P^n$. It is also important to take note of another comment that Hukki made. The use of the 80% mass passing size to describe the particle size is questioned. It does not describe the total size distribution and with inter-particle crushing, his point is even more valid. Work done by Kellerwessel (1989), to compare cone crushers with high-pressure grinding rolls, showed that for the same P_{80} the size distribution of the product of the high-pressure grinding rolls, is finer than that of the cone crusher. In this study comparison between the batch press and the pilot mills was based on the P_{80}, P_{50} and in some cases P_{25}, to take this into account.

1.2.2 PARTICLE SIZE DISTRIBUTIONS

The two most commonly used algorithms to describe the particle size distribution of an ore are the Gaudin-Schumann formula,

$$Y = (ax)^n \hspace{12cm} 12$$

Where: Y = Cumulative size distribution (mass % passing).

8

x = Screen aperture.

a, n = Constants,

and the Rosin-Rammler distribution,

$$Y = 1 - \exp(-(d/d_{63.5})^m) \hspace{4cm} 13$$

Where: Y = Cumulative size distribution (mass % passing)
d = Screen aperture size (µm)
$d_{63.5}$ = 63.5% mass passing this screen size (µm)
m = Constant, the so-called Rosin-Rammler slope

When plotting the data on a ln-ln scale, the graph is a straight line that represents Gaudin-Schumann's formula. When plotted as ln-ln on the y-axis and ln on the x-axis, the Rosin-Rammler slope m can be determined from the graph. Although not a fundamental approach, the Rosin-Rammler description is the most widely used of the two, and generally fits the data well. Hukki (1975), however, questioned the validity of this approach, as the data typically does not present a straight line, but deviates at the larger and smaller particle sizes. When material is milled in a rod or ball mill, a large percentage of the very fine material, normally –38 µm material is created through the abrasion of particles. Nipping of material between two balls will result in a range of particle sizes. However, abrasion of particles will result in only fine material, whilst the parent particle does not significantly change in size causing the deviation from the Rosin-Rammler plot at the fine end. It is not clear why it deviates at the coarse end. With inter-particle crushing the amount of abrasion is less, as there is less movement between particles. As this results in fewer fines and while larger particles are also crushed, the Rosin-Rammler plot is expected to be more of a straight line with a larger slope. Discussions with Foskor revealed that in their experience the Loesche pilot mill and the large Loesche mill do give products with size distributions closer to a Rosin-Rammler prediction. As the cumulative particle size distribution is a sigmoidal curve, other exponential descriptions were investigated in this study to determine if a more accurate description than the Rosin-Rammler description could be found.

1.2.3 BENCH SCALE EQUIPMENT

Facilities to do inter-particle crushing tests are limited to the manufacturers and few research facilities. Approximately one ton of material is required for the determination of the energy consumption and to get an idea of the product size distribution. To get this amount from drill cores is not a problem, but if a study on a heterogeneous ore has to be launched and any optimisation has to be done, up to a hundred tons could be needed. There is also a problem with the size of the rollers of the pilot plant equipment. The mill at Anglo American Research Laboratories (AARL) has 200 mm diameter rollers with a gap size of less than 3 mm. The Horomill at FCB has a gap of 10 mm. Tests with the Horomill were done with material with a top size of 30 mm. All the feed larger than the gap size is not subjected to inter-particle crushing. If one takes into account that the mill at Foskor is being fed with 80 mm top size, a large proportion of the behaviour of the ore is not included in the studies. Doing any fundamental work with pilot mills of this size, does yield good initial indications of communition behaviour, but cannot contribute to the understanding of the effect of large feed sizes, either on the energy consumption or the particle size distributions. The batch press is an apparatus that offers such an opportunity. The press is schematically shown and described in section 2.3.1.

This press could address the following disadvantages of the current equipment as the following may be done:

- Small scale tests with limited amount of material.
- Determination of the influence of the bed pressure on the product particle size distribution.
- Determination of the influence of bed pressure on the selective milling of the softer and harder minerals.
- Determination of the influence of oversize feed to the mill.
- Determination of the influence of the particle size distribution on downstream process.
- Determination of the influence of bed thickness on the particle size distributions.

- Comparison between different ore types and variations within an ore type in an ore body.

In any comminution system, the relationship between feed size, product size and energy consumption is needed to extrapolate beyond the test limits. In many cases the feed size to the full-scale mill, is larger than the samples available or treatable in the test program. In the case of Foskor, the feed size to the pilot mills was limited to 30 mm, but the feed size to the large mill is 80 mm. Since Foskor had been using cone crushers at the time to crush the material from 80 mm to 10 mm, the data from these crushers were used to extrapolate from a feed size of 30 mm to 80 mm. It was expected that to crush the material from 80 mm to 30 mm in a Horomill would use less energy than a cone crusher, with the result that a mistake would lead to a slight over-design of the Horomill. This could be justified, given the risk of the project. Any additional production would have been to the benefit of Foskor. However, if it is known from small tests how much energy is needed, the scale-up can be done more accurately. If there are good enough correlations between the batch press and the pilot mill, the test can include larger particles. This will also solve another problem. It is not known what the influence of the full scale feed size on the product size is. Increasing the feed size causes a less dense bed that could have an influence on the comminution process. It is not possible to test this on a pilot plant.

The determination of the bed pressure in a roller mill is an issue that has not yet been solved. The pressure presently measured is the force of the roller on the bed of particles divided by the product of the width and length of roller. The total force can be measured, but the definition of the area or the description of the force distribution is presently unsatisfactory. At the entrance of the bed, the force is nil and increases to a maximum where the material is packed to a maximum density. Small and large rollers have different nip or compression angles and according to Schönert (1988), the increase in pressure is a function of the compression angle. At present there is no certainty on how the bed pressure in a large mill should be measured.

With the batch press it is possible to vary the pressure on the bed and do numerous tests to study the influence of pressure and bed thickness on the fracture behaviour of the material. It also solves the problem of determining the influence of milling

conditions on downstream processes, as different samples can be prepared easily. Using the batch press, a better understanding of the material may be obtained at a relatively low cost before embarking on more expensive pilot plant work.

The approach in this study was to determine the relationship between energy consumption and product size for the particular material and size range. The Rosin-Rammler description will be compared to other similar descriptions to determine if the accuracy of the particle size distribution of a sample can be improved.

1.2.4 SUMMARY

To simulate inter-particle crushing processes, an energy relationship between the feed size and product size must be determined. Tests must indicate whether the size ranges as stated by Hukki can be used or whether it will be different for inter-particle crushing. To describe the particle size distribution of the products, the Rosin-Rammler relationship will be compared with other sigmoidal or S-curve descriptions.

CHAPTER 2

COMPARISON BETWEEN THE HOROMILL, LOESCHE MILL AND THE BATCH PRESS

2.1   INTRODUCTION

The main requirements for a comparative test between comminution devices of this nature are:

- Good sampling practices to ensure that the material tested in the press and mill is the same.
- The material must be milled to the same range of product sizes.
- The product sizes must stretch from coarser to finer than the liberation size of the minerals. The energy required to mill material from coarser to just finer than the liberation size, can increase suddenly as a result of the higher competency of single mineral particles.
- It is good practice to compare materials of different characteristics such as hard and soft materials, as well as coarse and fine-grained material.

Although not a specific requirement, it is a good idea to also evaluate the influence of the milling process on the downstream processing of the material, for example the influence of fines creation on flotation performance.

To fulfil these requirements four types of materials were tested:

- A mixed sulphide ore from the Rosh Pinah mine. This is an ore of medium hardness that typically have to be crushed to between 150μm and 50μm as the liberation size of the various minerals varies from 106 to 75μm.
- Titanium slag, which is very soft and which should be crushed to a top size of 850 μm with the specific requirement that the -106μm fraction must be minimized.
- Apatite ore from Foskor. This is a coarse grained ore of medium hardness. The main reason for using this ore is that it has been well researched in not only a Horomill but also a pilot ball mill.
- Banded iron stone with a liberation size of less than 100μm.

The objectives of the tests were to compare the batch press with a roller mill with regard to energy consumption, particle size distributions of the products and circulating load. The validity of Bond's law, Rittinger's law and the Rosin-Rammler descriptions of particle size distributions will be tested with the results obtained in the tests.

2.2 METHODOLOGY TO DETERMINE THE VALUE OF OPERATING WORK INDEX AND THE ENERGY VERSUS REDUCTION RATIO RELATIONSHIP

The method used to determine the values is based on the fact that the value of the operating work index equals the amount of energy to crush and mill material from a very large feed size to an 80% mass passing product size of 100 μm. Therefore this is a constant for the material. This is then calculated for each data point using equation 7 and a guessed value for the coefficient n. The value of n is changed until all the calculated operating indices are the same. If this is achieved, it means that the value of the coefficient is valid for all sizes from the smallest product size tested to the feed size. If it is not achieved, one reason could be that the value of the coefficient n is different for the feed size and the product size. This can be understood if remembering that the graph in figure 1 implies this value changes with product size. The value of $OWi*100^n/F_{80}^n$ is the amount of energy required to crush material from a very large size to the particular F_{80}. However, this will make predictions even more difficult because now two values must be guessed. Another reason could be that the relationship between energy and product size, while material is still being nipped into the gap, is different from that achieved when material is being crushed in the gap between the rollers.

2.3 EXPERIMENTAL SETUP

A pilot plant Horomill, a pilot plant Loesche mill, a laboratory roller mill and a batch press were used for the experiments, details of which will be given in the following paragraphs.

2.3.1 BATCH PRESS

The batch press consists of a cylinder with inside dimensions of 150 mm deep by 140 mm inside diameter as shown in figure 2 and a piston with an inside diameter of 138 mm and a height of 200 mm.

The presses were all fitted with load cells and displacement gauges and all the data were recorded. A 24-mV signal was sent to a personal computer where the force and displacement were recorded as an ASCII file. The bed of ore was compressed by controlling the maximum pressure applied.
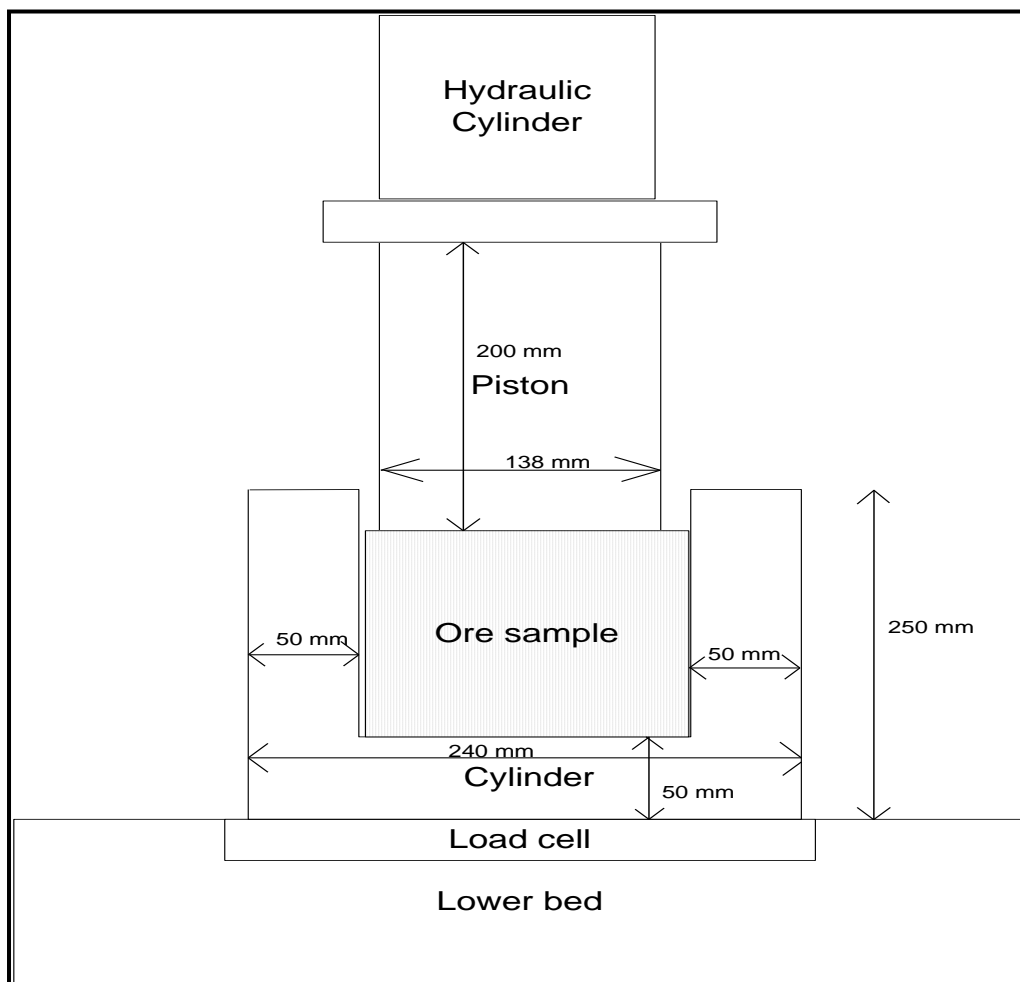
Figure 2: Schematic representation of the batch press.

The tests were done as follows:

- The cylinder was filled with a certain amount of material, approximately 1 kg, and the material pressed to the desired pressure. It was important not to handle the material extensively or vibrate it as this caused segregation.
- The material was removed, screened on a limiting screen, recording the mass of the coarse and fine fractions. Fresh feed was added to the coarse fraction to keep the amount of ore in the cylinder at 1 kg and homogenising by mixing in a bowl with a spatula taking care to prevent segregation of the material.
- The process was repeated until the mass of the fine fraction remained constant. Five to eight repetitions were normally necessary to achieve this.

Typical results obtained are shown in figures 3 to 5. In figure 3 it is shown how the energy was calculated.

Energy consumption was determined using the formula: energy equals force times distance. From a plot of force versus displacement this can be determined as the energy equals the surface area under the graph. This was done by determining the surface areas between discrete data points as shown in figure 6. The rectangular and triangle in the graph indicates the area between two sets of data points. As there are more than a thousand data points, the discrete areas are very small. Using this method will be as accurate and even more than trying to integrate the formula of the graph.

COMPRESSION TESTS WITH FOSKOR ORE
Determining energy consumption by measuring surface area under the graph
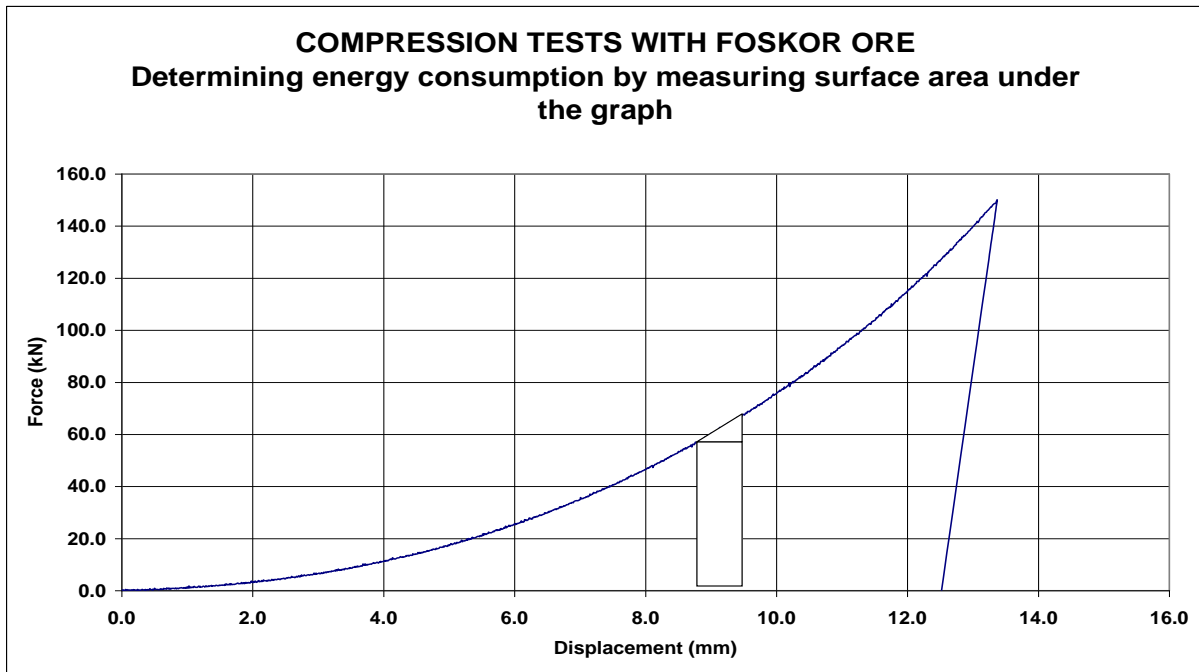
Figure 3: Force-Displacement graph indicating the method with which the energy consumption was determined (Example: Foskor ore).

With regard to figure 3, it is evident that when the pressure is released the bed seems to expand thereby releasing energy. In the mentioned figure this was measured to be 17% of the total energy. Tests done without any material in the bed indicted that the apparatus absorbed 4% of the total energy. The mechanical losses should be deducted when calculating the energy absorbed. The same must also be done for the pilot mills. In the case of the Horomill this was not measured at the time, but that of the Loesche mill varied between 25 and 35 % of the total measured and had to be deducted before any comparisons could be made with the results of the batch press.

The results shown in figures 4, 5 and 6 indicate graphs of successive presses. In figures 4 and 5 there is a pattern. The first time the material is compressed, the displacement is at its largest. After that it decreases until, under ideal conditions, it will reach a minimum and should settle at that minimum as the reduction ratio settles to a minimum. Figure 6 indicates that it will not always be the case and that repeatability could be a problem. One problem with experiments like these, is that mixing of the material is never ideal. Segregation of material always happens during handling, especially a mixture of fine and coarse material. This results in a variation of the bulk density throughout the bed leading to inconsistent results. The aim of the procedure is

17

to reach a stable state where the amount of energy per mass new product should be constant. Another factor that influenced the repeatability is the so called stiffness of the hydraulic system. Hydraulic systems do have inconsistency due to expansion of hydraulic hoses and valves. The presses used in the work with Foskor ore were not designed to be used with ore, but was available at Kumba as part of the steel testing facility. The one used at AARL was designed for the purpose of testing ore. When designing a press of this nature, stiffness must be maximised. If the inconsistency in the graphs is too big the experiments must be repeated, making sure experimental errors are kept to a minimum. The number of presses should also be increased until repeatability is achieved.

Figure 4: Force–displacement graphs obtained in compression tests on Foskor ore at a pressure of 50 kN indicating the graphs of progressing presses. Between presses the minus 300 µm material was removed with a screen.
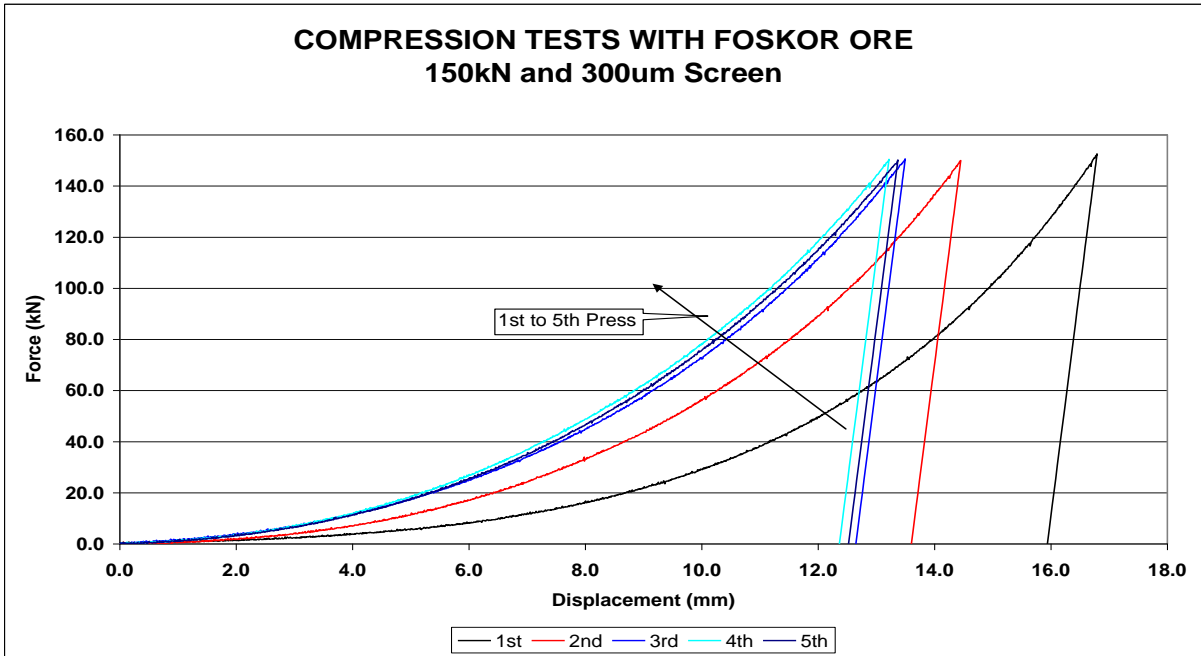
Figure 5: Force–displacement graphs obtained in compression tests on Foskor ore at a pressure of 150 kN indicating the graphs of progressing presses. Between presses the minus 300 µm material was removed with a screen.
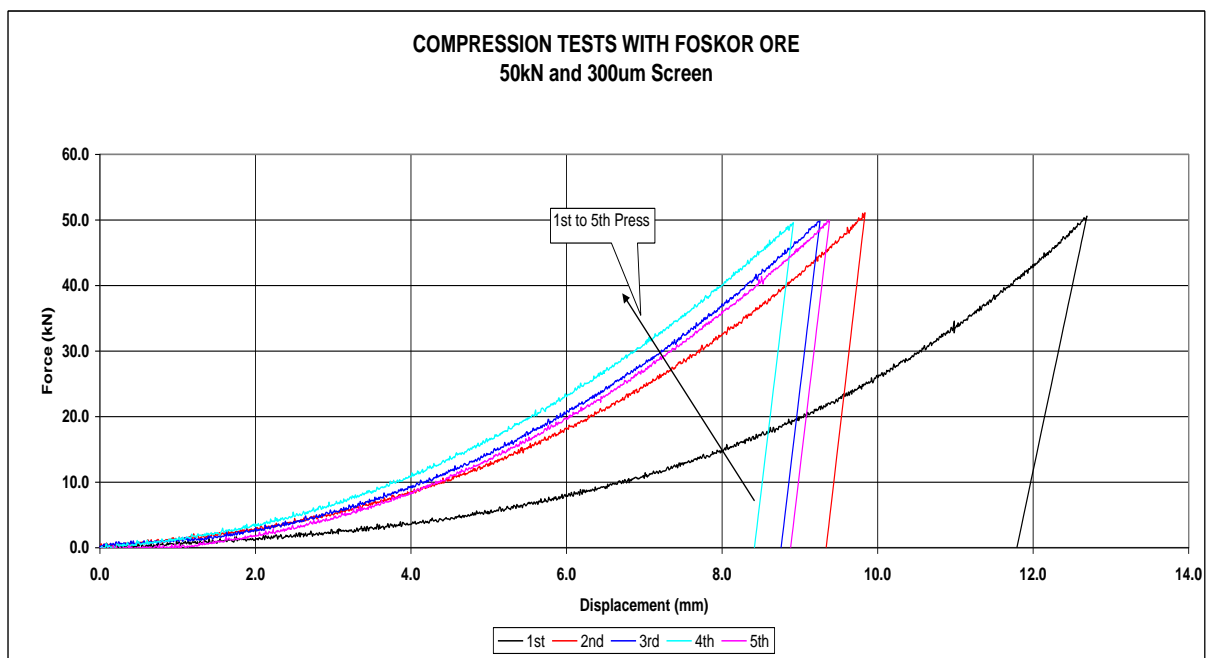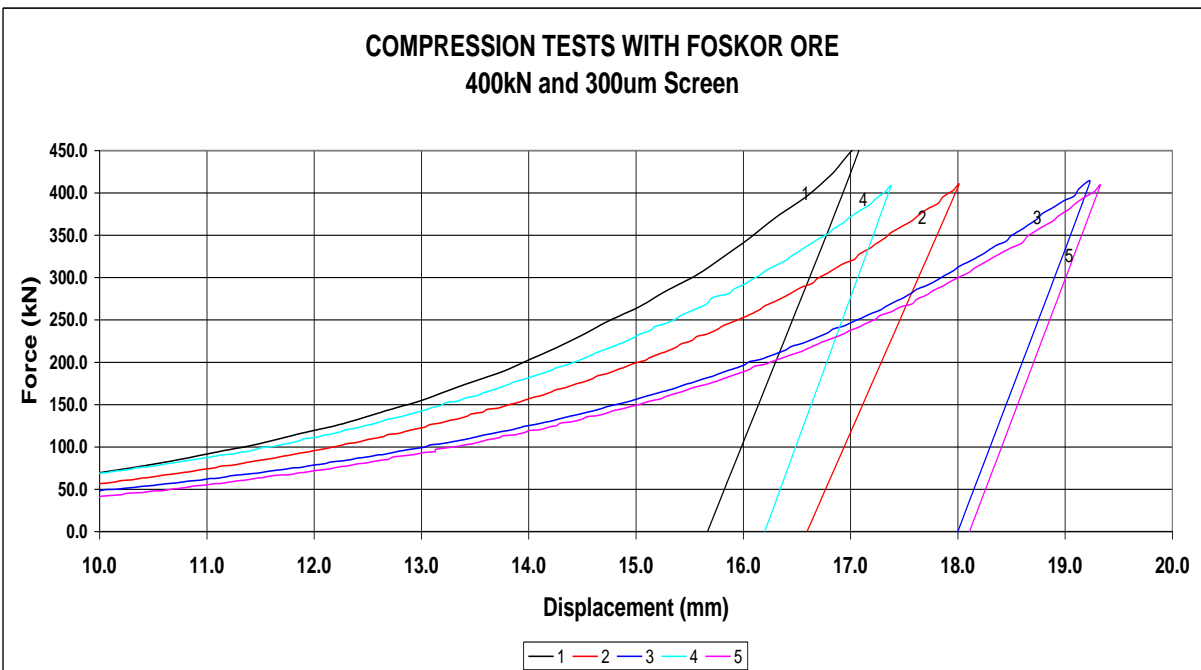

Figure 6: Force–displacement graphs obtained in compression tests on Foskor ore at a pressure of 400 kN indicating the graphs of progressing presses. Between presses the minus 300 µm material was removed with a screen.

19

2.3.2 PILOT HOROMILL

The detail of the test is given in the report by FCB on the project (Evrard and Cordonnier, 1995). The experimental set-up consisted of:

- Five-ton feed hopper.
- Feed conveyor with installed belt scale.
- Horomill.
- Feed conveyor to TSV air classifier.
- Coarse fraction recycle conveyor with installed belt scale.
- Fine fraction pneumatic conveying to a bag house.

The Horomill (see figure 53) used in this study consisted of a shell of 0.8 m diameter by 1 m long. Inside the mill a roller was installed onto which pressure was applied by a set of hydraulic cylinders. The shell was driven by an electric motor and gearbox. Material was fed into the feed end, pressed between the roller and shell and as the bed was compressed to a cake, it was loosened by a set of scrapers inside the mill before being pressed again. This technique enabled the mill to press the material three to five times before exiting the mill. The material was fed to the Horomill at feed rates that varied between 1.97 and 3.71 dry ton per hour at a top size of 30 mm and an 80% mass passing size of 16 mm. Pressures varied between 25 and 30 bar hydraulic pressure that gave approximately 30 MPa pressure on the bed. The latter figure was calculated by the FCB and they did not reveal the way they did it, as it was sensitive information at the time.

2.3.3 PILOT LOESCHE MILL AT AARL

The setup at AARL was as follows for the Rosh Pinah, titanium slag and iron ore tests:

- The mill consisted of two 200 mm diameter rollers applying pressure onto a 320 mm diameter table (see figure 51 and 52)
- The mill was fed from a bin with a conveyor equipped with a scale.

- The product was swept from the table by an air stream and transported through the internal classifier to a cyclone and bag house. The oversize joined the feed on the table.

- The total energy consumption used during each test was measured by a torque converter that was installed on the drive shaft of the mill.

- For the milling of the titanium slag an 850 μm aperture external screen was installed and the oversize was added to the feed.

- Samples were taken of the feed, circulating load and final product at regular intervals.

- The feed rate to the mill varied between 0.22 to 0.34 dry tons per hour for the Rosh Pinah ore and 0.3 tons per hour for the slag.

- Top size of Rosh Pinah ore varied between 10 and 3 mm. That of the slag was 5 mm.

- The top size of the banded iron stone varied between 5 and 3 mm and the feed rate was 0.3 ton per hour.

- The hydraulic pressures applied varied between 115 and 200 Bar. Unfortunately the specific pressure could not be measured due to lack of information by the manufacturer to convert the hydraulic pressure to specific pressure.

2.4 RESULTS AND DISCUSSION

2.4.1 COMPARISON BETWEEN THE ENERGY CONSUMPTION OF THE BATCH AND PILOT MILLS

2.4.1.1 FOSKOR ORE

Figures 7 to 9 illustrate the operating work index and the energy consumption required to crushed Foskor ore from a top size of 30 mm to product sizes smaller than 500 μm in the Horomill and from 10 mm to smaller than 500 μm in the batch press. These graphs indicate operating work index and the energy consumption as a function of product size for 80% mass passing size, 50% mass passing size and 25% mass passing size. In figure 10, the operating work index and energy consumption are shown when milling Foskor ore in a pilot plant ball mill. This was from tests done

at FCB and is taken from Evrard and Cordonnier (1995). The product size in this graph is defined as the 80% mass passing size. The experimental data and the calculated energy consumption are shown to indicate to what extent the calculated energy correlates with the experimental data.

Figure 11 is a plot of reduction ratio as a function of energy consumption for the Horomill and the batch press.

Table1 summarises the results from these tests.

Energy Consumption and Operating Work Index plotted as a function of Product Size P_{80} for Foskor Ore

$E_{Horomill} = 9.5*100^{1.01}(1/P^{1.01}-1/F^{1.01})$

$E_{Batch\ Press} = 5.3*100^{0.24}(1/P^{0.24}-1/F^{0.24})$

Legend:
- Horomill(experimental data)l
- Batch Press(experimental data)
- OWi(Horomill)
- OWi(Batch Press)
- Horomill(calculated energy)
- Batch Press(calculated energy)

Figure 7: Energy consumption and operating work index plotted as a function of the P_{80} obtained with the Horomill and batch press on apatite ore from Foskor.

22

Energy Consumption and Operating Work index plotted as a function of Product Size P_{50} for Foskor Ore

$E_{Horomill} = 7.5*100^{2.3}(1/P^{2.3}-1/F^{2.3})$

$E_{Batch\ Press} = 4.7*100^{0.85}(1/P^{0.85}-1/F^{0.85})$

Legend:
- Horomill(experimental data)
- Batch Press(experimental data)
- OWi(Horomill)
- Horomill(calculated energy)
- Batch Press(calculated energy)
- OWi(Batch Press)

Figure 8: Energy consumption and operating work index plotted as a function of the P_{50} obtained with the Horomill and batch press on apatite ore from Foskor.

Energy Consumption and Operating Work index plotted as a function of Product Size P_{25} for Foskor Ore

$E_{Horomill} = 2.4*100^{0.82}(1/P^{0.82}-1/F^{0.82})$

$E_{Batch\ Press} = 3.74*100^{0.68}(1/P^{0.68}-1/F^{0.68})$

Legend:
- Horomill(experimental data)
- Batch Press(experimental data)
- OWi(Horomill)
- Horomill(calculated energy)
- Batch Press(calculated energy)
- OWi(Batch Press)

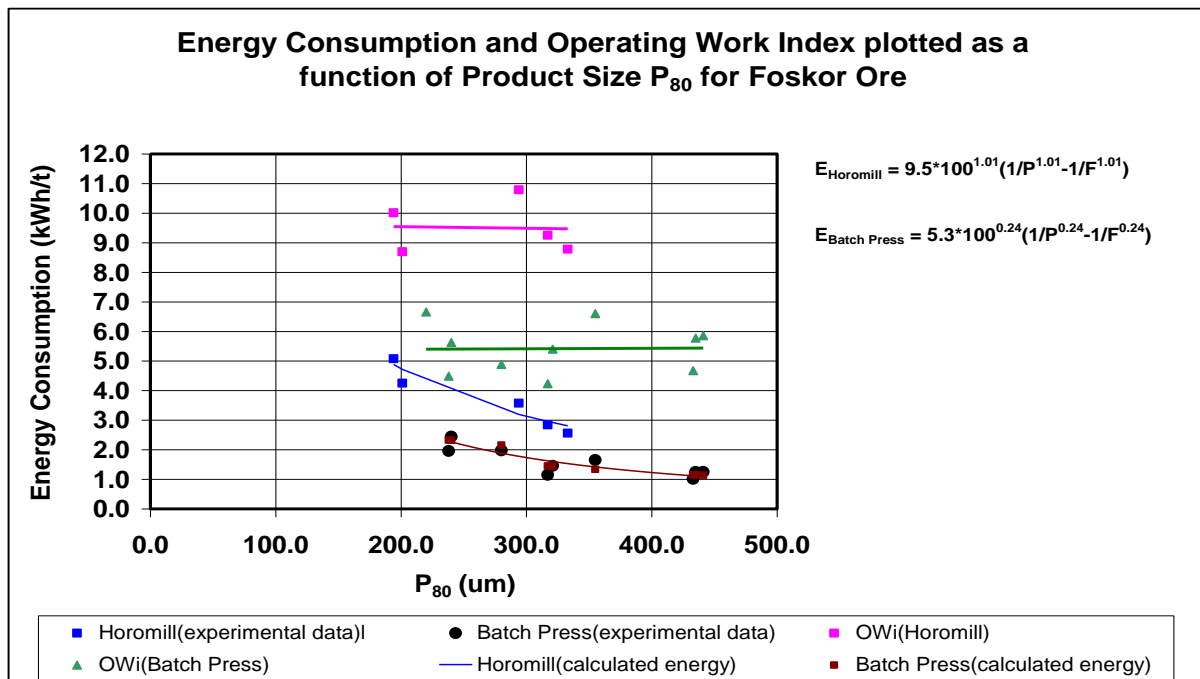Figure 9: Energy consumption and operating work index plotted as a function of the P_{25} obtained with the Horomill and batch press on apatite ore from Foskor.

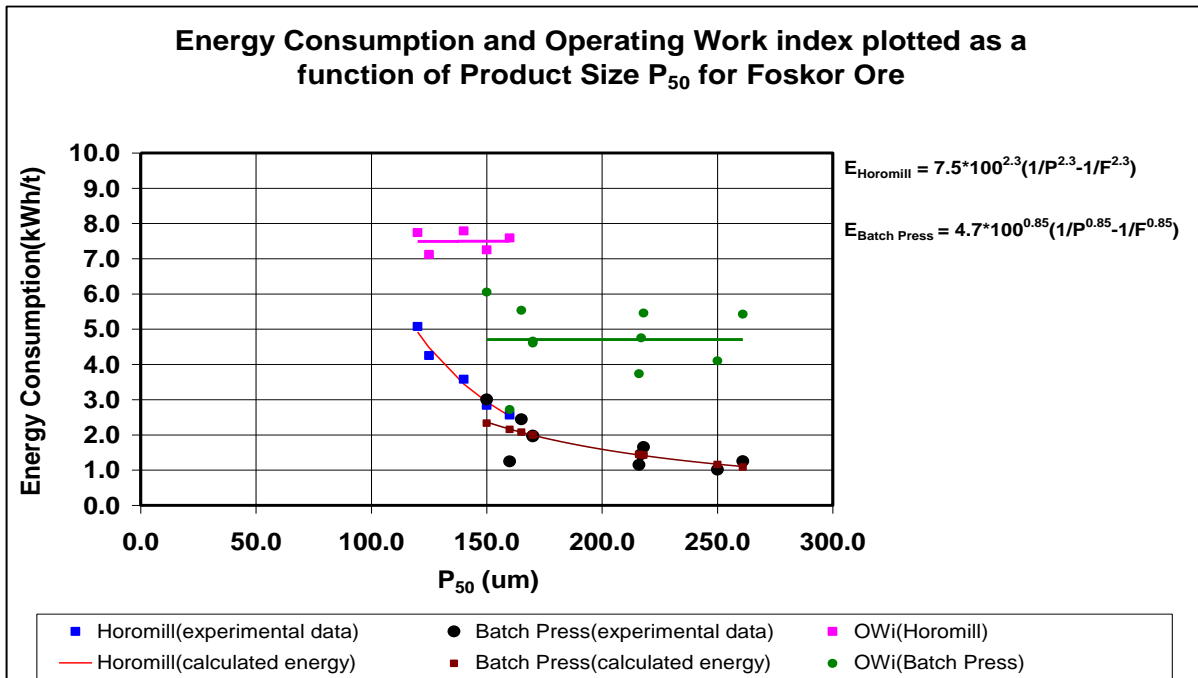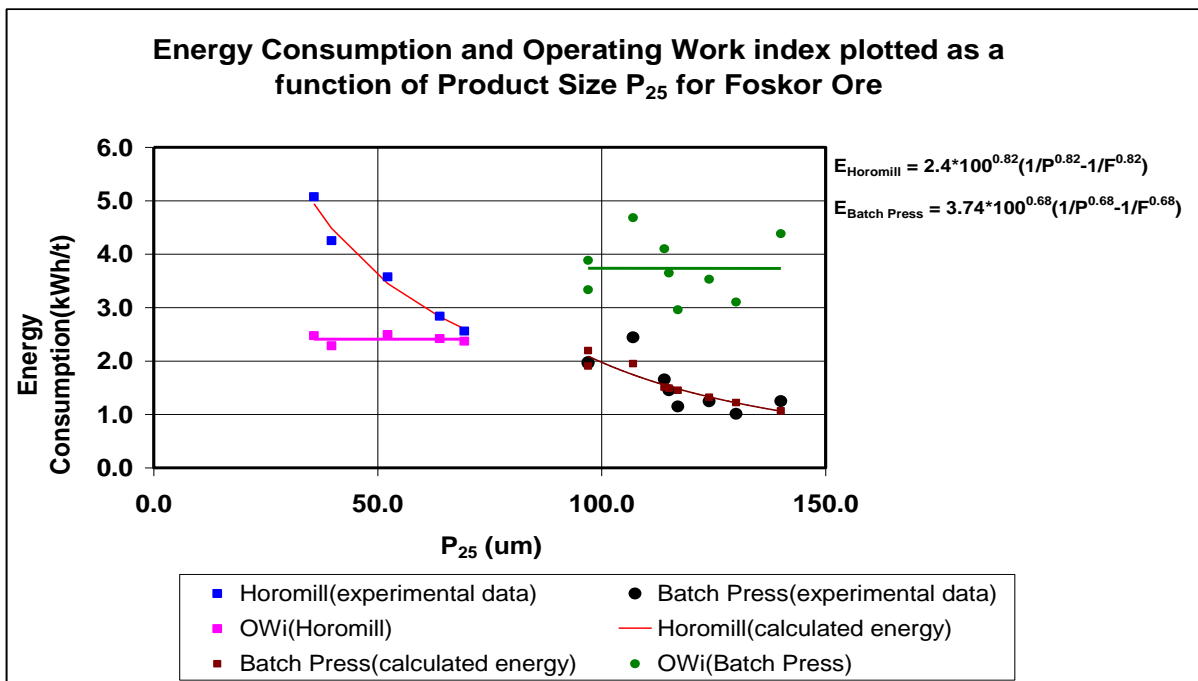23
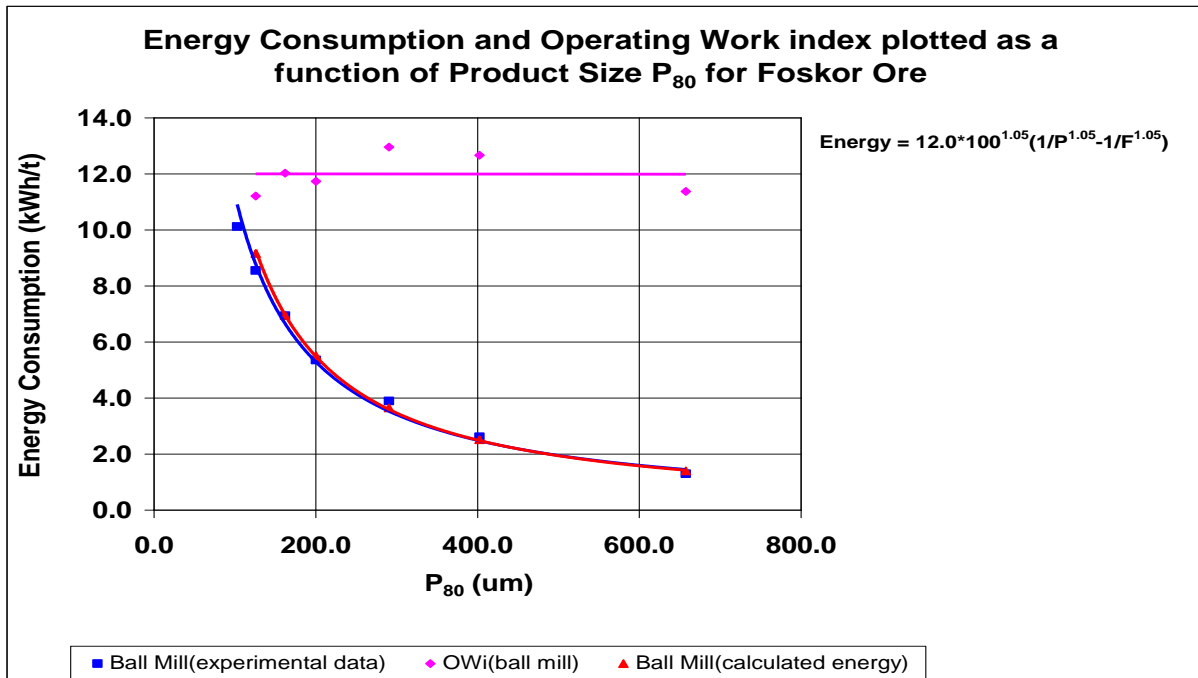
Figure 10: Plot of energy consumption and operating work index plotted as a function of product size and for Foskor ore in a pilot ball mill.
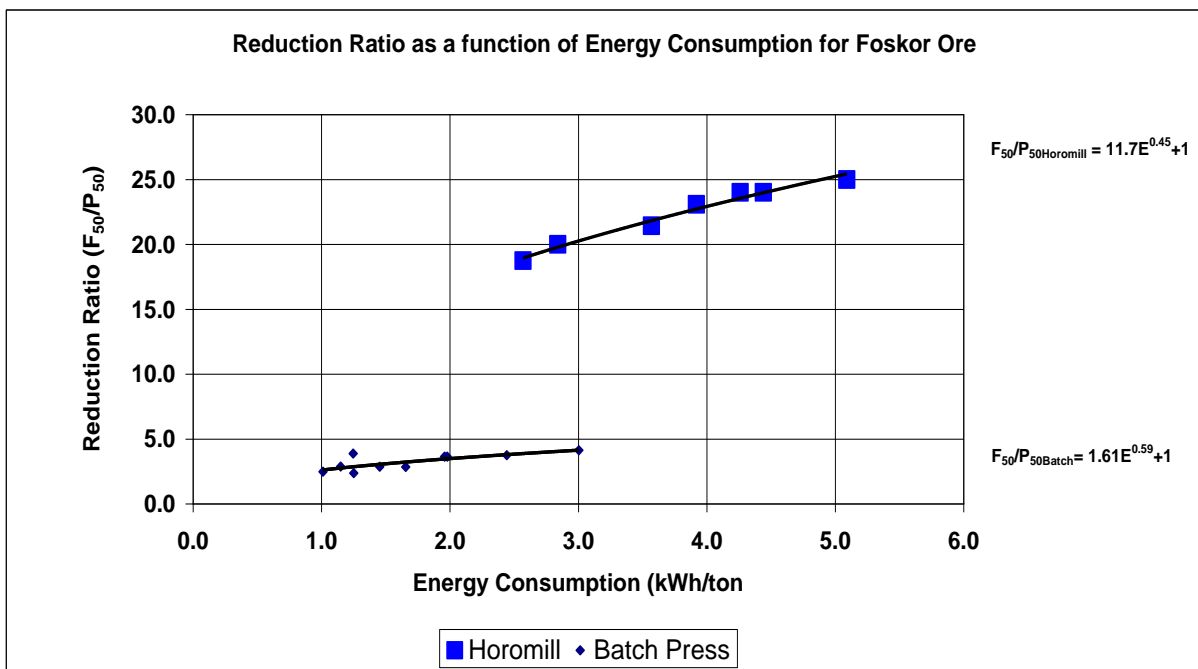
Figure 11: Relationship between reduction ratio and energy consumption for Foskor ore.

24

Table 1: Values of operating work indices and coefficient n for Foskor ore as well as the constants needed to describe the reduction ratio versus energy relationship.

Values of OWi and n for the Loesche mill, batch press and ball mill								
Horomill								
F_{80} (µm)	F_{50} (µm)	F_{25} (µm)	P_{80} (µm)		P_{50} (µm)		P_{25} (µm)	
			OWi	N	OWi	n	OWi	n
15300	3000	493	9.51	1.05	7.5	2.31	2.01	0.82
Batch press								
F_{80} (µm)	F_{50} (µm)	F_{25} (µm)	P_{80} (µm)		P_{50} (µm)		P_{25} (µm)	
			OWi	N	OWi	n	OWi	n
2008	620	270	5.33	0.24	4.7	0.85	3.74	0.68
Ball Mill								
Owi				n				
12				1.05				
Values describing the reduction ratio vs. energy relationship								
Horomill				Batch press				
F_{50} (µm)	a		n	F_{50} (µm)	a		n	
3000	11.7		0.45	620	1.62		0.59	

Comparison with the Bond/Rittinger formula and the suggested prediction of Kapur et al (1990), and Daniel (2001)

The first question to be answered, is to what extent the results compare with the formulas suggested by Bond and Rittinger. Bond postulated that energy is a function of $1/P^n$ where n equals 0.5 and Rittinger suggested that n equals 1. The results actually show the following:

- From figure 7 and table 1 in the case of 80% mass passing size of the product the value of n for the Horomill is 1.01 and for the batch press 0.24. From figure 8 and table 1 for the 50% mass passing size it is 2.31 and 0.85 respectively and for 25% mass passing size in figure 9 and table 1 these values are 0.82 and 0.68. No trends can be derived from these data.

- From figure 10, the results from the pilot plant ball mill show that the value of n equals 1.05. So even for a pilot ball mill this value differs from what Bond postulated.

- The operating work indices for 80% mass passing size are 9.51 kWh/ton for the Horomill and 5.33 kWh/ton for the batch press. For 50% mass passing size these are 7.50 kWh/ton and 4.7 kWh/ton and for 25% mass passing size, 2.41 kWh/ton and 3.74 kWh/ton.

Kapur et al (1990), as well as Daniel (2001), suggested that the reduction ratio for roller mills can be described as a function of (energy)^n where n equals 1. The value of n for the Horomill is 0.45 and 0.59 for the batch press. This can be seen in figure 11. The value of n for the Horomill is not near the suggested value of 1.0. If the reduction ratio-energy relationship is to be used, the batch press can not predict this relationship for the Horomill.

Comparison between Horomill and batch press.

- Figure 7 indicates that the operating work index for the Horomill is 9.51 kWh/ton and 5.33 kWh/ton for the batch press. The values of the coefficient are 1.01 versus 0.24. If there was a constant relationship between the work indices obtained from the Horomill and batch press, this could be used as a scale-up factor. The problem however, is the values of the coefficients are too far apart and therefore, in this case, the results from the batch press cannot be used to simulate the Horomill.

- In the case of the 50% mass passing size from figure 8 the work indices are 7.5 kWh/ton for the Horomill and 4.7 kWh/ton for the batch press. For the Horomill the values of the coefficient equals 2.31 and for the batch press 0.85. Again, the differences are too large for the batch press to be used as a simulator.

- Figure 9 shows that when using the 25% mass passing size the energy consumption of the batch press and the Horomill differ too. The operating work indices are 2.01 kWh/ton for the Horomill and 3.74 kWh/ton for the batch press. For the Horomill the values of the coefficient n equals 0.82 and for the batch press 0.68. One word of caution about using the 25% mass passing size or smaller, in many cases this particle size is smaller than 38 μm and screening below this size is not practical and inaccurate.

2.4.1.2   ROSH PINAH ORE

Figures 12 to 15 indicate the relationship between product size and energy consumption for the Loesche pilot mill and the batch press. This is done for 80% and 50% mass passing sizes. No 25% mass passing sizes was used as this was less than 10 μm. Figure 16 indicates the energy consumption of the mill and the operating work indices for the ball mill at Rosh Pinah. Only the trend line for the energy consumption is shown to keep the graph readable. This information is from data gathered by the author during a study done on this mill in 2002. This graph was added to emphasize that even with ball mills Bond's law does not always apply. Figures 17 to 18 indicate the relationship between reduction ratio and energy consumption to compare the data with the prediction of Kapur et al (1990), and Daniel (2001). In table 2 the values of OWi and n are shown.

Operating Work Index plotted as a function of Product Size P$_{80}$ for Rosh Pinah Ore

Legend:
- LM 3 mm top size
- LM 5 mm top size
- LM 10mm top size
- BP 3 mm top size
- BP 5 mm top size
- BP 10 mm top size

Figure 12: Operating work index plotted as a function of P$_{80}$ passing size for the product of the pilot Loesche mill and batch press on Rosh Pinah ore.

Energy Consumption plotted as a function of Product Size P$_{80}$ for Rosh Pinah Ore

$$E_{LM3mm} = 6.68*100^{1.10}(1/P^{1.10}-1/F^{1.10})$$
$$E_{LM5mm} = 7.68*100^{1.22}(1/P^{1.22}-1/F^{1.22})$$
$$E_{LM10mm} = 9.89*100^{1.36}(1/P^{1.36}-1/F^{1.36})$$

$$E_{BP3mm} = 2.67*100^{0.77}(1/P^{0.77}-1/F^{0.77})$$
$$E_{BP5mm} = 3.04*100^{0.65}(1/P^{0.65}-1/F^{0.65})$$
$$E_{BP10mm} = 3.04*100^{0.68}(1/P^{0.68}-1/F^{0.68})$$

Legend:
- LM 3 mm top size
- LM 5 mm top size
- LM 10 mm top size
- LM 3 mm top size(calculated energy)
- LM 5 mm top size(calculated energy)
- LM 10 mm top size(calculated energy)
- BP 3 mm top size
- BP 5 mm top size
- BP10 mm top size
- BP 3 mm top size(calculated energy)
- BP 5 mm top size(calculated energy)
- BP 10 mm top size(calculated energy)

Figure 13: Energy consumption as a function of the P$_{80}$ obtained with the pilot Loesche mill on Rosh Pinah ore.
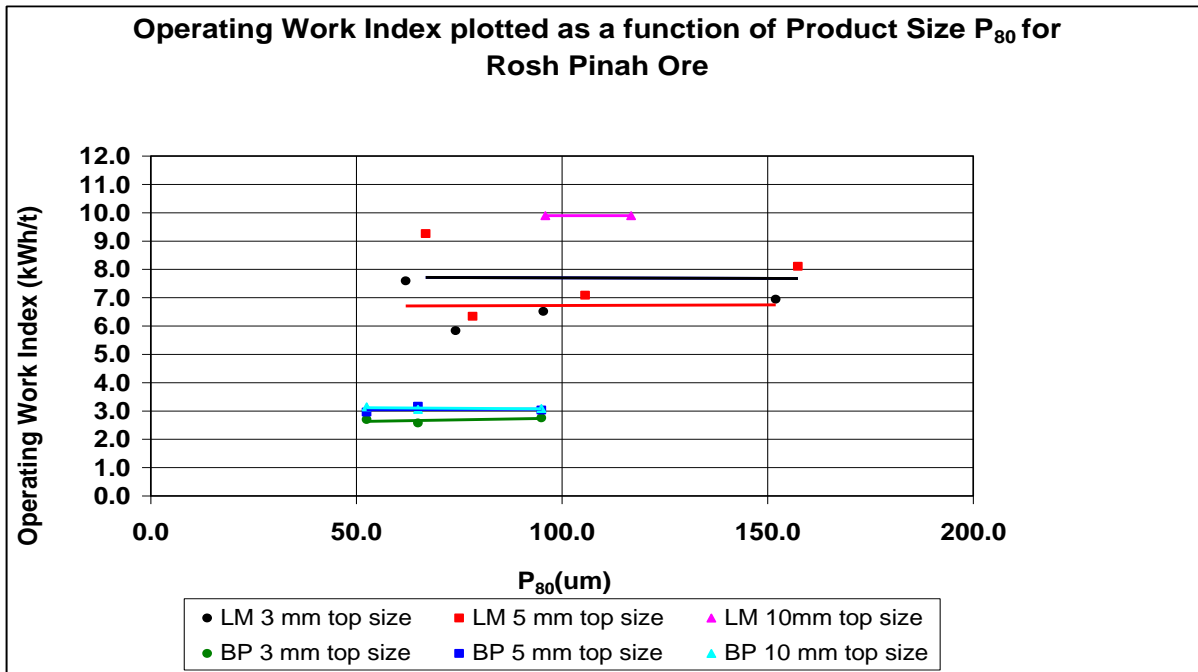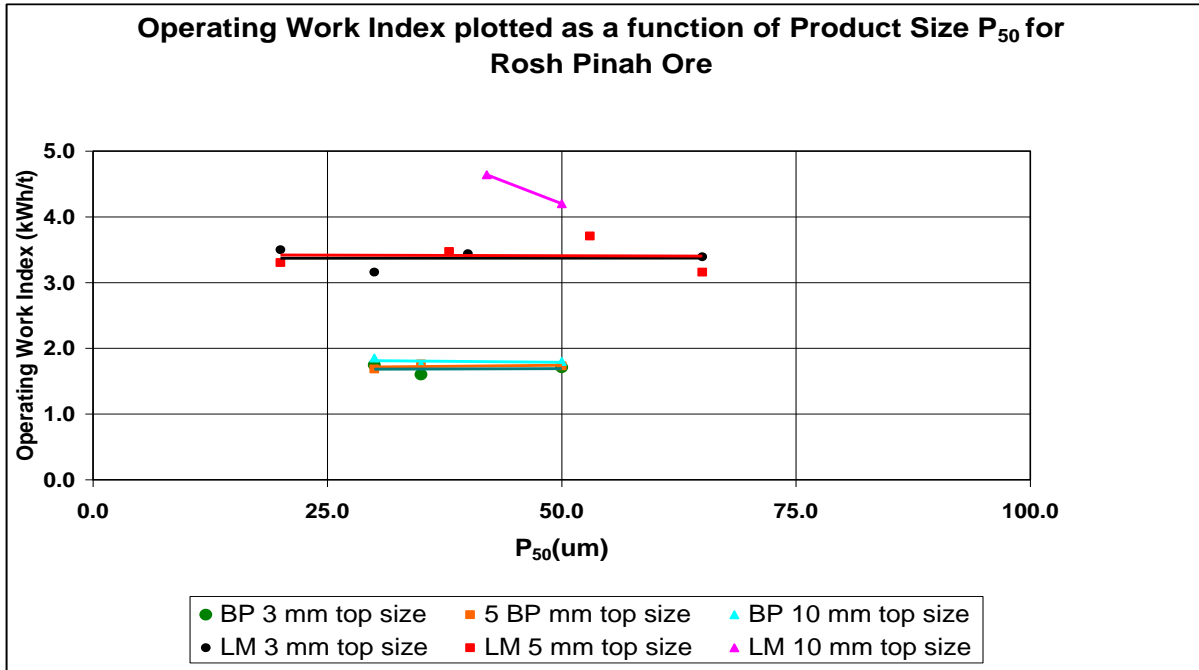
Figure 14: Operating work index plotted as a function of P_{50} passing size for the product of the pilot Loesche mill and batch press on Rosh Pinah ore.
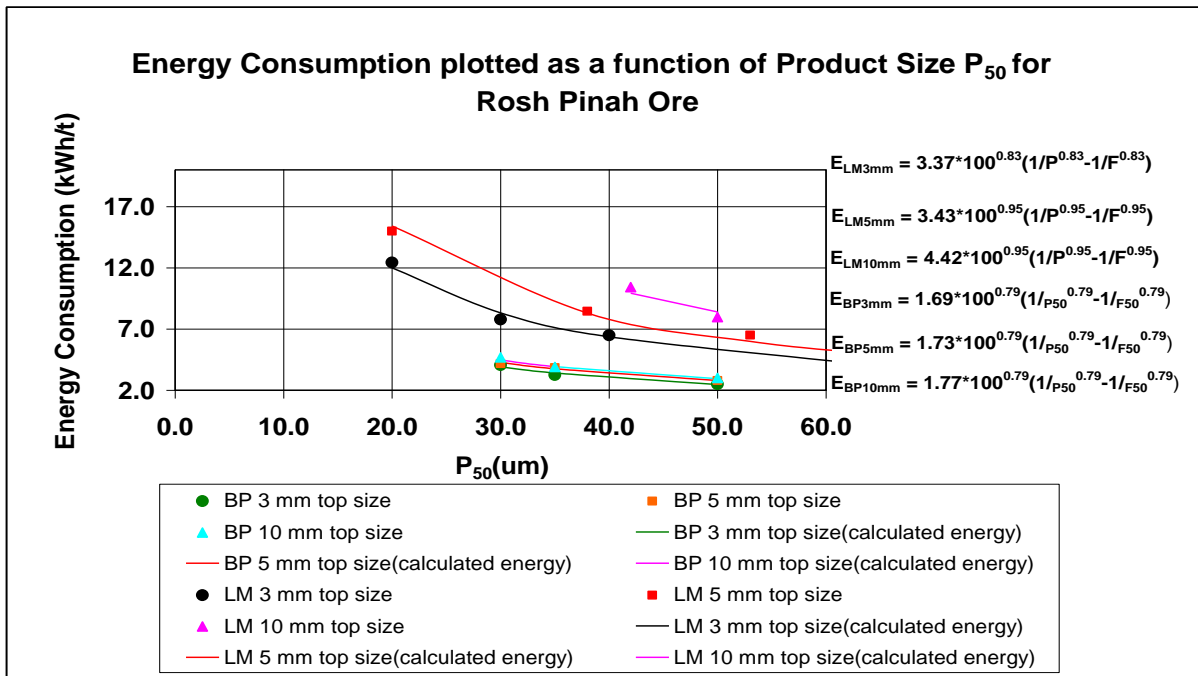
Figure 15: Energy consumption as a function of the P_{50} obtained with the pilot Loesche mill on Rosh Pinah ore.

Figure 16: Energy consumption and operating work indices plotted as a function of P_{80} passing size for the product of the Rosh Pinah ball mill. The latter is for two different size ranges
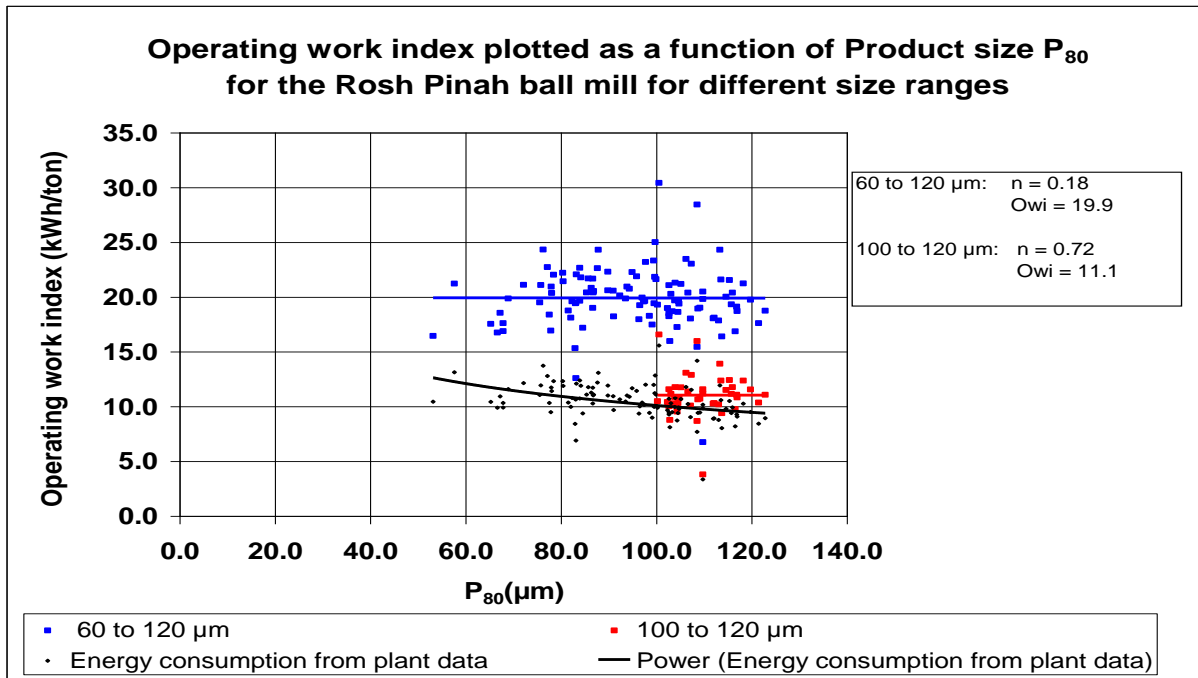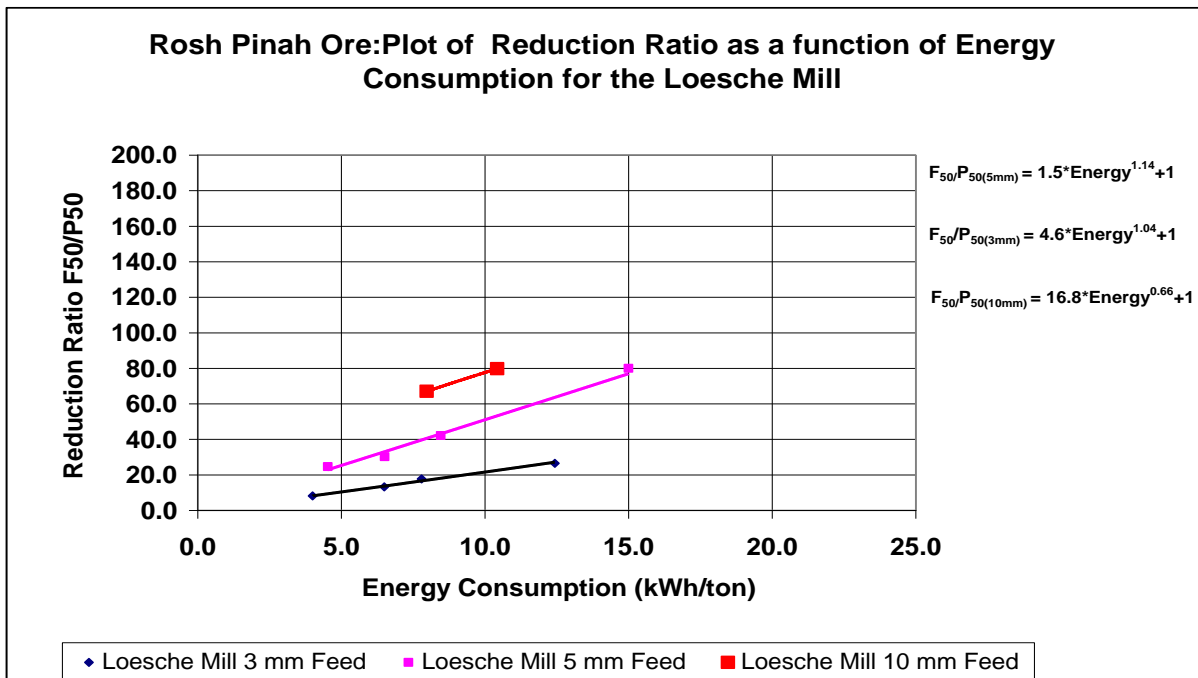

Figure 17: Plot of reduction ratio and energy consumption to indicate the values of the constants a and n in the formula $F_{50}/P_{50} = a*E^n+1$. The plot is for the Loesche pilot mill

Rosh Pinah Ore:Plot of Reduction Ratio as a function of Energy Consumption for the Batch Press

$F_{50}/P_{50(3mm)} = 3.4*Energy^{1.15}+1$

$F_{50}/P_{50(5mm)} = 8.3*Energy^{1.27}+1$

$F_{50}/P_{50(10mm)} = 19.6*Energy^{1.15}+1$

Y-axis: Reduction Ratio F50/P50 (0.0 to 140.0)

X-axis: Energy Consumption (kWh/ton) (0.0 to 5.0)

Legend: ◆ Batch press 3 mm Feed   ■ Batch press 5 mm Feed   ■ Batch press 10 mm Feed
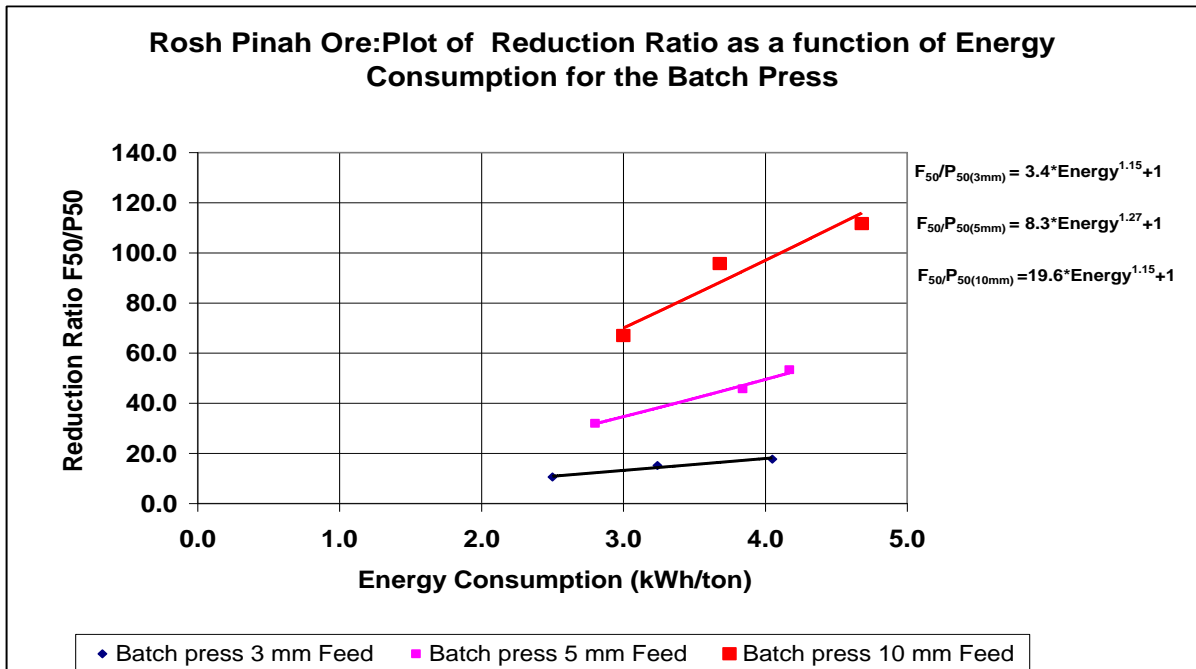
Figure 18: Plot of reduction ratio and energy consumption to indicate the values of the constants a and n in the formula $F_{50}/P_{50} = a*E^{n}+1$. This is for the pilot batch press.

Table 2: Values of operating work indices and coefficient n for the Loesche mill and batch press on Rosh Pinah ore.

Values of OWi and n for the Loesche mill and batch press													
Top size	Loesche mill						Batch press						
	$F_{80}(\mu m)$	$F_{50}(\mu m)$	P_{80}		P_{50}		$F_{80}(\mu m)$	$F_{50}(\mu m)$	P_{80}		P_{50}	
			OWi	n	OWi	n			OWi	n	OWi	n
3 mm	1500	530	6.68	1.10	3.33	0.83	1500	530	2.67	0.77	1.69	0.79
5 mm	3000	1600	7.18	1.22	3.43	0.95	3000	1600	3.04	0.65	1.73	0.80
10 mm	5800	3350	9.89	1.36	4.42	0.95	5800	3350	3.04	0.68	1.71	0.79

Comparison with the Bond/Rittinger formula and the suggested prediction of Kapur et al (1990), and Daniel (2001)

- The values of n for the Loesche mill, (80 % mass passing size), are quite different from that predicted by Bond and even higher than that predicted by Rittinger. The

values of n for the batch press are almost identical for the 80% and 50% mass passing size and is also different from that predicted by Bond and Rittinger

- When studying figures 12 to 14 it is clear that the values of OWi, although scattered, are constant for the range of product sizes in which the tests were conducted. As with Foskor ore, this leads to the conclusion that the formula $E = OWi(100^n)(1/P^n-1/F^n)$, is a valid description of the energy, product size and feed size relationship.

- Figure 16 is the calculated operating work index for the ball mill at Rosh Pinah. Two graphs are shown, for all the product sizes, 80% mass passing size of 60 to 120 µm and for the range 100 to 120 µm 80% mass passing product sizes. The operating work index for the total range of data is 19.9 kWh/ton and the value of the coefficient is 0.18. The values for only the 100 to 120 µm are 11.2 kWh/ton and 0.78. The latter operating work index is a good figure as the energy to crush the material at the plant from 80 % mass passing sizes of 80000 µm to 5460 µm is 1.7 kWh/ton. If this is added to the energy required by the ball mill to mill the ore to a P_{80} of 100 µm, 10.0 kWh/ton, from figure 16, a work index of 11.7 kWh/ton is expected. However, the value of 0.72 for the coefficient is quite different from what is expected from a Bond prediction.

- The values of the constants a and n in the model of Kapur et al (1990), and Daniel (2001), are shown in table 3.

Table 3: Values of the constants a and n in the formula describing reduction ratio as a function of energy.

Values of a and n in the formula $F_{50}/P_{50} = a*E^n+1$				
Top Size	Loesche mill		Batch press	
	a	n	A	n
3 mm	1.5	1.14	3.4	1.15
5 mm	4.6	1.04	8.3	1.27
10 mm	16.8	0.55	19.6	1.15

These results indicate that the value of n for both the Loesche mill and batch press are similar except for the 10 mm top size and not too far from the suggested value of 1. The value of a differs with top size and between the Loesche pilot mill and batch

press. If the model suggested by Kapur et al (1990), and Daniel (2001), for roller crushers is valid, the value of the constant a should be constant. This suggests that their proposal do not apply for the medium pressure roller crushers.

Comparison between the Loesche mill and the batch press.

In figures 12 to 15 the Loesche pilot mill is compared with the batch press. From these figures and table 2 for 80% mass passing it can be seen that the operating work index as well as the value of the coefficient of the batch press is much lower than that of the Loesche mill. The difference between the operating work indices for the 50% mass passing size is still high although the values of the coefficient for the Loesche mill and batch press are almost the same. The value of the operating work index as a function of top size is plotted in figure 19. From this graph the operating work index decreases with decreasing top size. This does give weight to the model by Daniel (2001), that there are two phases of breakage, the first when material is being nipped into the gap and the second when material is being crushed in the packed bed. The first phase from all these results is the less efficient phase. Roller presses are low pressure crushers with no packed bed crushing. To confirm that the operating work index of a roller crusher is high, Rosh Pinah material was crushed in a roller press. Using equation 6 and the value of the coefficient to be between 1.1 and 1.36, the same as with the Loesche mill tests, the values of the operating work indices in table 4 varied between 109.3 and 28.7 for a value of 1.1 for the coefficient and 354.9 to 52.6 for a coefficient of 1.36.

Table 4: Values of the operating work index for a roller crusher and Rosh Pinah ore.

F_{80} (μm)	P_{80} (μm)	Energy consumption (kWh/ton)	OWi: n = 1.1	OWi: n = 1.36
11400	6900	0.44	109.3	281.7
6900	2600	3.104	169.8	354.9
2600	2100	0.211	28.7	52.6

The reason why the first phase is inefficient has to do with the fact that while nipping of the material, slippage occurs and the selection function of material is low. In the packed bed the latter is high since, in theory, all particles have the same opportunity to be selected. The gap size between the rollers varied between 2 to 3 mm. If, from figures 19 and 20, the operating work index of the Loesche mill would decrease, at this gap size, to a value equal to that of the batch press, it could be said that the batch press does simulate the Loesche mill. This is not the case. The same argument applies for the value of the coefficient as indicated also in figures 19 and 20.
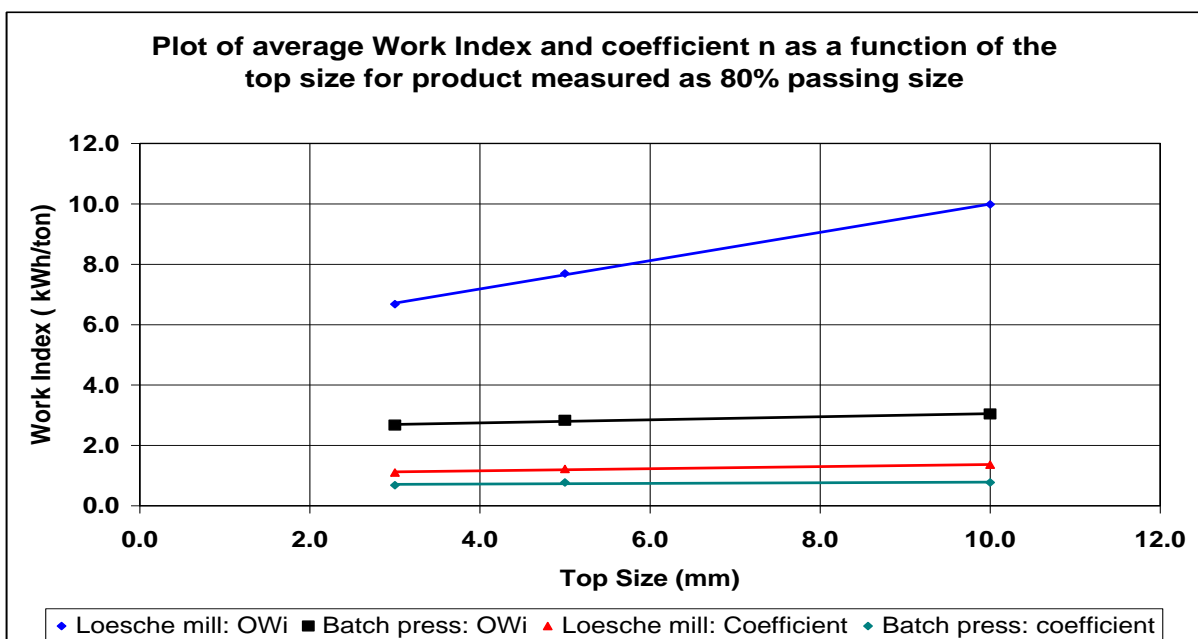
Figure 19: Operating work index and coefficient plotted as a function of top size to compare the pilot Loesche mill with the batch press on ore from Rosh Pinah. This is for 80% mass passing size.
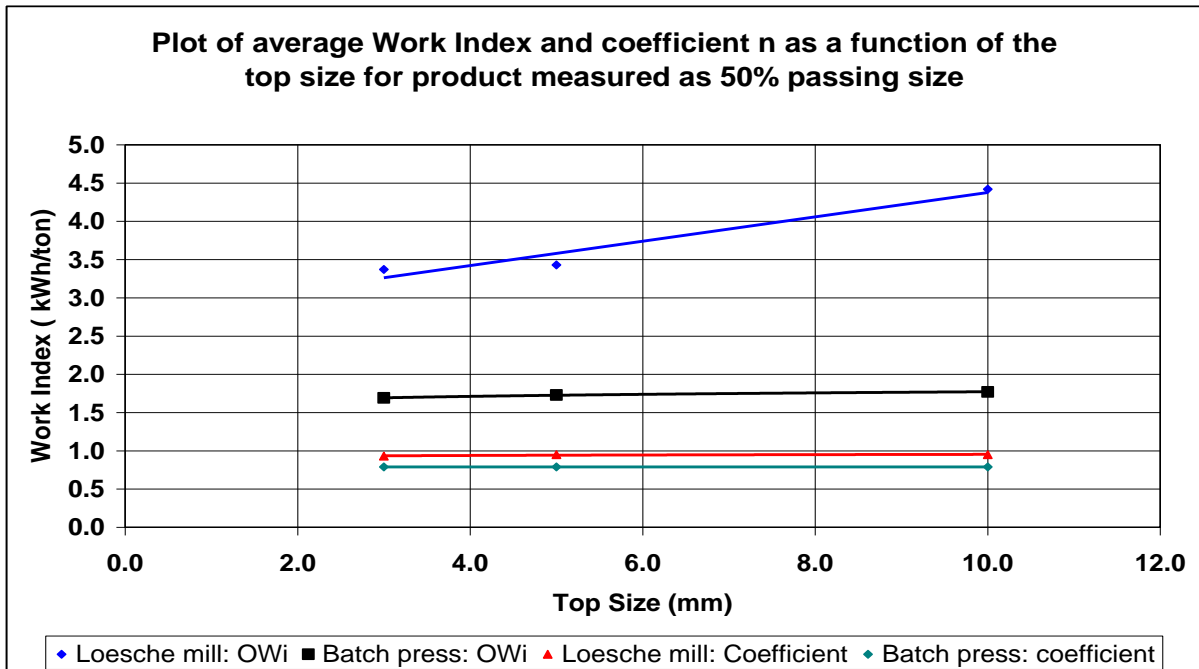
Figure 20: Operating work index and coefficient plotted as a function of top size to compare the pilot Loesche mill with the batch press on ore from Rosh Pinah. This is for 50% mass passing size.

2.4.1.3   TITANIUM SLAG

In figures 21 and 23 the operating work indices for the 80% and 50% mass passing sizes are shown. Figures 22 and 24 indicate the energy consumption of the Loesche mill compared with that of the batch press. This is for 80% and 50% mass passing size respectively. Figure 25 is the plot of reduction ratio as a function of energy consumption.

35

Operating Work Index plotted as a Function of Product Size P_{80} for Titanium slag

Operating Work Index (kWh/t)

45.00
40.00
35.00
30.00
25.00
20.00
15.00
10.00
5.00
-

0.0 100.0 200.0 300.0 400.0 500.0 600.0 700.0 800.0 900.0

P_{80}(µm)

■ Loesche Mill   ▲ Batch press

Figure 21: Operating work index as a function of 80% mass passing size for the batch press and the Loesche mill on titanium slag.

Energy Consumption plotted as a function of Product Size P_{80} for Titanium slag

Energy Consumption(kWh/t)

7.0
6.0
5.0
4.0
3.0
2.0
1.0
0.0

0.0 100.0 200.0 300.0 400.0 500.0 600.0 700.0 800.0 900.0

P_{80}(µm)

$E_{Loesche\ Mill} = 35*100^{0.9}*(1/P_{80}^{0.9}-1/F_{80}^{0.9})$

$E_{Batch\ press} = 3.6*100^{0.5}*(1/P_{80}^{0.5}-1/F_{80}^{0.5})$

■ Loesche Mill   ▲ Batch press
— Loesche Mill(calculated energy)   — Batch press(calculated energy)

Figure 22: Energy consumption as a function of 80% mass passing size for the batch press and the Loesche mill on titanium slag.
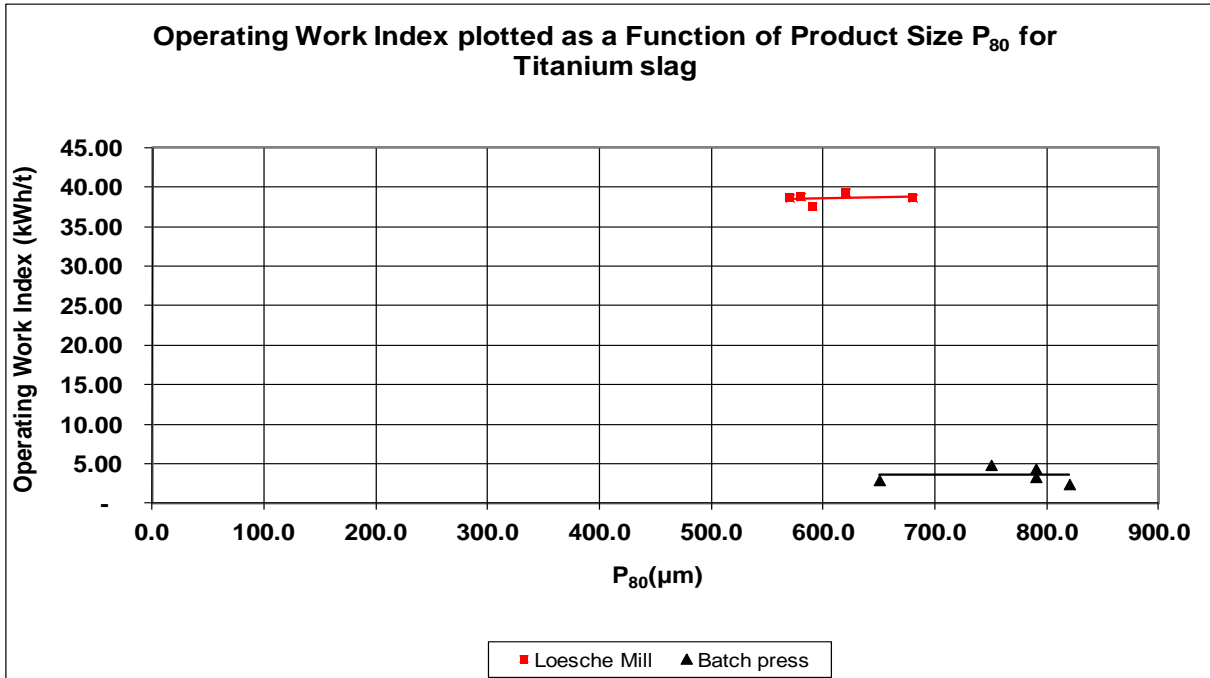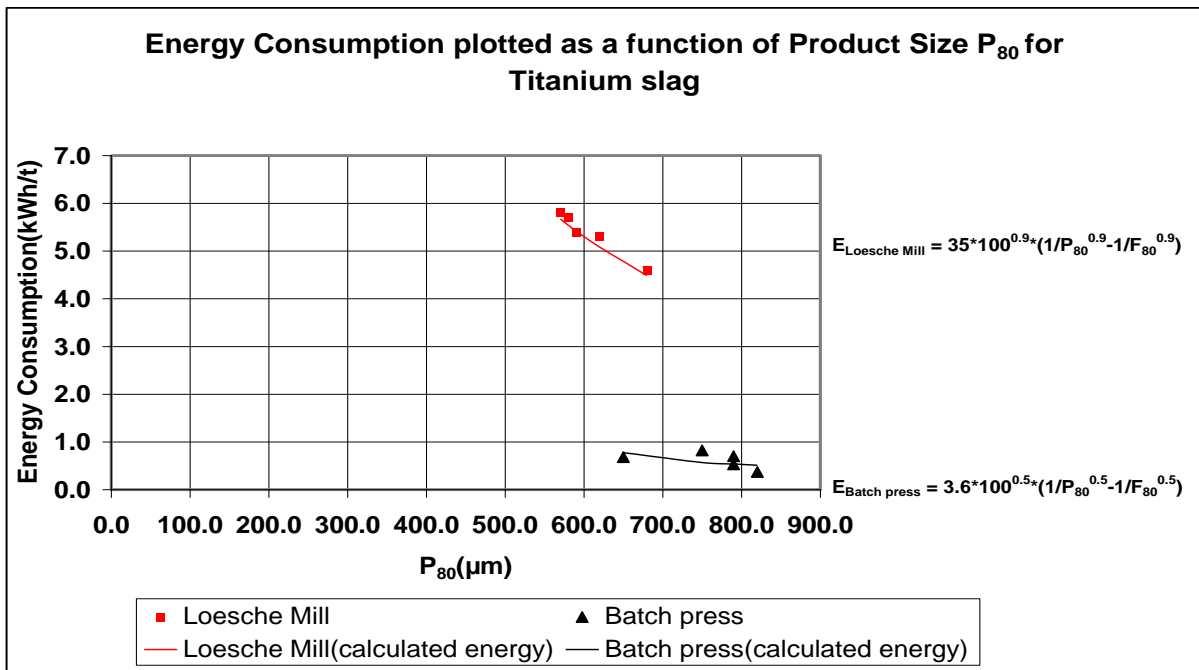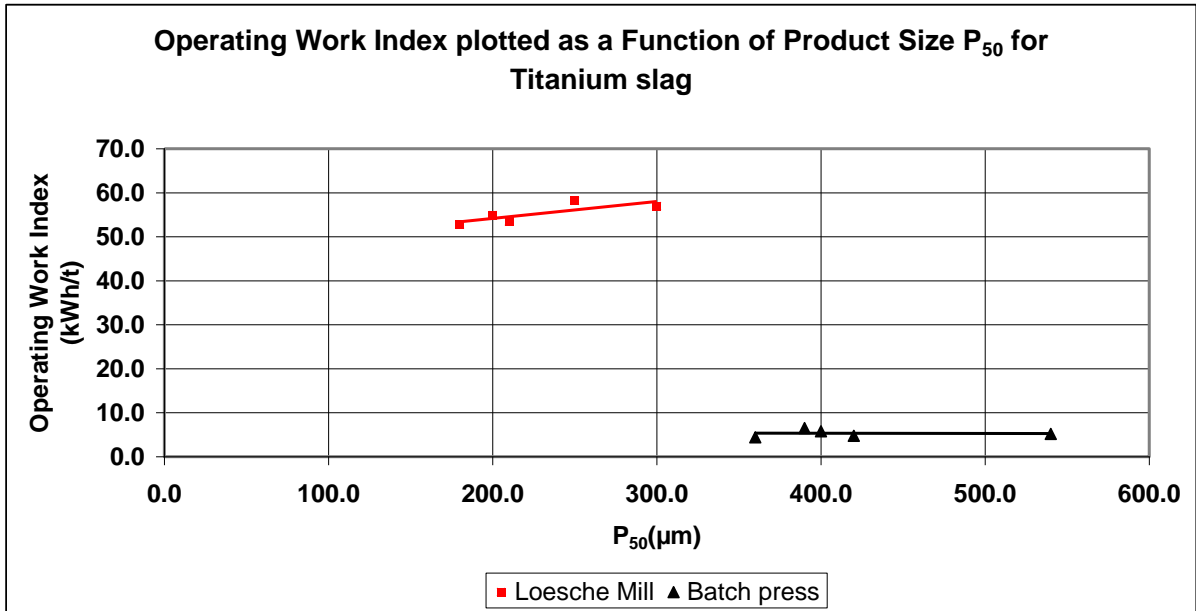
36

Figure 23: Operating work index as a function of 50% mass passing size for the batch press and the Loesche mill on titanium slag.
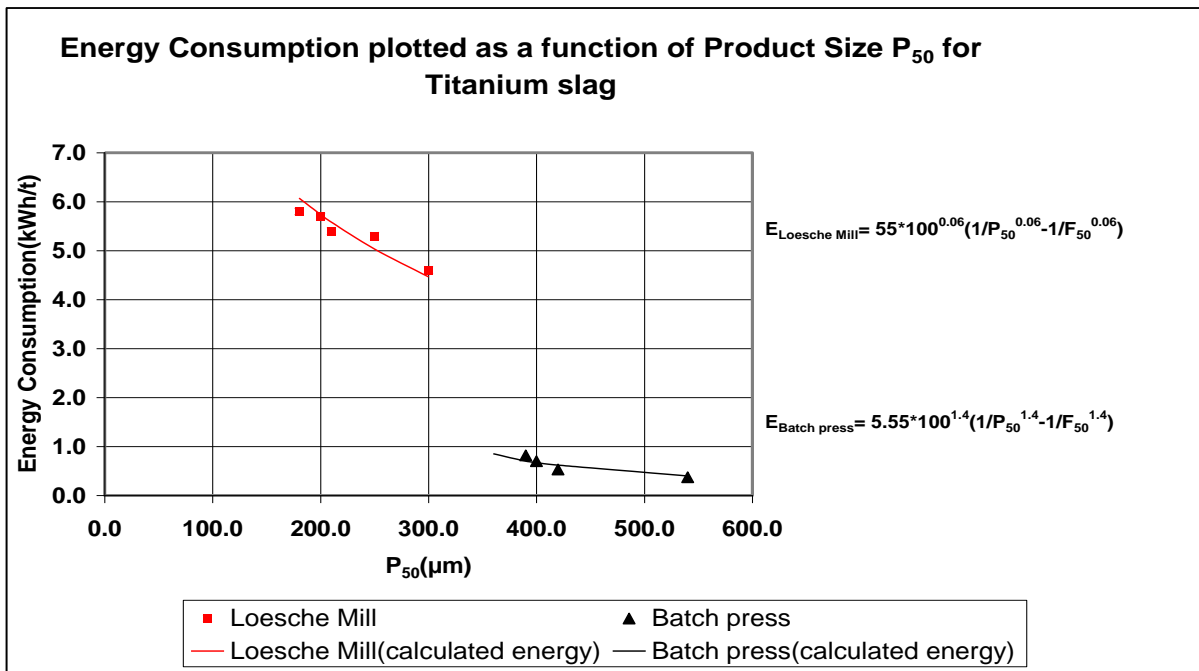

Figure 24: Energy consumption as a function of 50% mass passing size for the batch press and the Loesche mill on titanium slag.

Plot of Reduction Ratio to Energy Consumption for Titanium slag

$F_{50}/P_{50LM} = 0.73E^{1.75}+1$

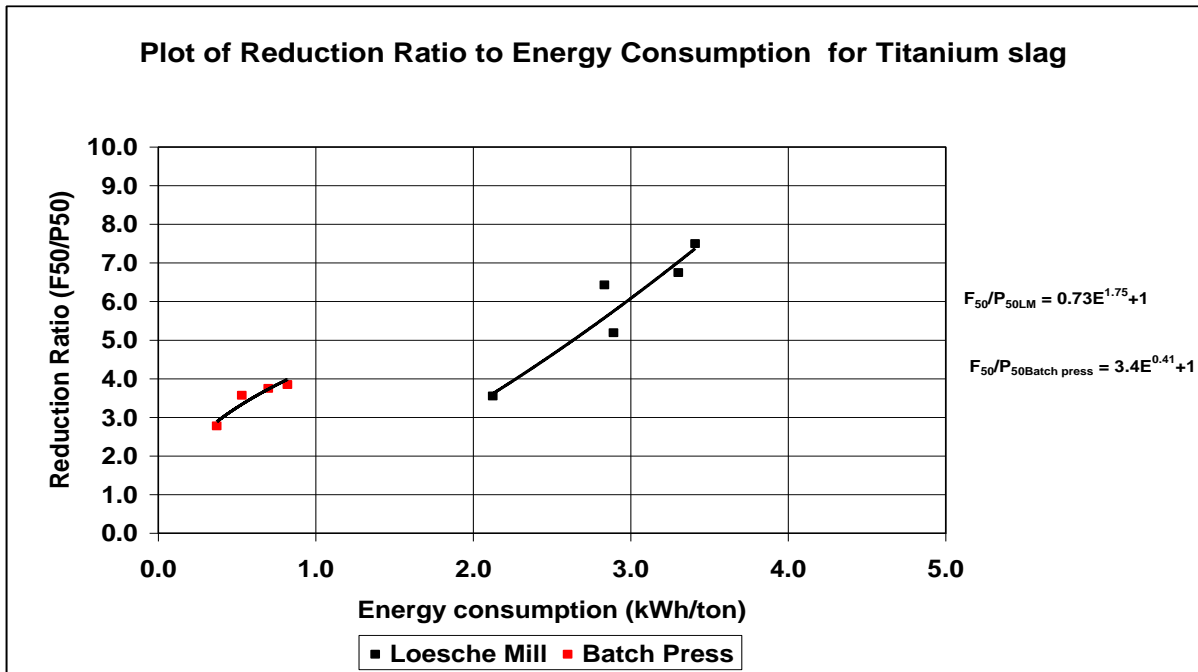$F_{50}/P_{50Batch\ press} = 3.4E^{0.41}+1$

Figure 25: Plot of reduction ratio to energy consumption for titanium slag using 50% mass passing size as the product size.

The following comments can be made from the results:

- In figure 21 it can be seen that the operating work index is a constant for both the Loesche mill and the batch press. However, in figure 23 the operating work index is not constant for the Loesche mill. This is the best fit that could be obtained. The value of the coefficient from figure 24 in this case is 0.06, an extremely low value. If the value of the operating index were to be more constant, the value of the coefficient must be even lower. For comparison with the batch press it is not important how much lower this value is, as it is already significant smaller than the value of 1.4 for the batch press.

- From figures 22 and 24, the values of the operating work indices for the Loesche mill are 35 kWh/ton and 55 kWh/ton for 80% and 50% mass passing size respectively. Those for the batch press are 3.6 kWh/ton and 5.6 kWh/ton for 80% and 50% mass passing size respectively. The differences are too big for the batch press to be used as a simulator for the Loesche mill.

- From figures 22 and 24 the values of the coefficients for the Loesche mill are 0.9 and 0.06 for 80% and 50% mass passing size respectively. Those obtained in the batch press are 0.5 and 1.4 for 80% and 50% mass passing size respectively.

Again the differences are too big for the batch press to be a used as a simulator for the Loesche mill.

- Figure 25 indicates that the coefficient n in the function: $F_{50}/P_{50} = aE^n+1$ is 1.75 for the Loesche mill and 0.4 for the batch press. Again, largely different from Kapur et al (1990), and Daniel's (2001), suggestions of 1. As with the energy-passing size relationships, there are large differences between the Loesche mill and batch press.

2.4.1.4   BANDED IRON STONE

Figures 26 and 28 are the graphs indicating the relationship between operating work index and products sizes. These are for different top sizes and product sizes as indicated in the graphs. Two top sizes, 3 mm and 5 mm were tested. The results of the batch press are also shown. In figures 27 and 29 the relationships between energy consumption and product size, are illustrated. Figure 30 is the plot of reduction ratio versus energy consumption for the Loesche mill.

Figure 26: Operating work index plotted as a function of 80% mass passing size for the Loesche mill and batch press for banded iron stone.

Figure 27: Energy consumption as a function of 80% mass passing size for the Loesche mill and batch press on banded iron stone.

Figure 28: Operating work index plotted as a function of 50% mass passing size for banded iron stone.

40
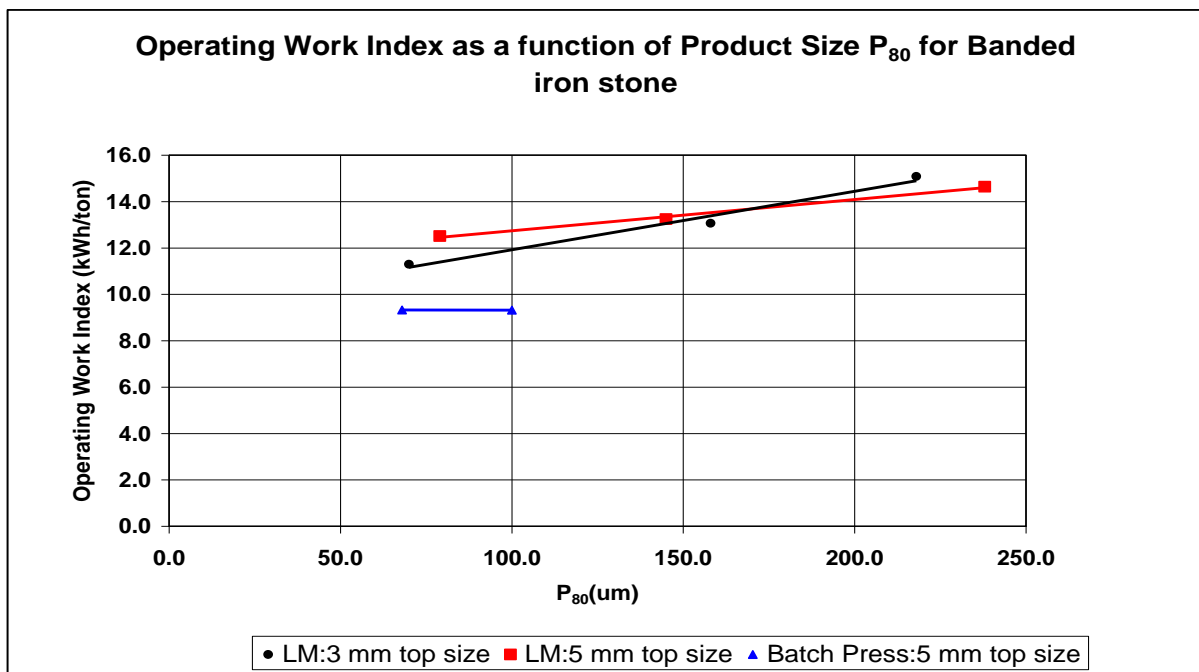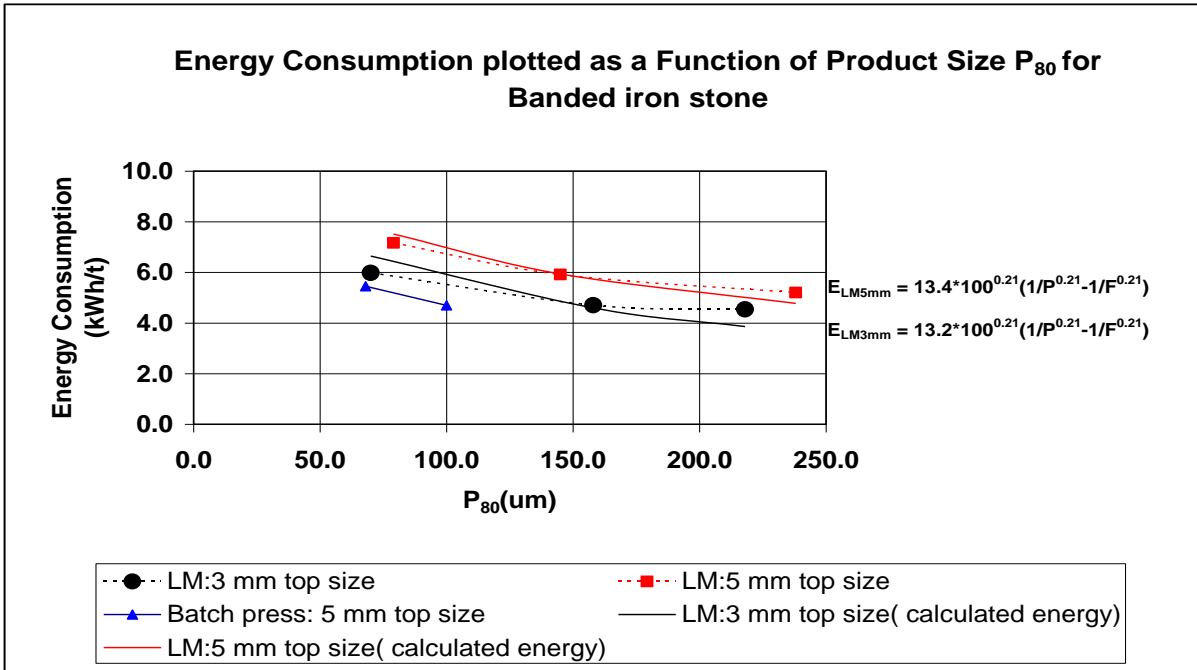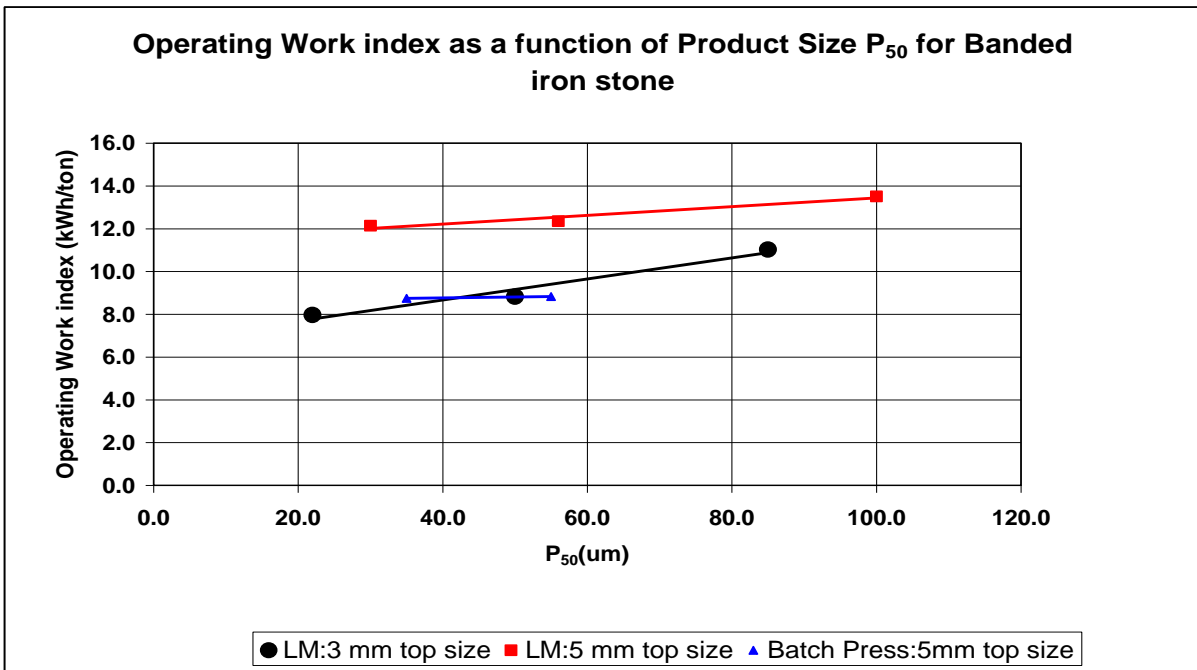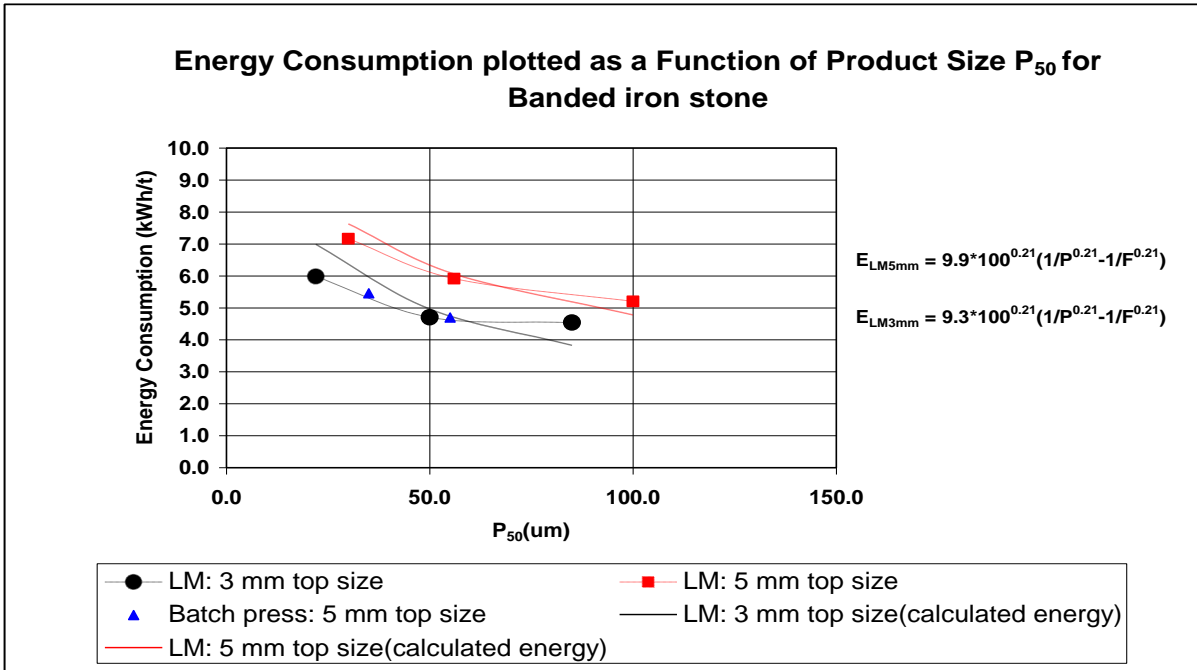
Figure 29: Energy consumption as a function of 50% mass passing size for the Loesche mill and batch press on banded iron stone.
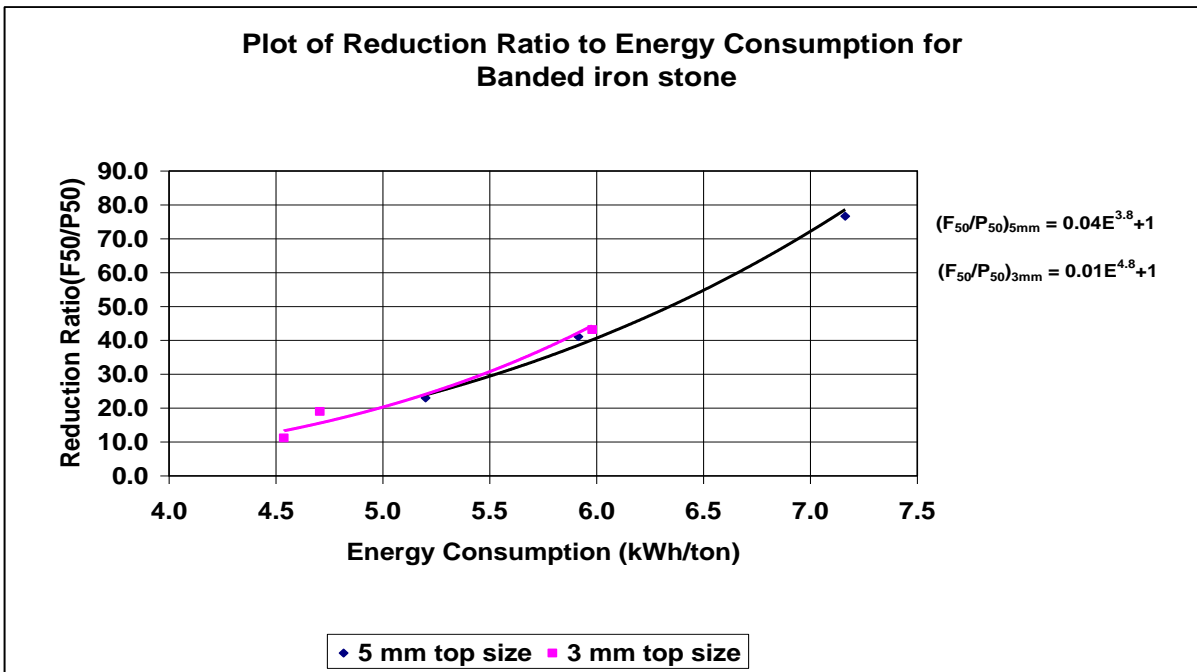

Figure 30: Plot of reduction ratio energy as a function of energy consumption in the Loesche mill for banded iron stone.

41

Comparison with the Bond/Rittinger formula and the suggested prediction of Kapur et al (1990), and Daniel (2001)

The operating work indices and coefficients from figures 27 and 29 are shown in table 5.

Table 5: Operating work indices and coefficients for banded iron stone.

Values of OWi and n for banded iron stone						
Top Size	F_{80}	Owi	n	F_{50}	OWi	N
5 mm	3350	13.4	0.21	2300	9.9	0.21
3 mm	1750	13.2	0.21	950	9.3	0.21
Batch press	3350	9.1	0.21	2300	15.7	0.18

The following deductions can be made from the data:

- In figures 26 and 28 the calculated operating work indices are shown. The operating work indices for 80% and 50% mass passing sizes for both the 3 mm and 5 mm top size are not constant over the range of particle sizes tested. To get the operating work indices to be constant, the value of the coefficient n must be reduced to even lower than 0.001. At these low values the value of the operating index would increase to as high as 2000. This is not a true reflection of the operating work index. From graph 27, the energy consumption to mill the 3 mm top size material to 100 µm is 5.5 kWh/ton. In this case the feed size is 1750 µm 80% mass passing size. The energy needed to crush the material from a relative large feed size to 100 µm equals the operating index of the material. To determine this energy, it is necessary to add the energy needed to crush the material to 1750 µm. In 2001 Bateman was tasked to do Bond work indices on this material (Cook, 2001). These values range from 20.5 at a P_{80} of 190 µm to 22.1 at a P_{80} of 96 um. Making the assumption that the Bond index is valid to crush the material to 3 mm and using equation 4, the amount of energy is 5.3 kWh/ton. Adding this to the 5.5 kWh/ton, the total energy to crush and therefore, operating work index would be 10.8 kWh/ton. If this value is then used to determine the value of the coefficient n from using equation 6, this amounts to 0.18. Similarly, for the top size of 5 mm the value of n would be 0.13. In figure 27 it is clear that the fit between the calculated

42

energy and tests results is not a good fit. In figure 29, if the value of the coefficient is taken to be the same, the operating work indices are 9.9 and 9.3 for the 5 mm and 3 mm material. Although an assumption, the fit in this case is not a good one either. It also does not improve with different values of the operating work index and the coefficient.

- From figure 30 the value of the coefficient n is 3.8 and 4.8 for 5 mm and 3 mm respectively and not 1 as suggested by Kapur et al (1990), and Daniel (2001).

Comparison between the Loesche mill and the batch press.

- From the graphs it can be seen that there is a marked difference between the energy needed to mill the material from 5 mm to 100 μm with the batch press and the Loesche mill. Because of the uncertainty around the values of the coefficients obtained from the tests, it is difficult to make a comparison between the batch press and the Loesche mill. Unfortunately, only two data points is shown for the batch press, as the rest of the tests with the batch press were not successful.

2.4.2   PARTICLE SIZE DISTRIBUTIONS

2.4.2.1   COMPARISON BETWEEN THE ROSIN-RAMMLER AND OTHER EXPRESSIONS

Hukki (1975), stated that the Rosin-Rammler expression does not sufficiently describe particle size distributions. In this study it will be shown that in some cases this is true and that this expression should be used with care. The advantages of the Rosin-Rammler model will be discussed and compared with other models for describing particle size distributions.

The other models used in this discussion are:

Gaussian Model:	$y = a\exp((-(b-x)^2)/(2c^2))$	14
Weibull Model:	$y = a - b\exp(-cx^d)$	15
Normalised Weibull:	$y = ((a\exp(-b(x/d_x)^d))100$	16
Truncated Rosin-Rammler	$y = 100(\exp(-a(x/b)^{dmax}))/(1-\exp(-a))$	17

Where: a,b,c and d are constants

x is the particle size defined as percentage retained on a specific screen aperture (μm)

d_x refers to a specific particle size, d_{50} is the 50% mass passing size, d_{80} the 80% mass passing size and d_{max} is the maximum particle size (μm)

A few reasons why the particle size distribution of an ore sample must be modelled are:

- Particle sizes are used to model unit processes such as mills, crushers, cyclones etc. From these models, mass balances are determined. Therefore accurate size distributions will result in accurate mass balances.
- Specific sizes play an important role in modeling, such as the P_{80} which is important in energy calculations.
- Comparisons between various unit processes, such as comparing the product of a rod mill with that of Loesche mill. In this case it is the slope of the graph that is the important measurement.

The Rosin-Rammler model is a normalised Weibull model. The value of the x-axis is divided by a constant d_x, which equals a specific value on the x-axis. There is a relationship between the constant b and the passing size d_x. In the case of d_x equals d_{50}, the constant is 0.693. With the constant b equals to 1, d_x changes to $d_{63.5}$ passing size. The value of these models are twofold; the constant d is an indication of the slope of the percentage passing size curve, whilst the term d_x indicates a point on the curve, such as d_{50}, d_{80} d_{25}, etc.. The value of a model such as this lies in the fact that before the mid '80s in the previous century, metallurgists used calculators and graph paper to determine the value of the slope of the curve. By integrating the equation, as discussed in Chapter 1, section 2.2.1, this gives a practical solution for determining the slope of the curve. Today, computers open other avenues. With curve fit packages the particle size description can be done with more ease and with different models. However, the problem with these packages is that many models could fit the data. Unfortunately there is no fundamental approach to guide metallurgists in selecting the most appropriate model and until such an approach has been developed, it is advisable to keep to sigmoid curves.

In the figures 31 to 39 the above models will be compared to see which describe the data the best and whether they are sufficient to be used for modeling. Table 6

contains the standard errors for the comparisons. This was determined using curveExpert 1.4, a fairly common and user friendly package.
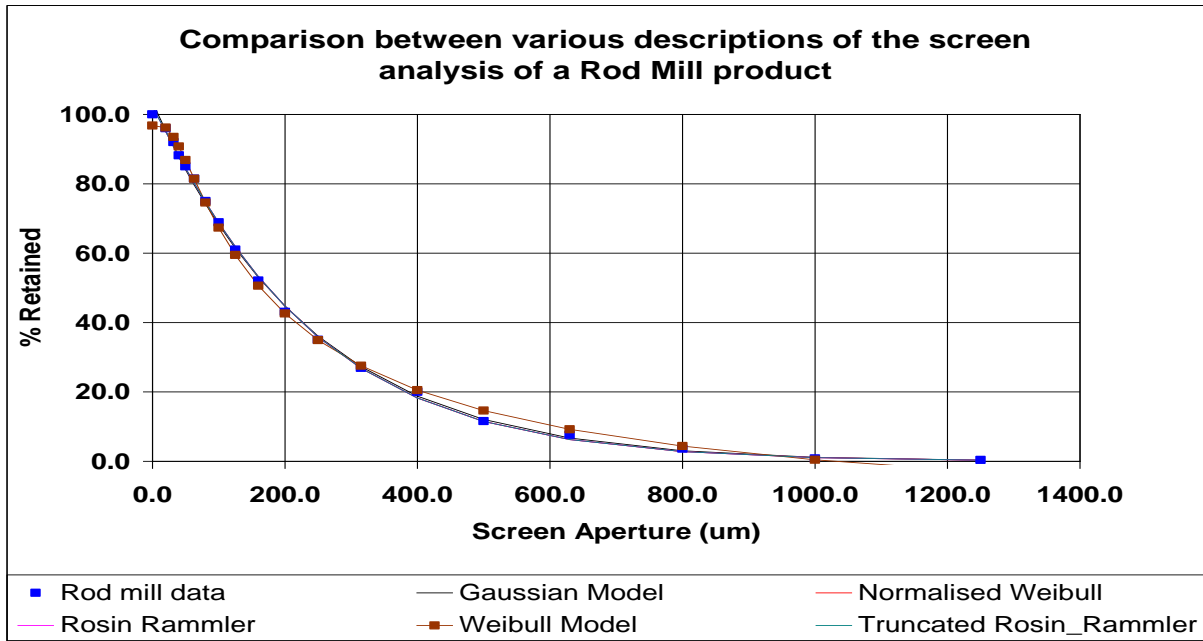
Figure 31: Particle size distribution of Foskor ore, milled in a rod mill, indicating different models describing the data.
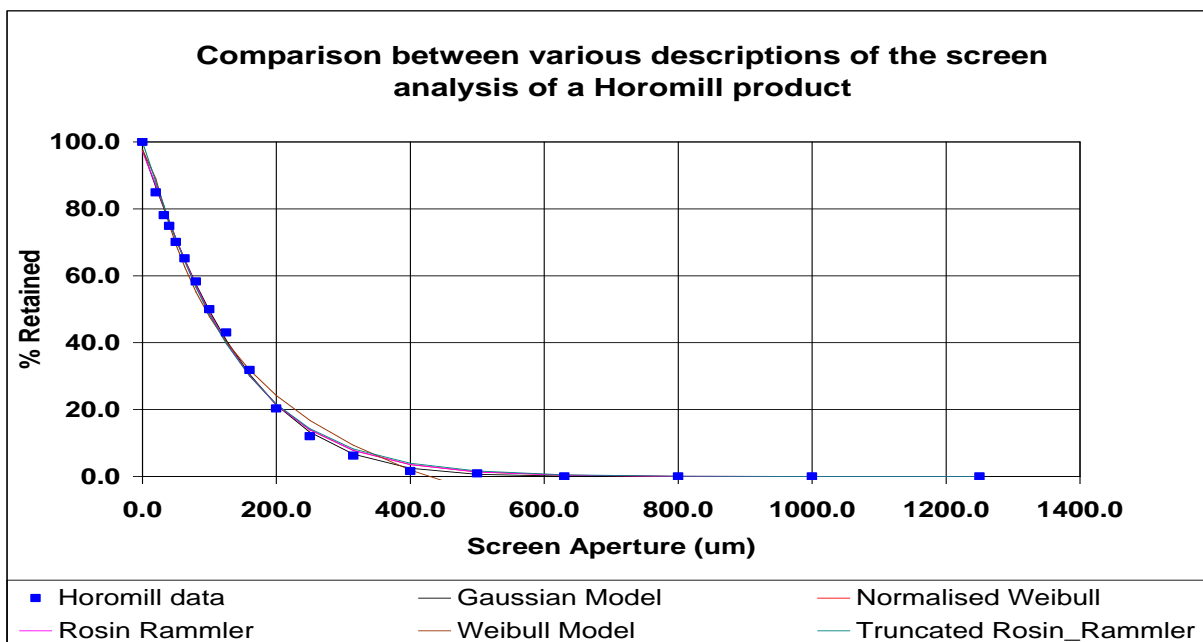
Figure 32: Particle size distribution of Foskor ore, milled in a Horomill, indicating different models describing the data

45

Figure 33: Particle size distribution of Foskor ore, milled in a batch press, indicating different models describing the data
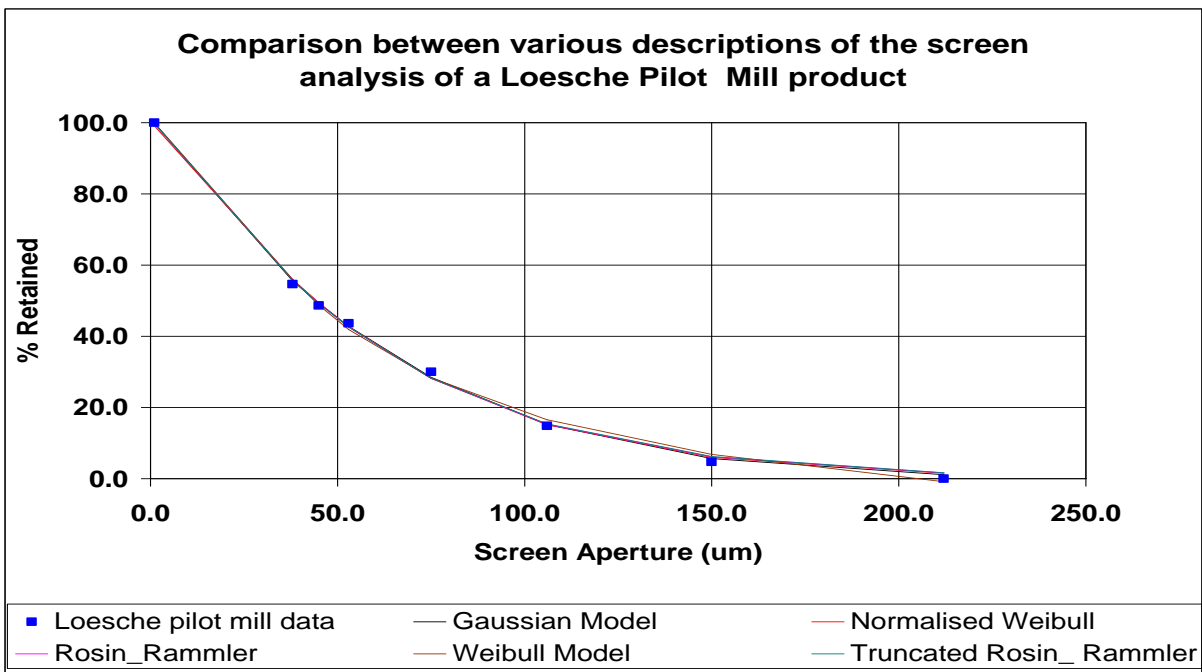
Figure 34: Particle size distribution of Rosh Pinah ore, milled in a Loesche pilot mill, indicating different models describing the data

46
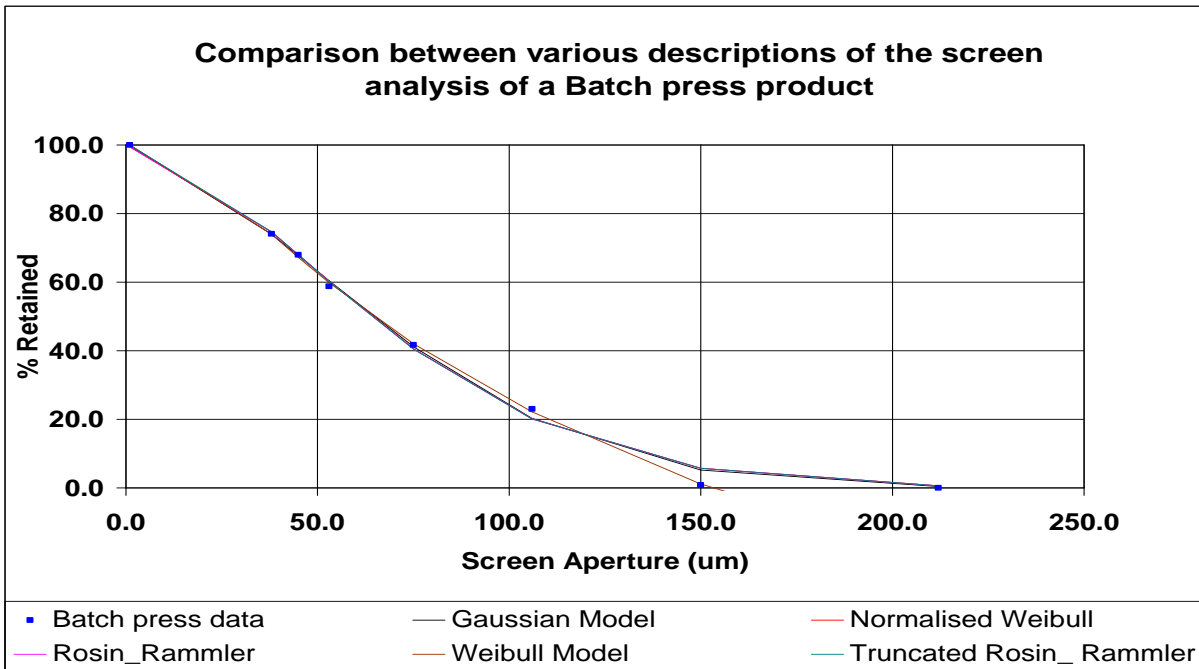
Figure 35: Particle size distribution of Rosh Pinah ore, milled in a batch press, indicating different models describing the data
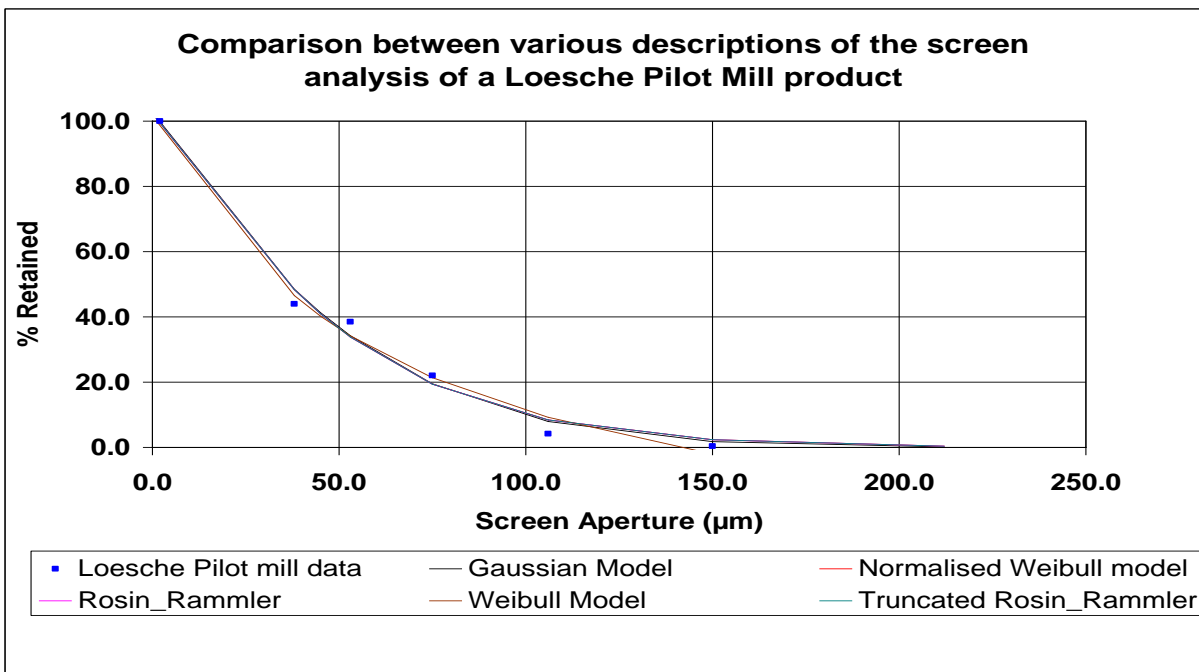
Figure 36: Particle size distribution of banded iron stone, milled in a Loesche pilot mill, indicating different models describing the data
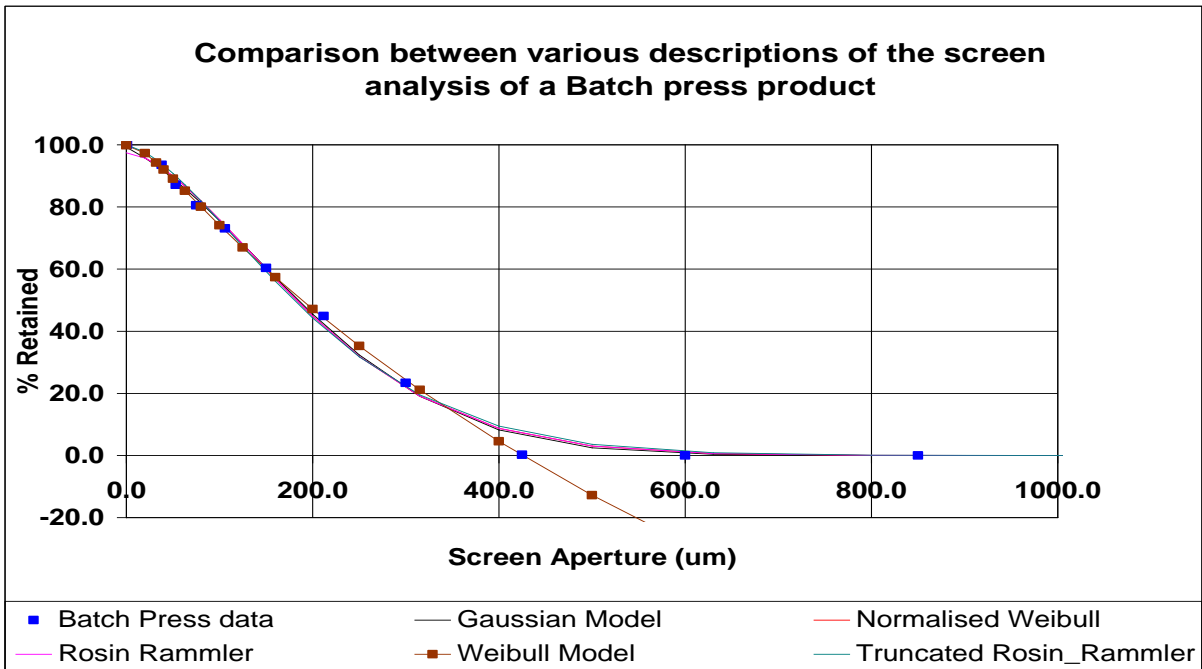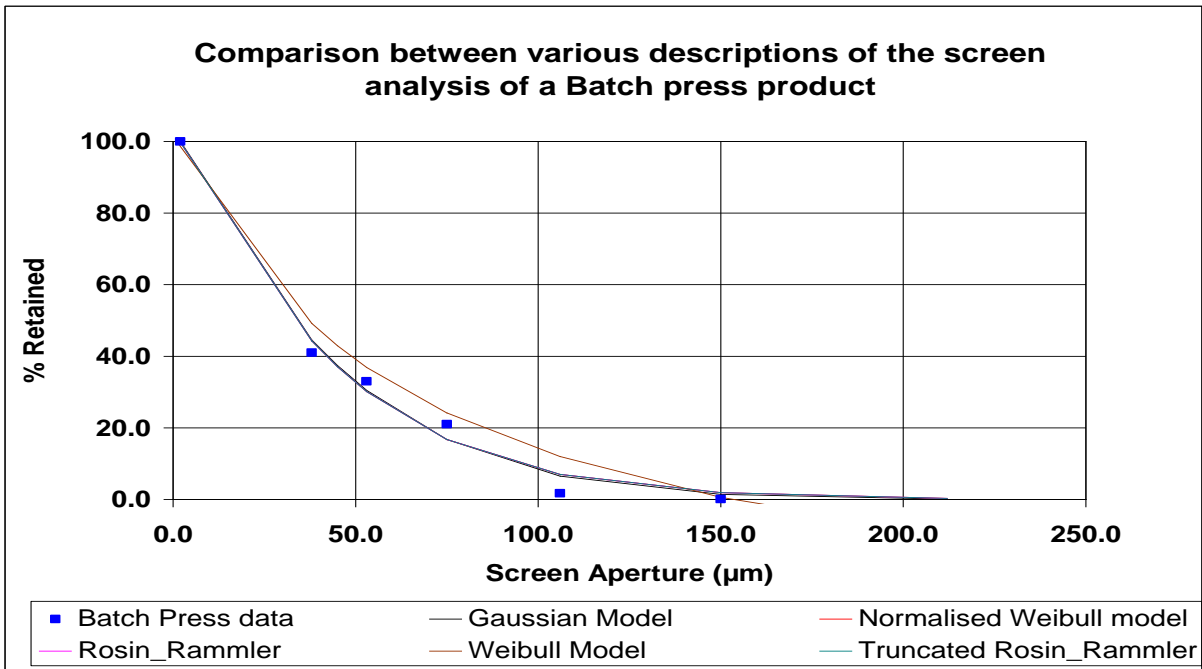
Figure 37: Particle size distribution of banded iron stone, milled in a batch press, indicating different models describing the data
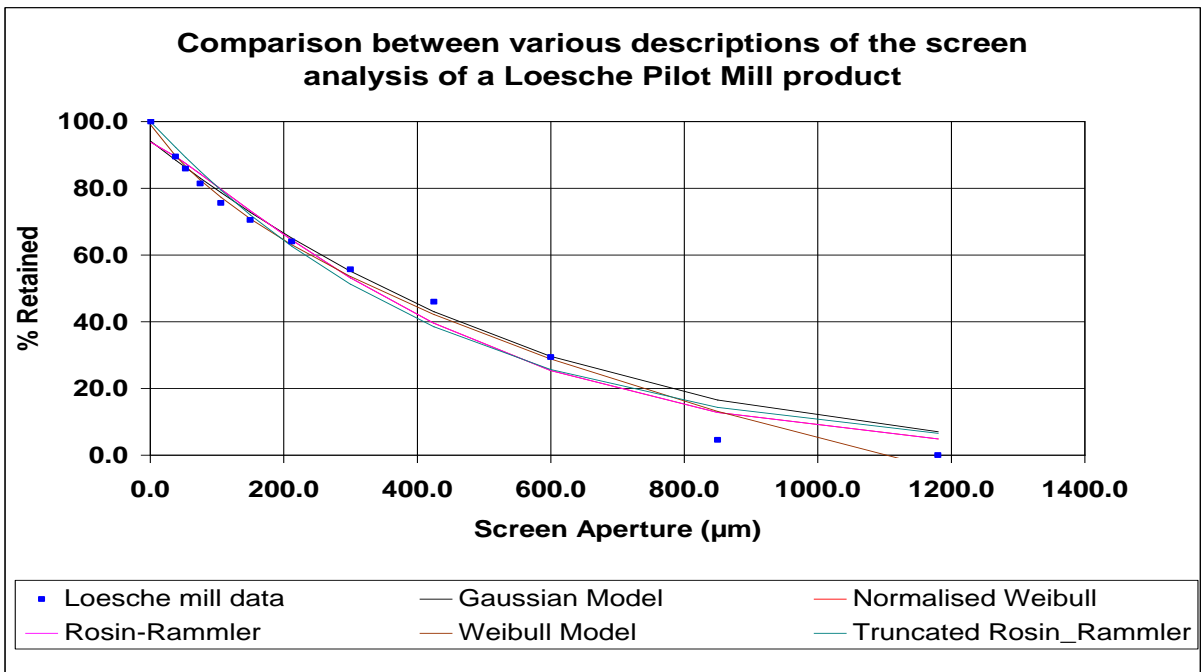
Figure 38: Particle size distribution of titanium slag, milled in a Loesche pilot mill, indicating different models describing the data
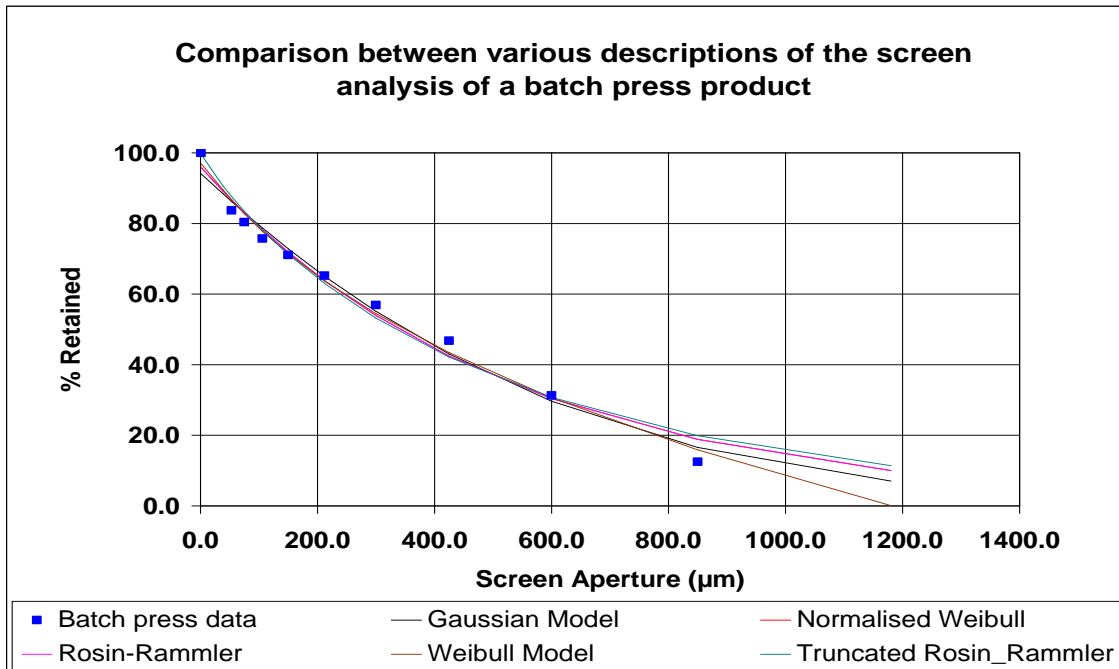
Figure 39: Particle size distribution of titanium slag, milled in a batch press, indicating different models describing the data

Figures 31 (rod mill), 32 (Horomill) and 34 (Loesche mill) indicate excellent fit with the data for all the models. From table 6, the Gaussian, normalised Weibull, and Rosin-Rammler models give standard deviations less than 2%, whilst that of the Weibull and Truncated Weibull model are up to 2.51%. The standard errors for Foskor ore (figure 33) and Rosh Pinah ore (figure 35) in the batch press are, but for the Weibull model, between 2.41% and 4.15% For the Weibull model it was less than 2%. However, as indicated in Figure 33, if the Weibull model is extended to higher values, it will result in negative values on the Y-axis. The rest of the figures indicate larger errors, up to 5.86%. The most important observation from figures 33, 35, 36, 37, 38 and 39, is that the models fit the data from 100% retained to 20% retained for Foskor, Rosh Pinah and banded iron stone. This value is about 30% for titanium slag. Another observation is that the data points that does not fit the models, are the lower numbers.

This gives weight to Hukki's (1975), observations that, the Rosin-Rammler distribution does not describe the particle size distribution sufficiently. This also applies for the other models. In this study it is particularly true for the batch press. To compare different milling and classification options, the models can be used as shown in section 2.3.2.2. To determine from the models a specific size fraction, if larger than 30% mass retained or 70% mass passing size, the sigmoid curve type is not

49

acceptable. This is an important reason why the P_{80} mass passing size is not a good choice to be used in energy calculations. If the need is to use the model to simulate a mineral processing flow sheet, there will be an error. It would be better not to use a model as an input into a mass balance, but rather use the actual data.

Table 6:   Standard errors of models in describing particle size distributions obtained from graphs 31 to 39.

Equipment	Ore	Gaussian	Normalised Weibull	Rosin-Rammler	Weibull	Truncated Weibull
Rod mill	Foskor	1.31	1.16	1.12	1.99	2.2
Horomill	Foskor	1.17	1.6	1.54	2.51	1.6
Batch press	Foskor	3.33	4.15	3.79	1.18	4.01
Loesche Pilot mill	Rosh Pinah	1.24	1.58	1.38	1.27	1.42
Batch press	Rosh Pinah	2.78	3.79	2.98	1.67	2.41
Loesche Pilot mill	Banded iron stone	4.13	5.66	4.56	5.07	4.56
Batch press	Banded iron stone	4.55	5.86	4.79	5.41	4.70
Loesche Pilot mill	Titanium slag	3.49	4.27	3.94	3.1	4.55
Batch press	Titanium slag	4.36	5.37	5.37	3.77	5.57

2.4.2.2 COMPARISON BETWEEN BATCH PRESS AND HOROMILL FOR FOSKOR ORE, AS WELL AS LOESCHE PILOT MILL FOR OTHER ORE TYPES

In this discussion the particle size distributions of the products of the different tests will be compared. This is done per ore type and the Rosin-Rammler formula is used in these comparisons.

2.4.2.2.1 Foskor Ore

The following graphs are shown for the Foskor ore:

- Figure 40 shows the particle size distributions of the products of the Horomill and batch press.
- In figure 41 the same data is plotted to indicate the Rosin-Rammler slope. This is lnln(% retained) as a function of ln(particle size).
- Figure 42 indicates the efficiency curves for a screen and a classifier. That of the classifier was taken from (Evrard and Cordonnier, 1995). The curve for the screen is taken to an ideal separation as will be the case when screening in a laboratory.
- Figure 43 is the particle size distribution for a screened and classified Horomill product.
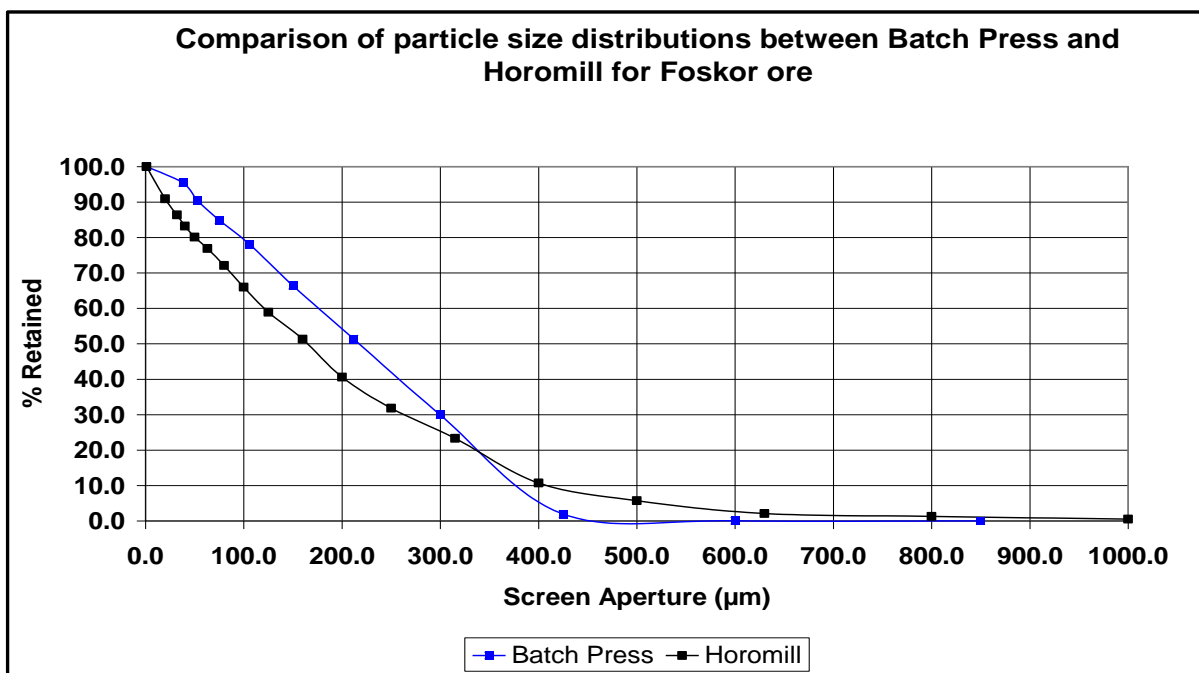
Figure 40: Screen analysis of Foskor ore products after comminution in the Horomill and batch tests.

Comparison between Batch Press and Horomill
Rosin-Rammler Plot

Batch = 1.36x + 0.01

Horomill = 1.10x + 0.08

Batch Press — Horomill
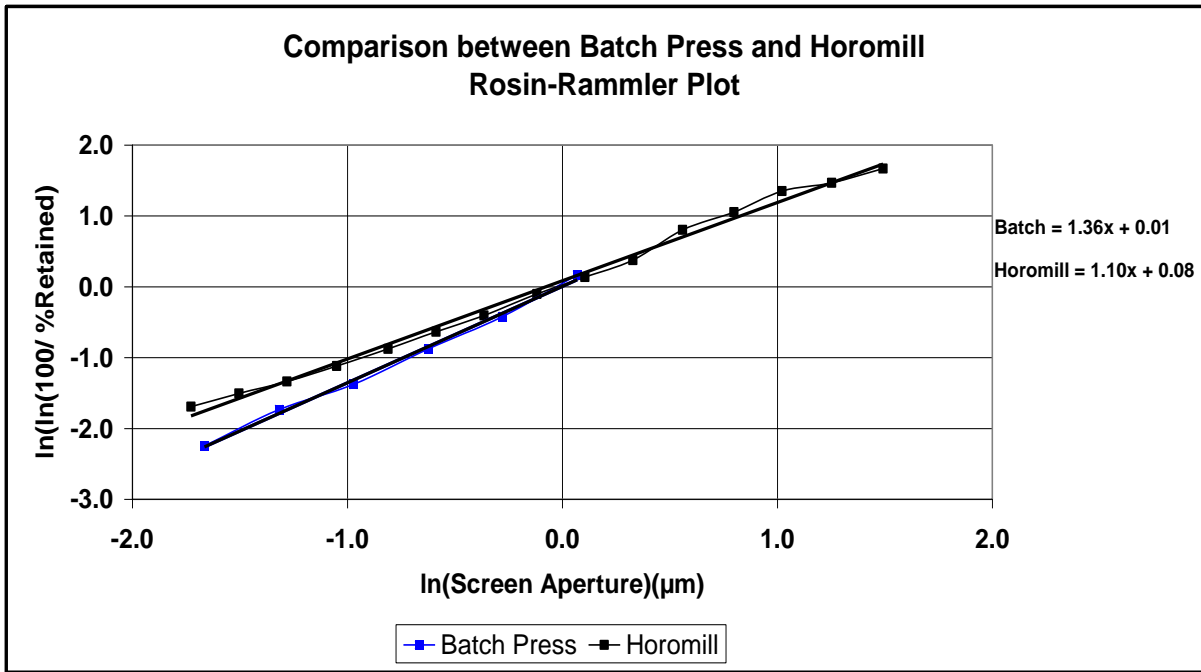
Figure 41: Rosin-Rammler plot of screen analysis of Foskor ore product after comminution in the Horomill and batch press.

Efficiency curve for a Classifier and a Screen
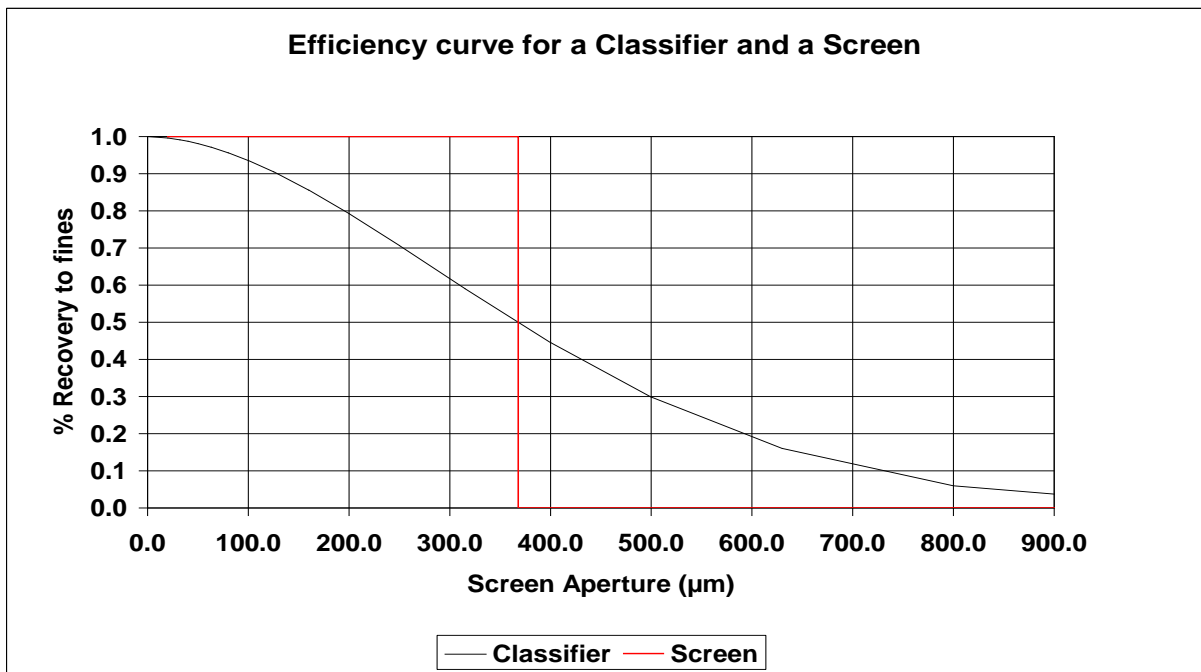
Classifier — Screen

Figure 42: Efficiency curves for a classifier and a screen.

52
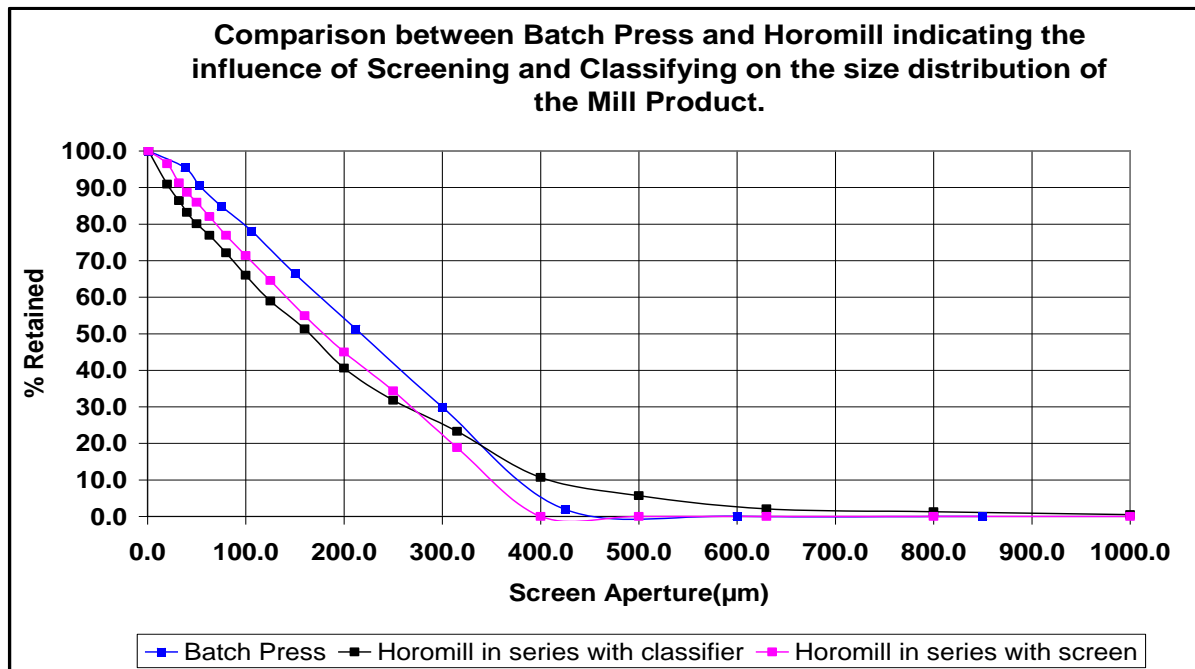
Figure 43: Screen analysis of Foskor ore indicating the difference between a classified and a screened product.

Discussion on Foskor ore

As shown in figure 40 and 41 there is a difference between the slopes of the particle size distribution for the Horomill and batch press. The slope according to the Rosin-Rammler model is 1.36 for the batch press and 1.10 for the Horomill. This difference could be partially explained in the way the mill or bath press discharge is classified. In the case of the Horomill, this was done with a classifier whilst the product of the batch press was screened. In figure 42 the partition curve for a classifier and screen is shown (Evrard and Cordonnier, 1995). From this it is clear why the screened product will have a steeper slope than the classified product. If the mill discharge is screened in stead of classified, it will result in a steeper slope for the screened product as can be seen in figure 43. However there is still some difference between the screen analysis of the batch press and that of the Horomill after screening.

2.4.2.2.2 Rosh Pinah ore
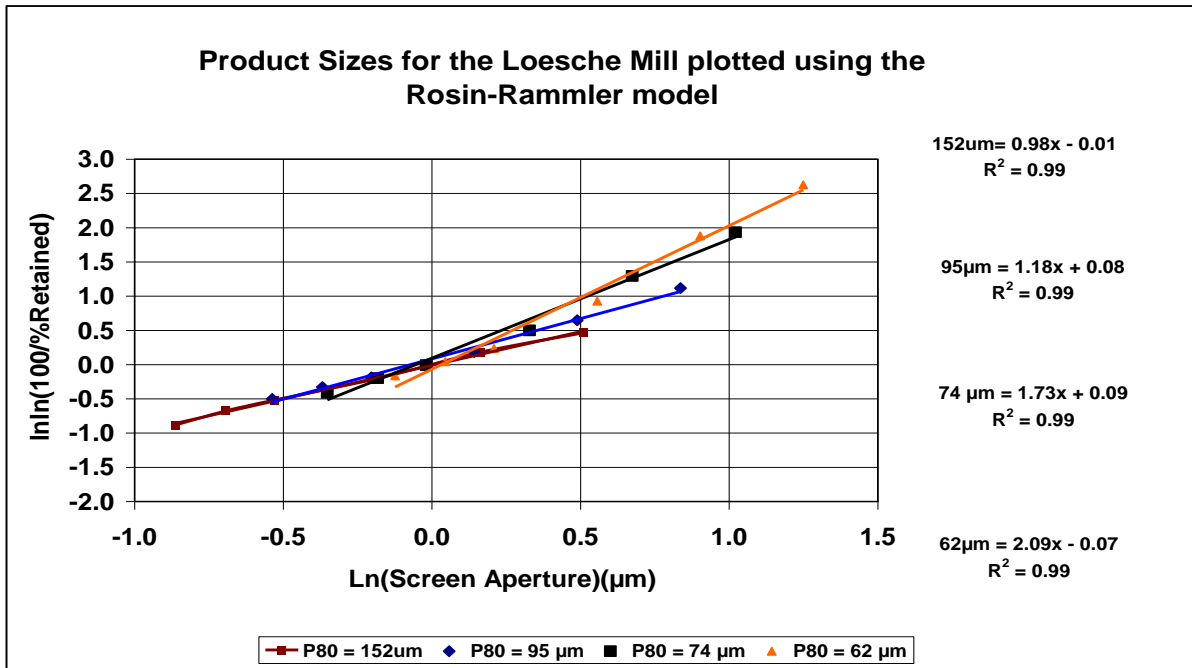
Figure 44: Screen analysis on a Rosin-Rammler plot for Rosh Pinah ore products after comminution in a Loesche mill.
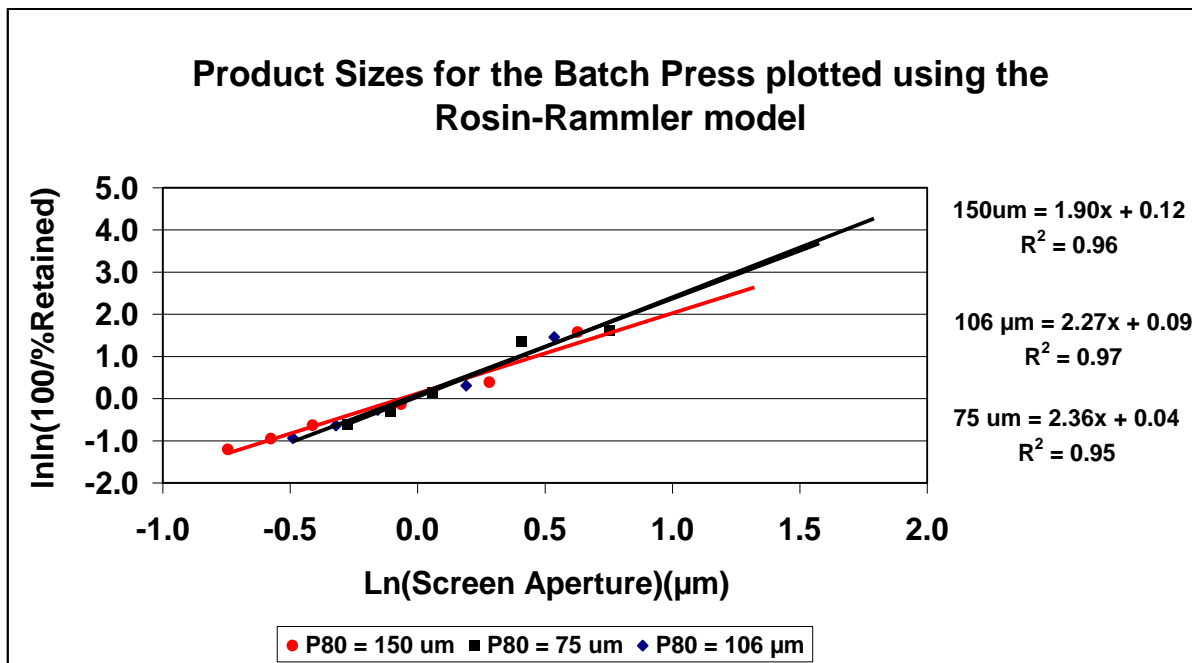
Figure 45: Screen analysis on a Rosin-Rammler plot for Rosh Pinah ore products after comminution in a batch press.

Discussion on Rosh Pinah ore

Figure 44 and 45 represents the size distribution of the products of the Loesche mill and batch press plotted using the Rosin-Rammler equation

- Figure 44 indicates that the Rosin-Rammler slope for Rosh Pinah ore varies between 0.98 and 2.09 for the Loesche mill product whilst, those of the batch press in figure 45 are between 1.9 and 2.36. This is a large difference. As the Loesche mill has an internal classifier, it is not possible to determine what the particle size of the product would look like if the mill discharge had been screened. Even then the difference would be still significant. With this ore the batch press did not represent the Loesche mill.
- The values of R^2 is in all cases larger than 0.95. This indicates that the Rosin-Rammler model can be used to describe the particle size distributions.

2.4.2.2.3 TITANIUM SLAG

The figures shown for titanium slag are:
- Figure 46 is the Rosin-Rammler plot for titanium slag in the Loesche mill.
- Figure 47 is the Rosin-Rammler plot for titanium slag in the batch press.

Comparison of the batch press and Loesche mills for titanium slag indicate some difference with averages for the Rosin-Rammler slopes of 0.82 for the batch press and 0.72 for the Loesche mill. In both cases the material were screened. All the R^2 values for the Rosin-Rammler slopes are well above 0.95 but it can be seen that at the top data points it deviates from a straight line. Again referring to Hukki, the Rosin-Rammler description can be used but the deviations must be taken into account.

Loesche Mill:Rosin-Rammler plot for Titanium Slag

33 Bar= 0.82x - 5.16
R^2 = 0.99

55 Bar = 0.69x - 4.16
R^2 = 0.99

100 Bar = 0.63x - 3.67
R^2 = 0.99

145 Bar = 0.59x - 3.35
R^2 = 0.99
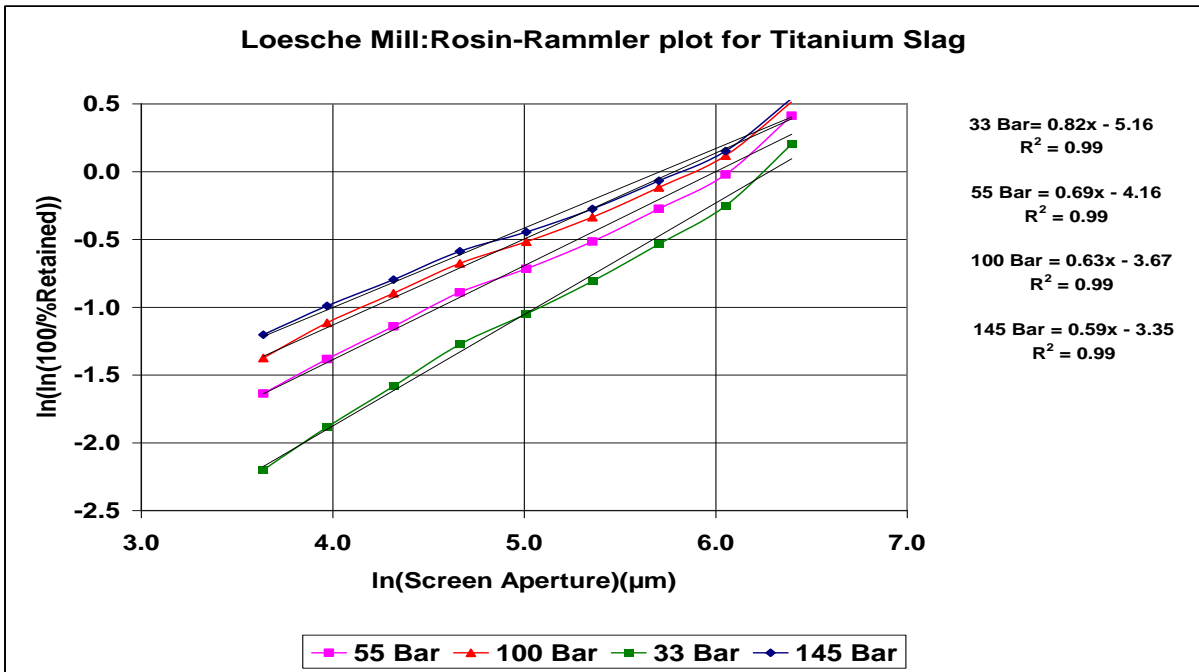
Figure 46: Rosin-Rammler plot for titanium slag in a Loesche pilot mill. The numbers in the legend indicate the hydraulic pressures at which the mill was set.

Batch Press:Rosin-Rammler plot for Titanium Slag

15MPa = 0.89x - 6.04
R^2 = 0.98

25MPa = 0.82x - 5.45
R^2 = 0.98

40MPa = 0.77x - 4.96
R^2 = 0.98

50MPa = 0.75x - 4.76
R^2 = 0.99
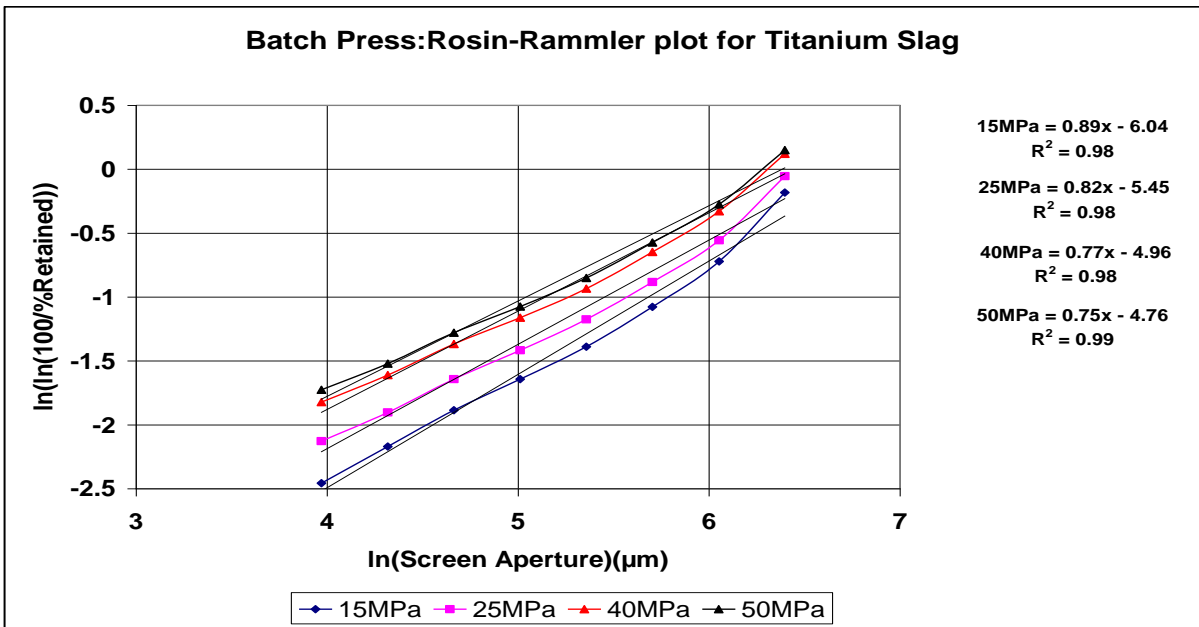
Figure 47: Rosin-Rammler plot for titanium slag in the batch press. The numbers in the legend indicate the pressures applied to the bed.

56

2.4.2.2.4 BANDED IRON STONE

Figure 48 is a comparison between the batch press and the Loesche mill for banded iron stone.

From this graph the following conclusions can be made:

- The Rosin-Rammler slope is 1.86 for the batch press and 1.80 for the Loesche mill which is not a significant difference.
- The graphs for both the Loesche mill and the batch press differ from a straight line but to the same extent, indicating that with this ore the batch press simulates the Loesche mill. Using the Rosin-Rammler description will introduce large errors.
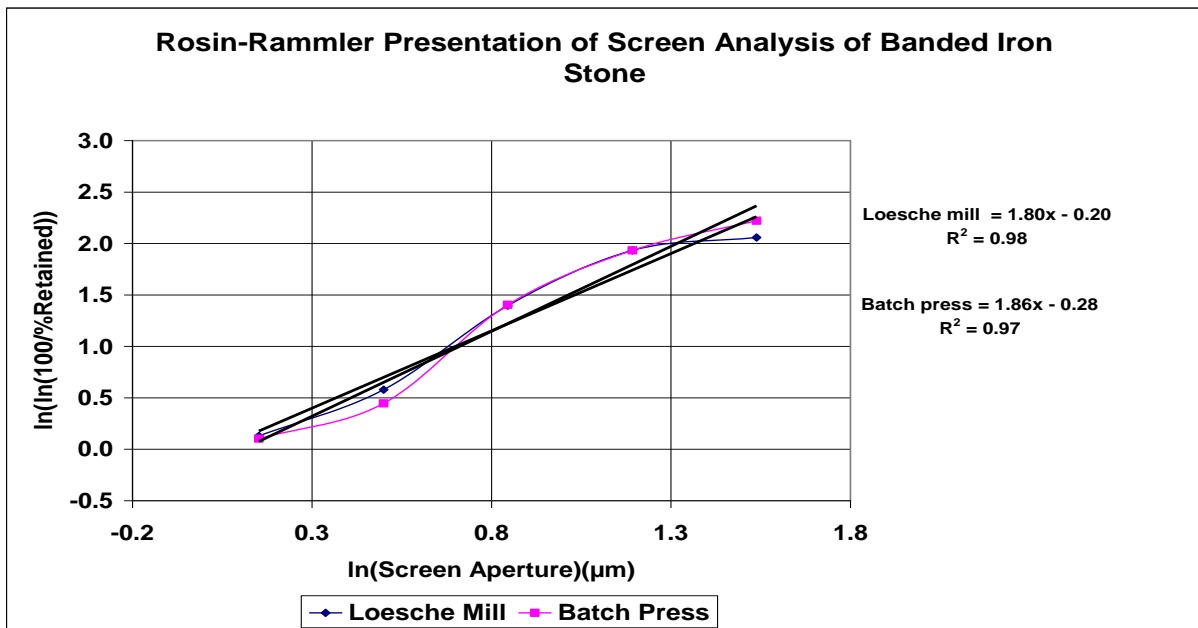
Figure 48: Rosin-Rammler Plot of Screen Analysis for Banded iron stone.

2.4.3 CIRCULATING LOAD

In Figure 49 the influence of applied pressure on the circulating load is summarised and compared with the results achieved with the Horomill on Foskor ore. The Loesche pilot mill has an internal classifier and therefore the circulating load could not be compared with the results from a batch press. As discussed previously, it is

important that there should be a good correlation between the circulating load ratios of the Horomill and the batch press
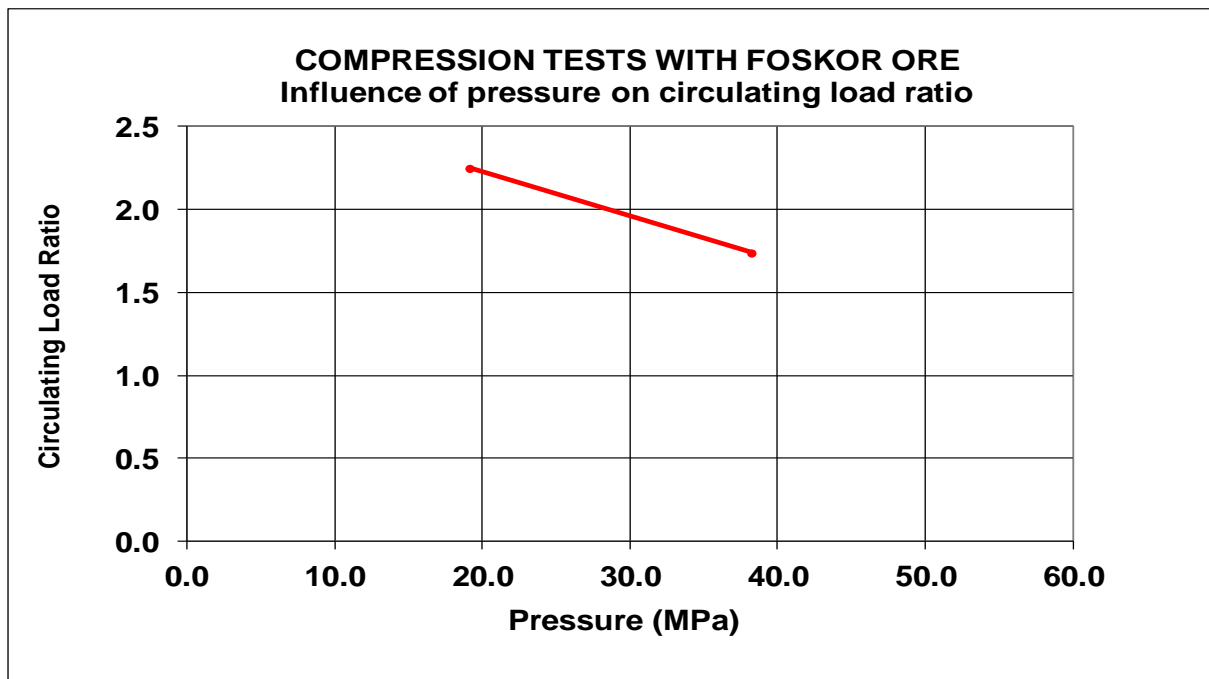
Figure 49: Circulating load ratio as a function of applied pressure for the Loesche and Horomill respectively for a product top size of 300μm.

Inside the Horomill is a unique design of a scraper/spreader installed. By adjusting the scraper the material can be pressed between 3 and 5 times before being discarded. In the tests this was assumed to be an average of 3 times. In the batch press the material was pressed and loosened three times before being taken out and screened. The process was repeated to simulate a circulating flow until the circulating load stabilised. This was done with pressures ranging from 20 to 40 MPa. According to the manufacturer the calculated bed pressures applied during the tests with the Horomill were of this order. From figure 49, it can be seen that the circulating load ratios in the batch press are approximately 2, the same value as was achieved with the Horomill.

CHAPTER 3

SUMMARY OF RESULTS AND COMPARISONS

3.1 ENERGY RELATIONSHIPS

Table 7: Summary of operating work indices and coefficients in the formula
$$E = OWi*(100^n)(1/P^n - 1/F^n)$$

Ore type	Top Size	Equipment	P_{80}		P_{50}	
			OWi	n	OWi	n
Foskor	30 mm	Horomill	9.51	1.05	7.5	2.31
Foskor		Batch Press	5.33	0.24	4.7	0.85
Foskor	5 mm	Pilot ball mill	12	1.05		
Titanium slag	10 mm	Loesche mill	35	0.9	55	0.06
Titanium slag	10 mm	Batch press	3.6	0.5	5.6	1.4
Banded iron stone	5 mm	Loesche mill	13.4	0.21	9.9	0.21
Banded iron stone	3 mm	Loesche mill	13.2	0.21	9.3	0.21
Banded iron stone	5 mm	Batch press	9.1	0.20	15.7	0.18
Rosh Pinah ore	10 mm	Loesche mill	9.89	1.36	4.42	0.95
Rosh Pinah ore	5 mm	Loesche mill	7.18	1.22	3.43	0.95
Rosh Pinah ore	3 mm	Loesche mill	6.68	1.1	3.33	0.83
Rosh Pinah ore	10 mm	Batch press	3.04	0.68	1.71	0.79
Rosh Pinah ore	5 mm	Batch press	3.04	0.65	1.73	0.8
Rosh Pinah ore	3 mm	Batch press	2.67	0.77	1.69	0.79
Rosh Pinah ore	10 mm	Ball mill	11.1	0.72		

Table 8: Summary of constants a and n in the formula $F_{50}/P_{50} = a*E^n+1$

Ore type	Top Size	Equipment	Constants	
			a	n
Foskor	30 mm	Horomill	11.7	0.45
Foskor		Batch Press	1.62	0.59
Titanium slag	10 mm	Loesche mill	0.73	1.75
Titanium slag	10 mm	Batch press	3.4	0.41
Banded iron stone	5 mm	Loesche mill	0.04	3.8
Banded iron stone	3 mm	Loesche mill	0.01	4.8
Rosh Pinah ore	5 mm	Loesche mill	1.5	1.14
Rosh Pinah ore	3 mm	Loesche mill	4.6	1.04
Rosh Pinah ore	10 mm	Batch press	16.8	0.55
Rosh Pinah ore	5 mm	Batch press	3.4	1.15
Rosh Pinah ore	3 mm	Batch press	8.3	1.27

Comparison with the Bond/Rittinger formula and the suggested prediction of Kapur et al (1990), and Daniel (2001),

To conclude the discussion on the comparison between Bond/Rittinger and experimental results, the following is repeated from the discussions on the individual ore types.

- For the Horomill, Loesche mill, batch press and even the two ball mills, the value of the coefficient n varies from ore type to ore type and for different % mass passing sizes.
- The energy/particle size relationship, $E = OWi(1/P^n-1/F^n)$, seems to be valid. Using the coefficient n for the specific experiment and calculating OWi, in almost all cases this calculated value is constant over the range of particle sizes tested.
- Whether the 80% or 50% mass passing size is the better choice for defining the product size, cannot be deduced from this project.

- The values of the coefficient in the reduction ratio/energy consumption model vary from between 0.86 and 1.24 for the Loesche mill with Foskor and Rosh Pinah ore. However, with banded iron stone and titanium slag, it is as high as 5.1. It follows that the suggestion of Kapur et al (1990), and Daniel (2001), that this should be 1, is not valid for the Loesche mill.

Comparison between the Loesche mill and the batch press.

The following deductions can be made from the results:
- The energy consumption of the batch press is consistently lower than the energy consumption of the Loesche and Horomill. The operating work indices and the values of the coefficients in the equation 6 and 7 differ significantly between that obtained from the batch press and that from the pilot mills.
- The operating work indices obtained from the batch press is in all cases lower than that from the pilot mills. In the case of titanium slag it is a tenth of that achieved in the pilot Loesche mill.
- The values of the coefficient are also, with the exception of the banded iron stone, lower than that obtained from the pilot mills.

3.2   PARTICLE SIZE DISTRIBUTIONS

The batch press produces a size distribution that deviates from the straight line relationship as described by the Rosin-Rammler model. However, it is still a valid method to describe the size distribution of the product of the Horomill and Loesche mill. The batch press, however, does not simulate the mills well. In the case of the banded iron stone and the slag, the differences in the Rosin-Rammler slope are small. The results with Foskor ore shows that by taking the method of classification into account the differences in the slope for the batch press and the Horomill could be explained. However, the results obtained with the Rosh Pinah ore can not be explained.

3.3 CONCLUSIONS

- The relationship between energy, a work index, the product and feed size as described by equation 6 and 7, was found to be useful for the comminution devices and ores investigated.

- The values of the coefficient in these equations are not constants as suggested by Bond and Rittinger, but vary and must be determined for each application.

- The relationship between the reduction ratio and energy consumption suggested by Kapur et al (1990), and Daniel (2001) has limited applicability. The results also indicates that the coefficient also differs from application to application.

- Using the batch press as a simulator can only be done with regard to particle size distributions. As far as energy descriptions are concerned, the differences between the batch press and pilot mills are too big. Even for simulating particle size distributions, unless proven for an application, it is suggested that it only be used for research purposes, for instance, to prepare material for bench scale tests such as flotation and magnetic separation.

REFERENCES

Austin, L.G., The theory of grinding, Industrial and Engineering Chemistry, Vol. 56, No. 11, 1964, 18-29.

Bond, F.C., The third theory of comminution, Mining Engineering, May 1952, 484-494.

Cook, P., Report on ball mill work indices of Thabazimbi ore, 2003.

Daniel, M., HPGR Model Verification and Scale-up, Amira International, 3rd Progress Report, May 2001.

Eicke, G., Grinding plants for special powders, Aufbereitungs-Technik, Vol. 20, No. 2, 1979, 99-103.

Evrard, R. and Cordonnier, A., Comparative study of grindability of pyroxenite from Phalaborwa: Results of test program conducted in November 1995, FCB.

Fandrich, R.G., Bearman, R.A., Boland, J. and Lim, W., Mineral liberation by particle bed breakage, Minerals Engineering, Vol. 10, No. 2, 1997, 175-187.

Guy, Elements of Physical Metallurgy, 1960, 330.

Hukki, R.T., The principles of comminution: an analytical summary. Engineering and Mining Journal, Vol. 5, May 1975, 106-110.

Jankovic, A., Dundar, H. and Mehta, R., Relationships between comminution energy and product size for a magnetite ore, SAIMM, Vol. 110, March 2010, 141-146.

Kanda, Y., Oyamada, T., Kanedo, K., and Sano, S., The compressive crushing of quartz in a powder bed: The effect of feed size on grindability, Minerals Engineering, Vol. 9, No. 4, 1996, 475-480.

Kapur, P.C., Schönert, K., Fuerstenau, D.W., Energy-size relationship for breakage of single particles in a rigidly mounted roll mill, International Journal of Mineral Processing, Vol. 29, 1990, 221-233.

Kapur, P.C., Sudhir, G.S. and Fuerstenhau, D.W., Grinding of heterogeneous mixtures in a high-pressure roll mill. Comminution: Theory and Practice, Society of Mining, Metallurgy, and Exploration, Inc., 1992, 109-123.

Kellerwessel, H., Extracts from Roller Press Symposium at Humboldt Wedag AG, Cologne, January 1989.

Kellerwessel, H., Extracts from Inter-particle Crushing Symposium, Johannesburg, 19th June 1990.

Lim, W.I.L. and Weller, K.R., Some benefits of studded surfaces in high pressure grinding mills, Comminution '98, Brisbane, Australia, February 1998.

63

Mayerhauser, D., Economical fine size reduction with a high compression roller mill, Industrial Minerals Processing Supplement, Vol. 4, 1990, 43-47.

Napier-Munn, T.J., Morrell, S., Morrison and R. D., Kojovic, T., Mineral Comminution Circuits: Their Operation and Optimisation, JKMRC Monograph Series in Mining and Mineral Processing 2, 1996.

Norgate, T.E., and Weller, K.R., Selection and operation of high pressure grinding rolls circuit for minimum energy consumption, Minerals Engineering, Vol. 7, No. 10, 1994, 1253-1267.

Schönert, K., A first survey of grinding with high-compression roller mills, International Journal of Mineral Processing, Vol. 22, 1988, 401-412.

Schönert, K., Advances in comminution fundamentals and impacts on technology, Aufbereitungs-Technik, Vol. 32, No. 9, 1991, 38-45.

Schwechten, D. and Milburn, G.H., Experiences in dry grinding with high compression roller mills for end product quality below 20 microns, Minerals Engineering, Vol. 3, No. 1/2, 1990, 23-34.

Van der Linde, G. and Bester, P., Improved apatite recovery from pyroxenite ore using dry milling, Foskor internal report, 1998.

Van der Meer, F., Roller press grinding of pellet feed, AusIMM Conference on Iron Ore Resources and Reserves Estimation, Perth, Australia, September 1997.

Viljoen, R.M., Smit, J.T., Du Plessis, I. and Ser, V., The development and application of in-bed compression breakage principles, Minerals Engineering, Vol. 14, No. 5, 2001, 465-471.

APPENDIX 1

A.1   INDUSTRIAL ROLLER MILLS

The industrial equipment available consists of three design types. All of these are equipped with high-pressure hydraulic systems which apply pressure to a roller and create a bed pressure of 15 MPa for the milling of coal and up to 100 MPa for the crushing of hard minerals such as quartz. The three designs are briefly described.

A.1.1 DUAL ROLLER PRESSES

These presses consist of two rollers of which one is a rigidly mounted roller with no drive train. It rotates freely and is driven by the ore passing through the gap. The other roller is electrical driven and pressure is applied to the roller by a hydraulic system through a set of hydraulic cylinders. It is expected that the rollers in this equipment will have the highest wear rate as the material is crushed only once when passing through the gap between the rollers. With the other designs the material can be pressed more than once whilst in the machine. Comparison between a dual roll crusher and the Horomill at FCB indicated that the pressure, as calculated by the manufacturers, is 100 MPa for the dual roller crusher and 30 MPa for the Horomill. The lower pressure required with the Horomill results from the fact that material is being pressed three times whilst in the mill. The lower applied pressure results in less wear of the metal surfaces. The action of such a mill on the ore and the pressure exerted on the bed of ore particles are shown schematically in figure 50.
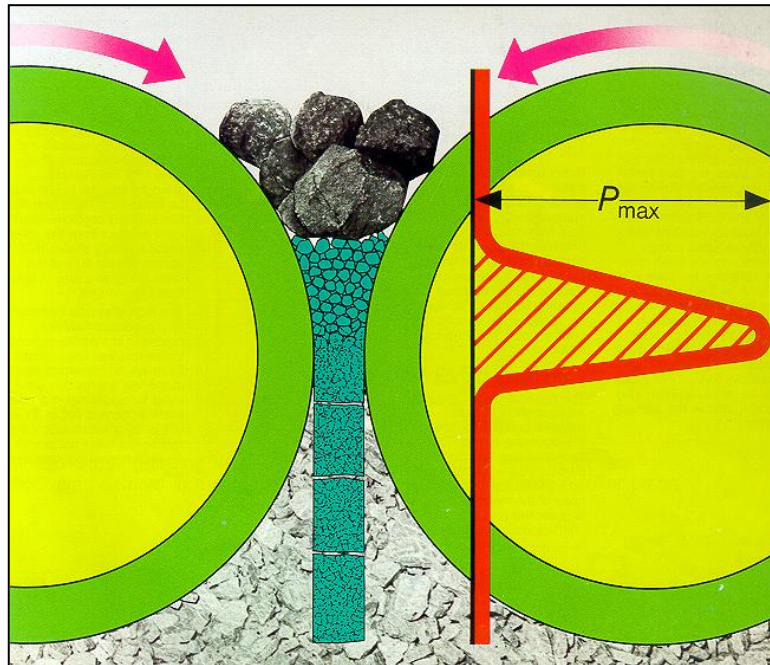
Figure 50: Diagram of a dual roller press indicating the size reduction of the ore and the pressure generated in the ore bed.

A.1.2 VERTICAL ROLLER MILLS

Loesche manufactures the best-known mill in this design type. Although the concept of inter-particle crushing is relatively new, these mills have existed for the better part of the last century. Their utilization was for the fine grinding of soft material, such as coal, or where the material needs to be milled to fineness such as 20μm. Ball mills are not efficient enough for milling to these fine sizes.

These mills consist of a horizontal rotating table and two or more free rotating rollers as shown in figures 51 and 52. Hydraulic pistons press the rollers onto the table. The small mills are equipped with two rollers, but larger mills may have four rollers. Because of the chance that the material can be pressed up to four times whilst on the table, these mills operate with the lowest pressures of all the designs and therefore the wear on the rollers are the least. At Foskor steel consumption of typically 18 grams of steel per ton of ore is achieved. It is expected that with only two rollers this figure could rise to 30 grams of steel per ton of ore.

The mill is equipped with an internal classifier that has the advantage of less ancillary equipment. The circulating load is transferred back onto the table as the classifier is situated right on top of the table. It is not advisable to use this arrangement where multiple classifications are necessary. However, the mill can be designed to be an overflow mill. The material is discharged over the edges of the table and dumped onto conveyors for classification. The bigger rollers are typically used for coarse material and operate at lower pressures while the smaller rollers will require higher pressures but comminution will be finer.
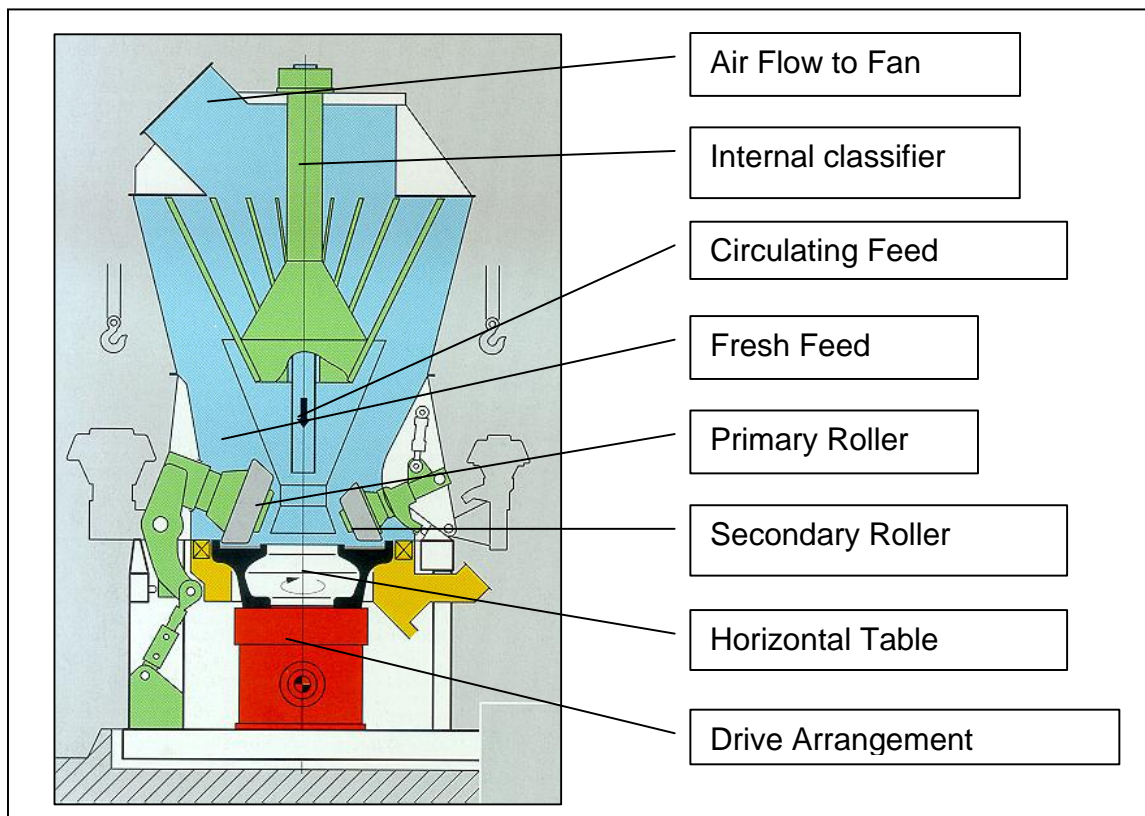
Figure 51: Schematic Representation of a Loesche Mill, Loesche GMPB [1994].

Figure 52: Views of the AARL Pilot Mill.

A.1.3 HOROMILL

The Horomill was developed by FCB in France to compete with the dual roller crushers in the cement industry. This mill consists of a pinion driven shell with a roller inside the shell as indicated in figure 53. This roller is free rotating and pressure is applied to the roller by hydraulic cylinders. Inside the shell is also a set of chutes that can be adjusted to change the residence time in the mill. The material can be pressed between 3 and 5 times before leaving the mill. These mills operate at moderate bed pressures of 30 to 50 MPa. This is lower than that of the dual roller that operates at 50 to 100 MPa and higher than that of the Loesche mill that operates at pressures as low as 15 MPa.
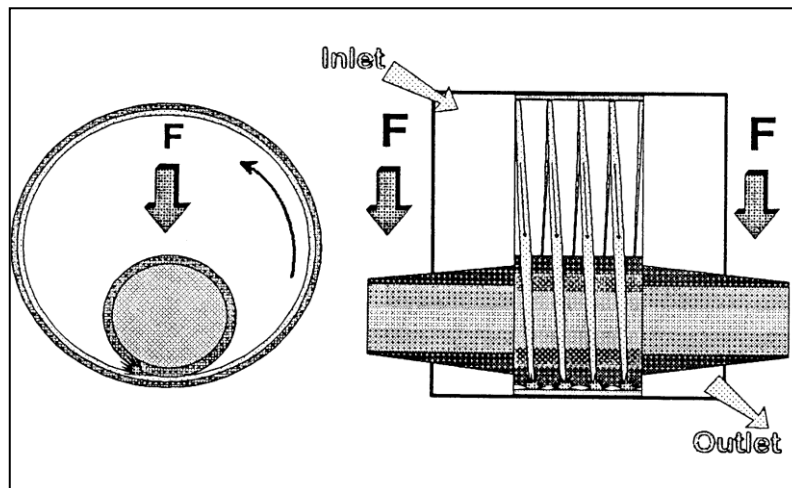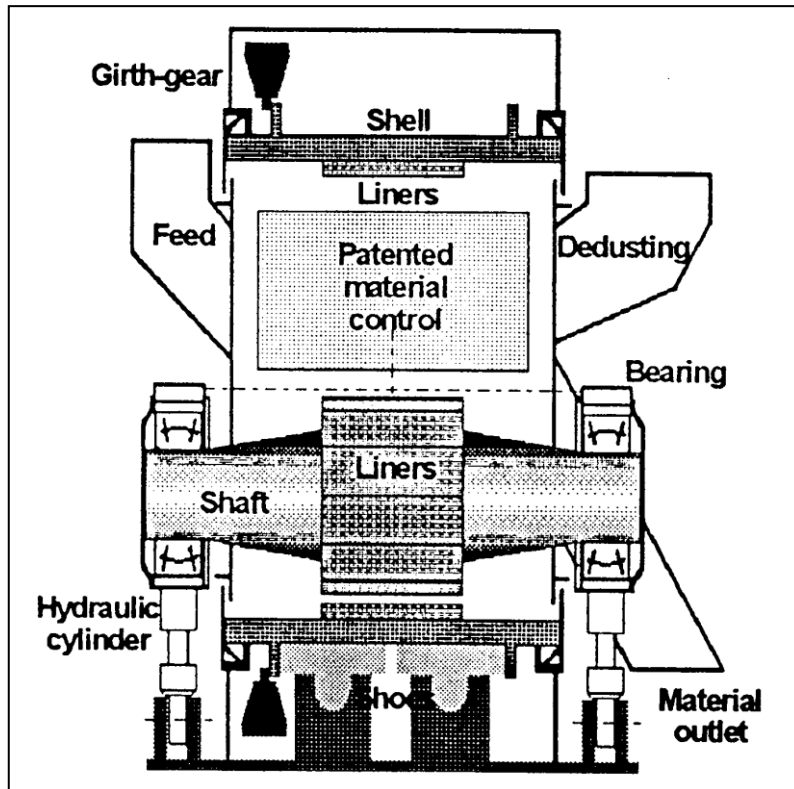
Figure 53: Schematic representation of a Horomill.

APPENDIX 2

DETAIL DATA FOR THE TESTS WITH FOSKOR ORE

Table A2.1:   Summary of detail of the tests performed with the batch press

.

BATCH PRESS: SUMMARY OF DETAILS OF TESTS												
Test Number	5030	1030	15030	40030	5040	1040	1540	5060	1060	1560	15030	30030
Force applied in the press (kN)	50	100	150	400	50	100	150	50	100	150	150	300
Pressure applied in the press (MPa)	6.36	12.73	19.09	50.91	6.36	12.73	19.09	6.36	12.73	19.09	19.09	38.18
Circulating load	15.0	9.0	6.2	3.3	11.9	5.1	3.8	6.6	2.8	2.3	2.2	1.7
Feed size $F_{80}(\mu m)$	2000	2000	2000	6000	2000	2000	2000	2000	2000	2000	6000	6000
Product size $P_{80}(\mu m$	280	280	280	240	390	390	345	470	450	450	260	220
Power consumption kWh/t	1.07	1.35	1.98	2.44	1.15	1.45	1.66	1.25	1.90	1.25	1.96	3.00
Reduction ratio F_{50}/P_{50}	7.1	7.1	7.1	25.0	5.1	5.1	5.3	4.3	4.4	4.4	23.1	27.3
Feed size $F_{50}(\mu m)$	750	750	750	900	750	750	750	750	750	750	750	750
Product size $P_{50}(\mu m$	140	140	140	165	215	215	190	165	155	160	155	150

Table A2.2:   Summary of detail of the tests performed with the Horomill.

SUMMARY OF RESULTS OF TESTS WITH HOROMILL			
HOROMILL			
Test Number	E49A	E49B	E49C	E49E
Feed size $F_{80}(\mu m)$	15300	15300	15300	15300
Product size $P_{80}(\mu m)$	194	201	294	333
Power consumption kWh/t	5.09	4.26	3.57	2.57
Xf/Xp	79	76	52	46
Feed size $F_{50}(\mu m)$	3000	3000	3000	3000
Product size $P_{50}(\mu m)$	120	125	140	160

Table A2.3: Screen analysis of the Horomill product.

| | SCREEN ANALYSIS OF THE HOROMILL PRODUCT | | | | | | | | | | | | | | |
| Test number | E49A | | | E49B | | | E49C | | | E49D | | | E49E | | |
Screen Aperture (um)	% Retained	%In Fraction	% Passing	% Retained	% In Fraction	% Passing	% Retained	%In Fraction	% Passing	% Retained	% In Fraction	% Passing	% Retained	% In Fraction	% mass passing
630	0.0	0.0	100	0.0	0.0	100	1.4	1.4	98.6	1.1	1.1	99.2	2.9	2.9	97.9
500	0.9	0.9	99.1	0.8	0.8	99.2	4.4	3.0	95.6	5.2	4.4	94.8	5.7	3.6	94.3
400	1.6	0.7	98.4	1.5	0.7	98.5	7.7	3.3	92.3	9.1	3.9	90.9	10.7	5	89.3
315	6.2	4.6	93.8	5.9	4.4	94.1	17.7	10.0	82.3	20.5	11.4	79.5	23.3	12.6	76.7
250	12.0	5.8	88	11.2	5.3	88.8	25.9	8.2	74.1	28.9	8.4	71.1	31.8	8.5	68.2
200	20.3	8.3	79.7	18.6	7.4	81.4	33.9	8.0	66.1	37.5	8.6	62.5	40.6	8.8	59.4
160	31.8	11.5	68.2	29.2	10.6	70.8	43.9	10.0	56.1	48.2	10.7	51.8	51.3	10.7	48.7
125	43.0	11.2	57.0	38.1	8.9	61.9	51.8	7.9	48.2	57.0	8.8	43.0	58.9	7.6	41.1
100	50.0	7.0	50.0	46.9	8.8	53.1	59.2	7.4	40.8	63.3	6.3	36.7	66	7.1	34
80	58.3	8.3	41.7	55.0	8.1	45.0	66.0	6.8	3.04	70.0	6.7	30.0	72.1	6.1	27.9
63	65.2	6.9	34.8	62.0	7.0	38.0	71.5	5.5	28.5	75.3	5.3	24.7	76.9	4.8	23.1
50	70.1	4.9	29.9	67.5	5.5	32.5	75.8	4.3	24.2	78.9	3.6	21.1	80.1	3.2	19.9
40	74.9	4.8	25.1	72.1	4.6	27.9	80.8	5.0	19.2	82.3	3.4	17.7	83.2	3.1	16.8
32	78.1	3.2	21.9	77.8	5.7	22.2	85.1	4.3	14.9	87.5	5.2	12.5	86.4	3.2	13.6
20	84.9	6.8	15.1	86.1	8.3	13.9	90.8	5.7	9.2	92.2	4.7	7.8	90.9	4.5	9.1
1	100.0	15.1	0.01	100.0	13.9	0.01	100.0	9.2	0.01	100.0	7.8	0.01	100.0	9.1	0.01

Table A2.4:   Screen analysis of Horomill feed.

SCREEN ANALYSIS OF HOROMILL FEED			
Screen Aperture	Feed		
(μm)	% Retained	% In Fraction	% mass passing
25000	5.1	5.1	94.9
20000	12.5	7.4	87.5
16000	18.6	6.1	81.4
12500	26.6	8.0	73.4
10000	32.3	5.7	67.7
8000	36.5	4.2	63.5
6300	39.9	3.4	60.1
5000	44.0	4.1	56.0
4000	46.3	2.3	53.7
3150	48.0	1.7	52.0
2500	50.7	2.7	49.3
1600	54.3	3.6	45.7
1250	57.0	2.7	43.0
1000	61.0	4.0	39.0
800	63.0	2.0	37.0
630	65.7	2.7	34.3
500	70.0	4.3	30.0
400	74.6	4.6	25.4
315	80.0	5.4	20.0
250	84.2	4.2	15.8
200	87.0	2.8	13.0
160	90.1	3.1	9.9
125	92.0	1.9	8.0
100	93.8	1.8	6.2
80	94.0	0.2	6.0
63	96.1	2.1	3.9
50	96.5	0.4	3.5
40	97.4	0.9	2.6
32	98.0	0.6	2.0
20	99.0	1.0	1.0
0	100.0	1.0	0.0

Table A2.5:   Screen analysis of the batch press product.

BATCH PRESS: SCREEN ANALYSIS OF FINE FRACTION																		
Test number	1540		1040		5040		1560		1060		5060		40300		15300		30300	
Screen Aperture	% In Fraction	% Passing	% In Fraction	% Passing	% In Fraction	% Passing	% In Fraction	% Passing	% In Fraction	% Passing	% In Fraction	% Passing	% In Fraction	% Passing	% In Fraction	% Passing	% In Fraction	% Passing
850	0.00	100.00	0.00	100	0.00	100	0.00	100.00	0.00	100.00	0.00	100.00						
600	0.00	100.00	0.00	100	0.00	100.00	1.40	98.60	1.40	98.60	1.89	98.11						
425	0.20	99.80	2.81	97.19	1.92	98.08	22.30	76.30	21.58	77.02	24.18	73.93						
300	23.14	76.66	27.73	69.46	28.01	70.07	18.25	58.05	18.51	58.51	17.18	56.74	6.57	93.43	2.35	97.65	9.51	90.49
212	21.55	55.11	21.31	48.15	21.38	48.68	15.89	42.16	16.63	41.87	17.40	39.34	25.70	67.73	26.62	71.03	10.49	80.00
150	15.47	39.63	14.09	34.07	15.05	33.63	11.74	30.42	12.16	29.71	12.33	27.02	24.49	43.24	23.91	47.12	19.14	60.86
106	12.71	26.92	11.77	22.29	11.71	21.93	9.62	20.80	9.86	19.86	9.59	17.43	19.03	24.20	15.76	31.37	15.71	45.15
75	7.45	19.47	6.06	16.23	6.82	15.11	6.01	14.79	5.93	13.93	5.73	11.70	4.19	20.01	11.33	20.03	16.52	28.63
53	6.56	12.91	6.16	10.08	5.54	9.56	4.91	9.88	5.06	8.87	4.50	7.20	14.25	5.76	16.85	3.18	23.00	5.63
38	6.41	6.50	7.43	2.65	4.97	4.59	4.62	5.26	4.79	4.07	3.94	3.26	4.69	1.07	2.75	0.44	4.70	0.93
1	6.50		2.65		4.59		5.26	0.00	4.07	0.00	3.26	0.00	1.07		0.44		0.93	0.00

APPENDIX 3

DETAIL DATA FOR THE TESTS WITH TITANIUM SLAG

Table A3.1:   Summary of pilot plant milling of titanium slag.

Test nr	FEED RATE (kg/hr)	CIRCULATING LOAD (kg/hr)	HYDRAULIC PRESSURE (MPa)	TABLE POWER (kWh/ton)	NO LOAD POWER (kWh)	POWER MEASURED USING TORQUE R(kWh/ton)	NETT TABLE POWER (kWh/ton) (table power less no load power)	P_{50} (μm)
1	306	363	3.0	4.6	0.75	0.7	2.1	680
2	294	203	5.5	5.4	0.75	1.6	2.9	620
3	300	240	8.0	5.3	0.75	2.5	2.8	590
4	318	257	10.0	5.7	0.75	3.3	3.3	580
5	308	202	14.5	5.8	0.75	3.7	3.4	580

Table A3.2: Screen analysis of pilot mill feed.

SCREEN ANALYSIS OF PILOT MILL FEED		
Screen Aperture(μm)	%In Fraction	%In Fraction
10000	0.00	0.22
6000	1.20	0.92
4750	1.22	0.92
3360	3.77	3.90
2350	11.43	12.03
1700	14.30	19.60
1180	23.68	27.34
850	21.90	20.57
600	16.86	11.41
425	3.97	2.27
300	0.77	0.49
212	0.41	0.19
150	0.23	0.03
106	0.17	0.03
75	0.03	0.03
53	0.01	0.01
38	0.02	0.01
-38	0.03	0.01

Table A3.3: Screen analysis of batch press feed.

SCREEN ANALYSIS OF BATCH PRESS FEED		
Screen Aperture(μm)	% In Fraction	% mass passing
6700	4.60	95.40
4750	2.32	93.08
3350	4.64	88.44
2360	12.67	75.77
1700	21.06	54.71
1180	22.18	32.53
850	17.45	15.08
600	11.11	3.97
425	2.32	1.65
300	0.62	1.03
212	0.31	0.71
150	0.18	0.54
106	0.13	0.40
75	0.13	0.27
53	0.13	0.13
1	0.13	0.00

Table A3.4:   Screen analysis of batch press products.

SCREEN ANALYSIS OF BATCH PRESS PRODUCTS								
	15MPa		25MPa		40MPa		50MPa	
Screen Aperture(µm)	% In Fraction	% mass passing	% In Fraction	% mass passing	% In Fraction	% mass passing	% In Fraction	% mass passing
850	17.14	82.86	16.85	83.15	12.83	87.17	12.48	87.52
600	26.29	56.57	21.91	61.24	19.51	67.66	18.80	68.72
425	18.08	38.50	17.60	43.63	16.34	51.32	15.47	53.24
300	9.62	28.87	9.74	33.90	10.54	40.77	10.15	43.09
212	6.81	22.07	7.30	26.59	8.26	32.51	8.32	34.78
150	4.46	17.61	5.06	21.54	5.62	26.89	5.82	28.95
106	3.52	14.08	3.93	17.60	4.39	22.50	4.66	24.29
75	3.29	10.80	3.75	13.86	4.39	18.10	4.66	19.63
53	2.58	8.22	2.62	11.24	3.16	14.94	3.33	16.31
1	8.22	0.00	11.24	0.00	14.94	0.00	16.31	0.00

APPENDIX 4

DETAIL DATA FOR THE TESTS WITH ROSH PINAH ORE

Table A4.1: Summary of results of Loesche tests done at AARL.

SUMMARY OF RESULTS OF LOESCHE TESTS DONE AT AARL								
Test No.	Top Size	Feed	Pressure	Table Power	No load	Table Power	Power measured from Torque	P$_{80}$
	mm	kg/h	MPa	Bruto	kWh	Nett(Bruto less no load)	kWh/ton	µm
1	3 mm	290	15.5	8.3	0.9	5.3	9.3	152
2	3 mm	298	17.5	9.4	0.9	6.5	10.8	95
3	3 mm	300	18	10.7	0.9	7.8	12.2	74
4	3 mm	220	19.5	16.4	0.9	12.4	17.7	62
5	5 mm	340	11.5	7.1	0.9	4.5	6.1	157
6	5 mm	298	13	9.4	0.9	6.5	10.2	106
7	5 mm	266	15.75	11.3	0.8	8.5	13.2	78
8	5 mm	224	18.5	14.3	0.8	10.9	16.2	67
9	10 mm	306	16.5	10.8	0.9	8.0	11.9	117
10	10 mm	234	18	14.1	0.9	10.4	16.3	96

Table A4.2: Summary of information needed to calculate the operating indices of the Loesche mill

INFORMATION NEEDED TO CALCULATE THE OPERATING WORK INDICES FOR LOESCHE MILL							
Test No.	Top size	Power consumption	F_{80}	P_{80}	F_{50}	P_{50}	F_{50}/P_{50}
	mm	kWh/t	µm	µm	µm	µm	
1	3	4.00	1400	152	530	65	8.15
2	3	6.50	1400	95	530	40	13.25
3	3	7.79	1400	74	530	30	17.67
4	3	12.43	1400	62	530	20	26.50
5	5	4.53	3000	157	1600	65	24.62
6	5	6.51	3000	106	1600	53	30.19
7	5	8.46	3000	78	1600	38	42.11
8	5	15.00	3000	67	1600	20	80.00
9	10	7.97	5800	117	3350	50	67.00
10	10	10.43	5800	96	3350	42	79.76
11	16	2.40	13800	495	11400	210	54.29
12	16	5.34	13800	230	11400	115	99.13
13	16	11.34	13800	106	11400	56	203.57
14	16	24.68	13800	66	11400	35	325.71
15	16	32.93	13800	44	11400	26	438.46

Table A4.3: Summary of work index calculations of the Batch press

WORK INDEX CALCULATIONS OF BATCH PRESS							
Test No.	Top size	Power consumption	F_{80}	P_{80}	F_{50}	P_{50}	F_{50}/P_{50}
	mm	kWh/ton	µm	µm	µm	µm	
Batch AARL 2	3	3.24	1400	65	530	35	15.14
Batch AARL 3	3	4.05	1400	53	530	30	17.67
Batch AARL 4	5	3	3000	95	1600	50	32.00
Batch AARL 5	5	3.84	3000	65	1600	35	45.71
Batch AARL 6	5	4.17	3000	53	1600	30	53.33
Batch AARL 7	10	3	5800	95	3350	50	67.00
Batch AARL 8	10	3.68	5800	65	3350	35	95.71
Batch AARL 9	10	4.68	5800	53	3350	30	111.67
Batch RP 1	16	3	13800	106	11400	65	175.38
Batch RP 2	16	2.55	13000	95	10250	65	157.69
Batch RP 3	16	3.05	2500	95	850	61	13.93
Batch RP 4	16	2.6	2500	105	850	65	13.08
Batch RP 5	16	3.35	2500	95	850	61	13.93
Batch RP 6	16	3.02	2500	90	850	61	13.93

Table A4.4: Screen analysis of products of Loesche tests.

SCREEN ANALYSIS OF PRODUCTS OF LOESCHE TESTS										
Top Size = 3 mm					Top size = 5 mm				Top size = 10 mm	
	P_{80}				P_{80}				P_{80}	
Test No.	1	2	3	4	5	6	7	8	9	10
Screen Aperture(µm)	62	74	95	152	67	78	106	157	78	117
150	0.0	0.1	4.7	20.3	0.0	0.3	8.0	21.4	2.7	11.5
106	0.1	2.5	10.1	9.8	0.2	5.3	11.8	11.9	10.5	11.3
75	7.9	16.7	15.2	14.0	15.3	16.0	16.4	11.7	21.1	13.3
53	20.3	17.8	13.6	11.0	12.1	15.6	13.8	12.4	11.0	12.5
45	7.0	7.0	5.0	5.0	5.0	6.0	5.0	4.0	4.0	5.0
38	7.5	7.5	6.0	6.0	5.2	6.8	3.6	4.2	3.4	4.3
1	57.2	48.4	45.4	33.9	62.2	49.9	41.3	34.4	47.4	42.1

Table A4.5: Screen analysis of products of batch tests.

SCREEN ANALYSIS OF PRODUCTS OF BATCH TESTS										
	Top Size = 3 mm			Top Size = 5 mm				Top Size = 10 mm		
	P_{80}			P_{80}				P_{80}		
Test No.	1	2	3	4	5	6	7	8	9	10
Screen Aperture(µm)	110	81	60	110	97	81	60	110	81	60
150	0.8	0.0	0.0	0.2	0.3	0.0	0.0	1.0	0.0	0.0
106	22.2	1.4	0.7	21.0	13.7	2.1	0.8	20.7	2.1	0.5
75	18.6	24.3	1.4	18.4	19.2	24.3	1.0	18.0	24.1	0.5
53	17.1	21.0	29.4	16.6	17.0	20.9	26.5	16.2	21.2	28.1
45	9.2	12.5	16.5	9.4	8.4	13.2	15.1	11.5	13.0	17.9
38	6.1	8.7	10.3	7.9	7.0	7.2	10.9	5.0	7.6	10.4
1	25.9	32.3	41.7	26.5	34.4	32.4	45.6	27.6	32.1	42.6